

3. TOXICOKINETICS

Trichloroethylene (TCE) is a lipophilic compound that readily crosses biological membranes. Exposures may occur via the oral, dermal, and inhalation route, with evidence for systemic availability from each route. TCE is rapidly and nearly completely absorbed from the gut following oral administration, and studies with animals indicate that exposure vehicle may impact the time-course of absorption: oily vehicles may delay absorption whereas aqueous vehicles result in a more rapid increase in blood concentrations.

Following absorption to the systemic circulation, TCE distributes from blood to solid tissues by each organ's solubility. This process is mainly determined by the blood:tissue partition coefficients, which are largely established by tissue lipid content. Adipose partitioning is high, adipose tissue may serve as a reservoir for TCE, and accumulation into adipose tissue may prolong internal exposures. TCE attains high concentrations relative to blood in the brain, kidney, and liver—all of which are important target organs of toxicity. TCE is cleared via metabolism mainly in three organs: the kidney, liver, and lungs.

The metabolism of TCE is an important determinant of its toxicity. Metabolites are generally thought to be responsible for toxicity—especially for the liver and kidney. Initially, TCE may be oxidized via cytochrome P450 (CYP) xenobiotic metabolizing isozymes or conjugated with glutathione by glutathione S-transferase enzymes. While CYP2E1 is generally accepted to be the CYP form most responsible for TCE oxidation at low concentrations, others forms may also contribute, though their contributions may be more important at higher, rather than lower, environmentally-relevant exposures.

Once absorbed, TCE is excreted primarily either in breath as unchanged TCE or carbon dioxide (CO₂), or in urine as metabolites. Minor routes of elimination include excretion of metabolites in saliva, sweat, and feces. Following oral administration or upon cessation of inhalation exposure, exhalation of unmetabolized TCE is a major elimination pathway. Initially, elimination of TCE upon cessation of inhalation exposure demonstrates a steep concentration-time profile: TCE is rapidly eliminated in the minutes and hours postexposure, and then the rate of elimination via exhalation decreases. Following oral or inhalation exposure, urinary elimination of parent TCE is minimal, with urinary elimination of the metabolites trichloroacetic acid and trichloroethanol accounting for the bulk of the absorbed dose of TCE.

Sections 3.1–3.4 below describe the absorption, distribution, metabolism, and excretion of TCE and its metabolites in greater detail. Section 3.5 then discusses physiologically based pharmacokinetic modeling of TCE and its metabolites.

This document is a draft for review purposes only and does not constitute Agency policy.

1 **3.1. ABSORPTION**

2 Trichloroethylene is a low-molecular-weight lipophilic solvent; these properties explain
3 its rapid transfer from environmental media into the systemic circulation after exposure. As
4 discussed below, it is readily absorbed into the bloodstream following exposure via oral
5 ingestion and inhalation, with more limited data indicating dermal penetration.

6
7 **3.1.1. Oral**

8 Available reports on human exposure to TCE via the oral route are largely restricted to
9 case reports of occupational or intentional (suicidal) ingestions and suggest significant gastric
10 absorption (e.g., Perbellini et al., 1991; Yoshida et al., 1996; Brüning et al., 1998). Clinical
11 symptoms attributable to TCE or metabolites were observed in these individuals within a few
12 hours of ingestion (such as lack of consciousness), indicating absorption of TCE. In addition,
13 TCE and metabolites were measured in blood or urine at the earliest times possible after
14 ingestion, typically upon hospital admission, while urinary excretion of TCE metabolites was
15 followed for several days following exposure. Therefore, based on these reports, it is likely that
16 TCE is readily absorbed in the gastrointestinal tract; however, the degree of absorption cannot be
17 confidently quantified because the ingested amounts are not known.

18 Experimental evidence in mice and rats supports rapid and extensive absorption of TCE,
19 although variables such as stomach contents, vehicle, and dose may affect the degree of gastric
20 absorption. D'Souza et al. (1985) reported on bioavailability and blood kinetics in fasted and
21 nonfasted male Sprague-Dawley rats following intragastric administration of TCE at 5–25 mg/kg
22 in 50% polyethylene glycol (PEG 400) in water. TCE rapidly appeared in peripheral blood (at
23 the initial 0.5 minutes sampling) of fasted and nonfasted rats with peak levels being attained
24 shortly thereafter (6–10 minutes), suggesting that absorption is not diffusion limited, especially
25 in fasted animals. The presence of food in the gastro-intestinal (GI) tract, however, seems to
26 influence TCE absorption based on findings in the nonfasted animals of lesser bioavailability
27 (60–80% vs. 90% in fasted rats), smaller peak blood levels (2–3 fold lower than nonfasted
28 animals), and a somewhat longer terminal half-life ($t_{1/2}$) (174 vs. 112 minutes in fasted rats).

29 Studies by Prout et al. (1985) and Dekant et al. (1986a) have shown that up to 98% of
30 administered radiolabel was found in expired air and urine of rats and mice following gavage
31 administration of [¹⁴C]-radio labeled TCE ([¹⁴C]TCE). Prout et al. (1985) and Green and Prout
32 (1985) compared the degree of absorption, metabolites, and routes of elimination among two
33 strains each of male rats (Osborne-Mendel and Park Wistar) and male mice (B6C3F1 and Swiss-
34 Webster) following a single oral administration of 10, 500, or 1,000 [¹⁴C]TCE. Additional dose
35 groups of Osborne-Mendel male rats and B6C3F1 male mice also received a single oral dose of

This document is a draft for review purposes only and does not constitute Agency policy.

1 2,000 mg/kg [¹⁴C]TCE. At the lowest dose of 10 mg/kg, there were no major differences
2 between rats and mice in routes of excretion with most of the administered radiolabel (nearly
3 60–70%) being in the urine. At this dose, the expired air from all groups contained 1–4% of
4 unchanged TCE and 9–14% CO₂. Fecal elimination of the radiolabel ranged from 8.3% in
5 Osborne-Mendel rats to 24.1% in Park Wistar rats. However, at doses between 500 and 2,000
6 mg/kg, the rat progressively excreted a higher proportion of the radiolabel as unchanged TCE in
7 expired air such that 78% of the administered high dose was found in expired air (as unchanged
8 TCE) while only 13% was excreted in the urine.

9 Following exposure to a chemical by the oral route, distribution is determined by delivery
10 to the first organ encountered in the circulatory pathway—the liver (i.e., the first-pass effect),
11 where metabolism and elimination may limit the proportion that may reach extrahepatic organs.
12 Lee et al. (1996) evaluated the efficiency and dose-dependency of presystemic elimination of
13 TCE in male Sprague-Dawley rats following administration into the carotid artery, jugular vein,
14 hepatic portal vein, or the stomach of TCE (0.17, 0.33, 0.71, 2, 8, 16, or 64 mg/kg) in a 5%
15 aqueous Alkamus emulsion (polyethoxylated vegetable oil) in 0.9% saline. The first-pass
16 elimination, decreased from 57.5 to <1% with increasing dose (0.17–16 mg/kg) which implied
17 that hepatic TCE metabolism may be saturated at doses above 16 mg/kg in the male rat. At
18 doses of 16 mg/kg or higher, hepatic first-pass elimination was almost nonexistent indicating
19 that, at relatively large doses, virtually all of TCE passes through the liver without being
20 extracted (Lee et al., 1996). In addition to the hepatic first-pass elimination findings, pulmonary
21 extraction, which was relatively constant (at nearly 5–8% of dose) over the dose range, also
22 played a role in eliminating TCE.

23 In addition, oral absorption appears to be affected by both dose and vehicle used. The
24 majority of oral TCE studies have used either aqueous solution or corn oil as the dosing vehicle.
25 Most studies that relied on an aqueous vehicle delivered TCE as an emulsified suspension in
26 Tween 80[®] or PEG 400 in order to circumvent the water solubility problems. Lee et al.
27 (2000a, b) used Alkamuls (a polyethoxylated vegetable oil emulsion) to prepare a 5% aqueous
28 emulsion of TCE that was administered by gavage to male Sprague-Dawley rats. The findings
29 confirmed rapid TCE absorption but reported decreasing absorption rate constants (i.e., slower
30 absorption) with increasing gavage dose (2–432 mg/kg). The time to reach blood peak
31 concentrations increased with dose and ranged between 2 and 26 minutes postdosing. Other
32 pharmacokinetics data, including area under the blood concentration time curve (AUC) and
33 prolonged elevation of blood TCE levels at the high doses, indicated prolonged GI absorption
34 and delayed elimination due to metabolic saturation occurring at the higher TCE doses.

This document is a draft for review purposes only and does not constitute Agency policy.

1 A study by Withey et al. (1983) evaluated the effect of dosing TCE with corn oil versus
2 pure water as a vehicle by administering four volatile organic compounds separately in each
3 dosing vehicle to male Wistar rats. Based on its limited solubility in pure water, the dose for
4 TCE was selected at 18 mg/kg (administered in 5 mL/kg). Times to peak in blood reported for
5 TCE averaged 5.6 minutes when water was used. In comparison, the time to peak in blood was
6 much longer (approximately 100 minutes) when the oil vehicle was used and the peaks were
7 smaller, below the level of detection, and not reportable.

8 Time-course studies reporting times to peak in blood or other tissues have been
9 performed using both vehicles (Withey et al., 1983; Larson and Bull, 1992 a, b; D'Souza et al.,
10 1985; Green and Prout, 1985; Dekant et al., 1984). Related data for other solvents (Kim et al.,
11 1990; Dix et al., 1997; Lilly et al., 1994; Chieco et al., 1981) confirmed differences in TCE
12 absorption and peak height between the two administered vehicles. One study has also evaluated
13 the absorption of TCE from soil in rats (Kadry et al., 1991) and reported absorption within 16
14 hours for clay and 24 hours for sandy soil. In summary, these studies confirm that TCE is
15 relatively quickly absorbed from the stomach, and that absorption is dependent on vehicle used.
16

17 **3.1.2. Inhalation**

18 Trichloroethylene is a lipophilic volatile compound that is readily absorbed from inspired
19 air. Uptake from inhalation is rapid and the absorbed dose is proportional to exposure
20 concentration and duration, and pulmonary ventilation rate. Distribution into the body via
21 arterial blood leaving the lungs is determined by the net dose absorbed and eliminated by
22 metabolism in the lungs. Metabolic clearance in the lungs will be further discussed in
23 Section 3.3, below. In addition to metabolism, solubility in blood is the major determinant of the
24 TCE concentration in blood entering the heart and being distributed to the each body organ via
25 the arterial blood. The measure of TCE solubility in each organ is the partition coefficient, or the
26 concentration ratio between both organ phases of interest. The blood-to-air partition coefficient
27 (PC) quantifies the resulting concentration in blood leaving the lungs at equilibrium with
28 alveolar air. The value of the blood-to-air partition coefficient is used in physiologically based
29 pharmacokinetic (PBPK) modeling (see Section 3.5). The blood-to-air partition has been
30 measured *in vitro* using the same principles in different studies and found to range between
31 8.1–11.7 in humans and somewhat higher values in mice and rats (13.3–25.8) (see
32 Tables 3-1–3-2, and references therein).

1
2

Table 3-1. Blood:air PC values for humans

Blood:air partition coefficient	Reference/notes
8.1 ± 1.8	Fiserova-Bergerova et al., 1984; mean ± SD (SD converted from SE based on <i>n</i> = 5)
8.11	Gargas et al., 1989; (<i>n</i> = 3–15)
9.13 ± 1.73 [6.47–11]	Fisher et al., 1998; mean ± SD [range] of females (<i>n</i> = 6)
9.5	Sato and Nakajima, 1979; (<i>n</i> = 1)
9.77	Koizumi, 1989
9.92	Sato et al., 1977; (<i>n</i> = 1)
11.15 ± 0.74 [10.1–12.1]	Fisher et al., 1998; mean ± SD [range] of males (<i>n</i> = 7)
11.2 ± 1.8 [7.9–15]	Mahle et al., 2007; mean ± SD; 20 male pediatric patients aged 3–7 years [range; USAF, 2004]
11.0 ± 1.6 [6.6–13.5]	Mahle et al., 2007; mean ± SD; 18 female pediatric patients aged 3–17years [range; USAF, 2004]
11.7 ± 1.9 [6.7–16.8]	Mahle et al., 2007; mean ± SD; 32 male patients aged 23–82 years [range; USAF, 2004]
10.6 ± 2.3 [3–14.4]	Mahle et al., 2007; mean ± SD; 27 female patients aged 23–82 years [range; USAF, 2004]

3
4

SD = standard deviation, SE = standard error.

1
2

Table 3-2. Blood:air PC values for rats and mice

Blood:air partition coefficient	Reference/notes
Rat	
15 ± 0.5	Fisher et al., 1989; mean ± SD (SD converted from SE based on <i>n</i> = 3)
17.5	Rodriguez et al., 2007
20.5 ± 2.4	Barton et al., 1995; mean ± SD (SD converted from SE based on <i>n</i> = 4)
20.69 ± 3.3	Simmons et al., 2002; mean ± SD (<i>n</i> = 7–10)
21.9	Gargas et al., 1989 (<i>n</i> = 3–15)
25.8	Koizumi, 1989 (pooled <i>n</i> = 3)
25.82 ± 1.7	Sato et al., 1977; mean ± SD (<i>n</i> = 5)
13.3 ± 0.8 [11.6–15]	Mahle et al., 2007; mean ± SD; 10 PND 10 male rat pups [range; USAF, 2004]
13.4 ± 1.8 [11.8–17.2]	Mahle et al., 2007; mean ± SD; 10 PND 10 female rat pups [range; USAF, 2004]
17.5 ± 3.6 [11.7–23.1]	Mahle et al., 2007; mean ± SD; 9 adult male rats [range; USAF, 2004]
21.8 ± 1.9 [16.9–23.5]	Mahle et al., 2007; mean ± SD; 11 aged male rats [range; USAF, 2004]
Mouse	
13.4	Fisher et al., 1991; male
14.3	Fisher et al., 1991; female
15.91	Abbas and Fisher, 1997

3
4
5
6
7
8
9
10
11
12
13

SD = standard deviation, SE = standard error, PND = postnatal day.

TCE enters the human body by inhalation quickly and at high concentrations may lead to death (Coopman et al., 2003), unconsciousness, and acute kidney damage (Carrieri et al., 2007). Controlled exposure studies in humans have shown absorption of TCE to approach a steady state within a few hours after the start of inhalation exposure (Monster et al., 1976; Fernandez et al., 1977; Vesterberg et al., 1976; Vesterberg and Astrand, 1976). Several studies have calculated the net dose absorbed by measuring the difference between the inhaled concentration and the exhaled air concentration. Soucek and Vlachova (1959) reported between 58–70% absorption of

1 the amount inhaled for 5-hour exposures between 93–158 ppm. Bartonicek (1962) obtained an
 2 average retention value of 58% after 5 hours of exposure to 186 ppm. Monster et al. (1976) also
 3 took into account minute ventilation measured for each exposure, and calculated between
 4 37–49% absorption in subjects exposed to 70 and 140 ppm. The impact of exercise, the increase
 5 in workload, and its effect on breathing has also been measured in controlled inhalation
 6 exposures. Astrand and Ovrum (1976) reported 50–58% uptake at rest and 25–46% uptake
 7 during exercise from exposure at 100 or 200 ppm (540 or 1,080 mg/m³, respectively) of TCE for
 8 30 minutes (see Table 3-3). These authors also monitored heart rate and pulmonary ventilation.
 9 In contrast, Jakubowski and Wieczorek (1988) calculated about 40% retention in their human
 10 volunteers exposed to TCE at 9 ppm (mean inspired concentration of 48–49 mg/m³) for 2 hours
 11 at rest, with no change in retention during increase in workload due to exercise (see Table 3-4).

12
 13 **Table 3-3. Air and blood concentrations during exposure to TCE in humans**
 14 **(Astrand and Ovrum, 1976)**
 15

TCE conc. (mg/m ³)	Work load (watt)	Exposure series	TCE concentration in			Uptake as % of amount available	Amount taken up (mg)
			Alveolar air (mg/m ³)	Arterial blood (mg/kg)	Venous blood (mg/kg)		
540	0	I	124 ± 9	1.1 ± 0.1	0.6 ± 0.1	53 ± 2	79 ± 4
540	0	II	127 ± 11	1.3 ± 0.1	0.5 ± 0.1	52 ± 2	81 ± 7
540	50	I	245 ± 12	2.7 ± 0.2	1.7 ± 0.4	40 ± 2	160 ± 5
540	50	II	218 ± 7	2.8 ± 0.1	1.8 ± 0.3	46 ± 1	179 ± 2
540	50	II	234 ± 12	3.1 ± 0.3	2.2 ± 0.4	39 ± 2	157 ± 2
540	50	II	244 ± 16	3.3 ± 0.3	2.2 ± 0.4	37 ± 2	147 ± 9
1,080	0	I	280 ± 18	2.6 ± 0.0	1.4 ± 0.3	50 ± 2	156 ± 9
1,080	0	III	212 ± 7	2.1 ± 0.2	1.2 ± 0.1	58 ± 2	186 ± 7
1,080	50	I	459 ± 44	6.0 ± 0.2	3.3 ± 0.8	45 ± 2	702 ± 31
1,080	50	III	407 ± 30	5.2 ± 0.5	2.9 ± 0.7	51 ± 3	378 ± 18
1,080	100	III	542 ± 33	7.5 ± 0.7	4.8 ± 1.1	36 ± 3	418 ± 39
1,080	150	III	651 ± 53	9.0 ± 1.0	7.4 ± 1.1	25 ± 5	419 ± 84

16 Series I consisted of 30-minute exposure periods of rest, rest, 50W and 50W; Series II consisted of
 17 30-minute exposure periods of rest, 50W, 50W, 50W; Series III consisted of 30-minute exposure
 18 periods of rest, 50W, 100W, 150W.
 19

1 **Table 3-4. Retention of inhaled TCE vapor in humans (Jakubowski and**
 2 **Wieczorek, 1988)**
 3

Workload	Inspired concentration (mg/m ³)	Pulmonary ventilation (m ³ /hour)	Retention	Uptake (mg/h)
Rest	48 ± 3*	0.65 ± 0.07	0.40 ± 0.05	12 ± 1.1
25 W	49 ± 1.3	1.30 ± 0.14	0.40 ± 0.05	25 ± 2.9
50 W	49 ± 1.6	1.53 ± 0.13	0.42 ± 0.06	31 ± 2.8
75 W	48 ± 1.9	1.87 ± 0.14	0.41 ± 0.06	37 ± 4.8

4
 5 *Mean ± standard deviation, n = 6 adult males.

6
 7 W = watts.
 8
 9

10 Environmental or occupational settings may results from a pattern of repeated exposure
 11 to TCE. Monster et al. (1979) reported 70-ppm TCE exposures in volunteers for 4 hours for
 12 5 consecutive days, averaging a total uptake of 450 mg per 4 hours exposure (see Table 3-5). In
 13 dry-cleaning workers, Skender et al. (1991) reported initial blood concentrations of 0.38 µmol/L,
 14 increasing to 3.4 µmol/L 2 days after. Results of these studies support rapid absorption of TCE
 15 via inhalation.
 16

17 **Table 3-5. Uptake of TCE in human volunteers following 4 hour exposure to**
 18 **70 ppm (Monster et al., 1979)**
 19

	BW (kg)	MV (L/min)	% Retained	Uptake (mg/day)	Uptake (mg/kg/d)
A	80	9.8 ± 0.4	45 ± 0.8	404 ± 23	5.1
B	82	12.0 ± 0.7	44 ± 0.9	485 ± 35	5.9
C	82	10.9 ± 0.8	49 ± 1.2	493 ± 28	6.0
D	67	11.8 ± 0.8	35 ± 2.6	385 ± 38	5.7
E	90	11.0 ± 0.7	46 ± 1.1	481 ± 25	5.3
Mean					5.6 ± 0.4

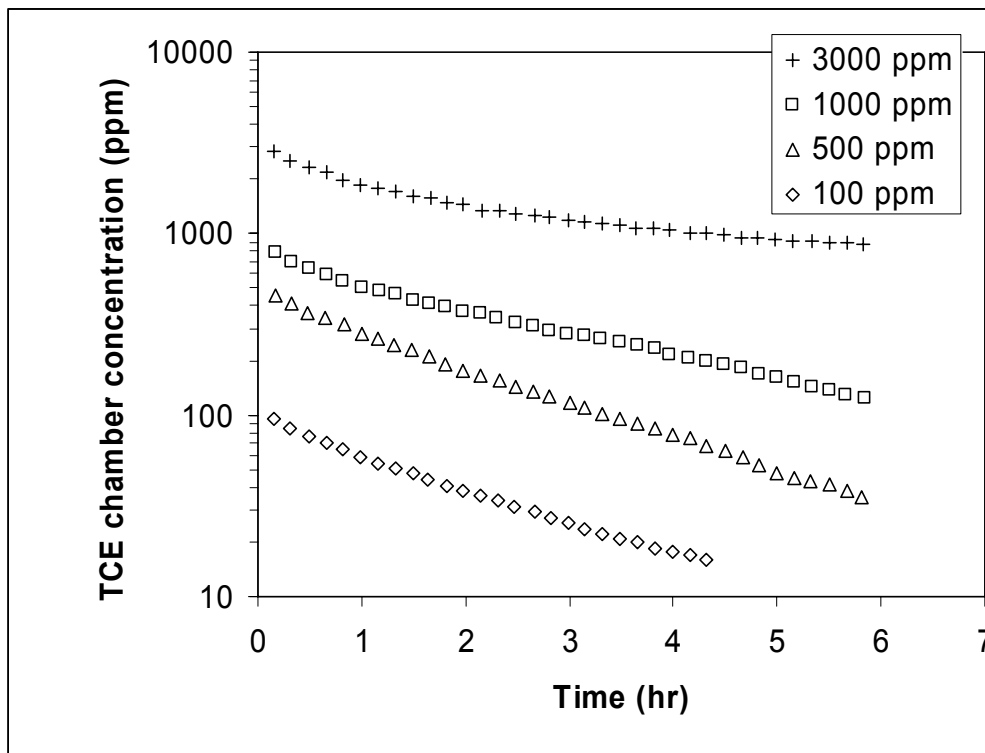
20
 21 BW = body weight.
 22
 23

1 Direct measurement of retention after inhalation exposure in rodents is more difficult
2 because exhaled breath concentrations are challenging to obtain. The only available data are
3 from Dallas et al. (1991), who designed a nose-only exposure system for rats using a facemask
4 equipped with one-way breathing valves to obtain measurements of TCE in inspired and exhaled
5 air. In addition, indwelling carotid artery cannulae were surgically implanted to facilitate the
6 simultaneous collection of blood. After a 1-hour acclimatization period, rats were exposed to 50-
7 or 500-ppm TCE for 2 hours and the time course of TCE in blood and expired air was measured
8 during and for 3 hours following exposure. When air concentration data were analyzed to reveal
9 absorbed dose (minute volume multiplied by the concentration difference between inspired and
10 exhaled breath), it was demonstrated that the fractional absorption of either concentration was
11 more than 90% during the initial 5 minutes of exposure. Fractional absorption then decreased to
12 69 and 71% for the 50 and 500-ppm groups during the second hour of exposure. Cumulative
13 uptake appeared linear with respect to time over the 2-hour exposure, resulting in absorbed doses
14 of 8.4 mg/kg and 73.3 mg/kg in rats exposed to 50 and 500 ppm, respectively. Given the 10-fold
15 difference in inspired concentration and the 8.7-fold difference in uptake, the authors interpreted
16 this information to indicate that metabolic saturation occurred at some concentration below
17 500 ppm. In comparing the absorbed doses to those developed for the 70-ppm-exposed human
18 (see Monster et al., 1979), Dallas et al. (1991) concluded that on a systemic dose (mg/kg) basis,
19 rats receive a much higher TCE dose from a given inhalation exposure than do humans. In
20 particular, using the results cited above, the absorption per ppm-hour was 0.084 and
21 0.073 mg/kg-ppm-hour at 50 and 500 ppm in rats (Dallas et al., 1991) and
22 0.019 mg/kg-ppm-hour at 70 ppm in humans (Monster et al., 1979)—a difference of around
23 4-fold. However, rats have about a 10-fold higher alveolar ventilation rate per unit body weight
24 than humans (Brown et al., 1997), which more than accounts for the observed increase in
25 absorption.

26 Other experiments, such as closed-chamber gas uptake experiments or blood
27 concentration measurements following open-chamber (fixed concentration) experiments,
28 measure absorption indirectly but are consistent with significant retention. Closed-chamber
29 gas-uptake methods (Gargas et al., 1988) place laboratory animals or *in vitro* preparations into
30 sealed systems in which a known amount of TCE is injected to produce a predetermined
31 chamber concentration. As the animal retains a quantity of TCE inside its body, due to
32 metabolism, the closed-chamber concentration decreases with time when compared to the start of
33 exposure. Many different studies have made use of this technique in both rats and mice to
34 calculate total TCE metabolism (i.e., Andersen, 1987; Fisher et al., 1991; Simmons et al., 2002).
35 This inhalation technique is combined with PBPK modeling to calculate metabolic parameters,

This document is a draft for review purposes only and does not constitute Agency policy.

1 and the results of these studies are consistent with rapid absorption of TCE via the respiratory
2 tract. Figure 3-1 shows an example from Simmons et al. (2002), in Long Evans rats, that
3 demonstrates an immediate decline in chamber concentrations of TCE indicating absorption,
4 with multiple initial concentrations needed for each metabolic calculation. At concentrations
5 below metabolic saturation, a secondary phase of uptake appears, after 1 hour from starting the
6 exposure, indicative of metabolism. At concentrations above 1,000 ppm, metabolism appears
7 saturated, with time course curves having a flat phase after absorption. At intermediate
8 concentrations, between 100–1,000 ppm, the secondary phase of uptake appears after
9 distribution as continued decreases in chamber concentration as metabolism proceeds. Using a
10 combination of experiments that include both metabolic linear decline and saturation obtained by
11 using different initial concentrations, both components of metabolism can be estimated from the
12 gas uptake curves, as shown in Figure 3-1.
13



14
15 **Figure 3-1. Gas uptake data from closed-chamber exposure of rats to TCE.**
16 **Symbols represent measured chamber concentrations. Source: Simmons et**
17 **al. (2002).**
18

19
20 Several other studies in humans and rodents have measured blood concentrations of TCE
21 or metabolites and urinary excretion of metabolites during and after inhalation exposure (e.g.,

1 Fisher et al., 1998, 1991, 1990; Filser and Bolt, 1979). While qualitatively indicative of
2 absorption, blood concentrations are also determined by metabolism, distribution, and excretion,
3 so comparisons between species may reflect similarities or differences in any of the absorption,
4 distribution, metabolism, and excretion (ADME) processes.

6 **3.1.3. Dermal**

7 Skin membrane is believed to present a diffusional barrier for entrance of the chemical
8 into the body, and TCE absorption can be quantified using a permeability rate or permeability
9 constant, though not all studies performed such a calculation. Absorption through the skin has
10 been shown to be rapid by both vapor and liquid TCE contact with the skin. Human dermal
11 absorption of TCE vapors was investigated by Kezic et al. (2000). Human volunteers were
12 exposed to 3.18×10^4 ppm around each enclosed arm for 20 minutes. Adsorption was found to
13 be rapid (within 5 minutes), reaching a peak in exhaled breath around 30 minutes, with a
14 calculated dermal penetration rate averaging 0.049 cm/hour for TCE vapors.

15 With respect to dermal penetration of liquid TCE, Nakai et al. (1999) used surgically
16 removed skin samples exposed to TCE in aqueous solution in a chamber designed to measure the
17 difference between incoming and outgoing [^{14}C]TCE. The *in vitro* permeability constant
18 calculated by these researchers averaged 0.12 cm/hour. *In vivo*, Sato and Nakajima (1978)
19 exposed adult male volunteers dermally to liquid TCE for 30 minutes, with exhaled TCE
20 appearing at the initial sampling time of 5 minutes after start of exposure, with a maximum
21 observed at 15 minutes. In Kezic et al. (2001), human volunteers were exposed dermally for
22 3 minutes to neat liquid TCE, with TCE detected in exhaled breath at the first sampling point of
23 3 minutes, and maximal concentrations observed at 5 minutes. Skin irritancy was reported in all
24 subjects, which may have increased absorption. A dermal flux of 430 ± 295 (mean \pm standard
25 error [SE]) nmol/cm²/minute was reported in these subjects, suggesting high interindividual
26 variability.

27 Another species where dermal absorption for TCE has been reported is in guinea pigs.
28 Jakobson et al. (1982) applied liquid TCE to the shaved backs of guinea pigs and reported peak
29 blood TCE levels at 20 minutes after initiation of exposure. Bogen et al. (1992) estimated
30 permeability constants for dermal absorption of TCE in hairless guinea pigs between
31 0.16–0.47 mL/cm²/hour across a range of concentrations (19–100,000 ppm).

33 **3.2. DISTRIBUTION AND BODY BURDEN**

34 TCE crosses biological membranes and quickly results in rapid systemic distribution to
35 tissues—regardless of the route of exposure. In humans, *in vivo* studies of tissue distribution are

This document is a draft for review purposes only and does not constitute Agency policy.

1 limited to tissues taken from autopsies following accidental poisonings or from surgical patients
2 exposed environmentally, so the level of exposure is typically unknown. Tissue levels reported
3 after autopsy show wide systemic distribution across all tested tissues, including the brain,
4 muscle, heart, kidney, lung, and liver (Ford et al., 1995; De Baere et al., 1997; Dehon et al.,
5 2000; Coopman et al., 2003). However, the reported levels themselves are difficult to interpret
6 because of the high exposures and differences in sampling protocols. In addition, human
7 populations exposed environmentally show detectable levels of TCE across different tissues,
8 including the liver, brain, kidney, and adipose tissues (McConnell et al., 1975; Pellizzari et al.,
9 1982; Kroneld, 1989).

10 In addition, TCE vapors have been shown to cross the human placenta during childbirth
11 (Laham, 1970), with experiments in rats confirming this finding (Withey and Karpinski, 1985).
12 In particular, Laham (1970) reported determinations of TCE concentrations in maternal and fetal
13 blood following administration of TCE vapors (concentration unreported) intermittently and at
14 birth (see Table 3-6). TCE was present in all samples of fetal blood, with ratios of
15 concentrations in fetal:maternal blood ranging from approximately 0.5 to approximately 2. The
16 concentration ratio was less than 1.0 in six pairs, greater than 1 in 3 pairs, and approximately 1 in
17 1 pair; in general, higher ratios were observed at maternal concentrations below
18 2.25 mg/100 mL. Because no details of exposure concentration, duration, or time postexposure
19 were given for samples taken, these results are of minimal quantitative value, but they do
20 demonstrate the placental transfer of TCE in humans. Withey and Karpinski (1985) exposed
21 pregnant rats to TCE vapors (302, 1,040, 1,559, or 2,088 ppm for 5 hours) on gestation Day 17
22 and concentrations of TCE in maternal and fetal blood were determined. At all concentrations,
23 TCE concentration in fetal blood was approximately one-third the concentration in
24 corresponding maternal blood. Maternal blood concentrations approximated 15, 60, 80, and
25 110 µg/gram blood. When the position along the uterine horn was examined, TCE
26 concentrations in fetal blood decreased toward the tip of the uterine horn.

27 TCE appears to also distribute to mammary tissues and is excreted in milk.
28 Pellizzari et al. (1982) conducted a survey of environmental contaminants in human milk using
29 samples from cities in the northeastern region of the United States and one in the southern
30 region. No details of times postpartum, milk lipid content, or TCE concentration in milk or
31 blood are reported, but TCE was detected in 8 milk samples taken from 42 lactating women.
32 Fisher et al. (1990) exposed lactating rats to 600-ppm TCE for 4 hours and collected milk
33 immediately following the cessation of exposure. TCE was clearly detectable in milk, and, from
34 a visual interpretation of the graphic display of their results, concentrations of TCE in milk
35 approximated 110 µg/mL milk.

This document is a draft for review purposes only and does not constitute Agency policy.

1
2

Table 3-6. Concentrations of TCE in maternal and fetal blood at birth

TCE concentration in blood (mg/100 mL)		Ratio of concentrations fetal:maternal
Maternal	Fetal	
4.6	2.4	0.52
3.8	2.2	0.58
8	5	0.63
5.4	3.6	0.67
7.6	5.2	0.68
3.8	3.3	0.87
2	1.9	0.95
2.25	3	1.33
0.67	1	1.49
1.05	2	1.90

Source: Laham (1970).

3
4
5
6
7
8
9
10
11
12
13
14
15
16
17
18
19
20
21
22

In rodents, detailed tissue distribution experiments have been performed using different routes of administration (Savolainen et al., 1977; Pfaffenberger et al., 1980; Abbas and Fisher, 1997; Greenberg et al., 1999; Simmons et al., 2002; Keys et al., 2003). Savolainen et al. (1977) exposed adult male rats to 200-ppm TCE for 6 hours/day for a total of 5 days. Concentrations of TCE in the blood, brain, liver, lung, and perirenal fat were measured 17 hours after cessation of exposure on the fourth day and after 2, 3, 4, and 6 hours of exposure on the fifth day (see Table 3-7). TCE appeared to be rapidly absorbed into blood and distributed to brain, liver, lungs, and perirenal fat. TCE concentrations in these tissues reached near-maximal values within 2 hours of initiation of exposure on the fifth day. Pfaffenberger et al. (1980) dosed rats by gavage with 1 or 10 mg TCE/kg/day in corn oil for 25 days to evaluate the distribution from serum to adipose tissue. During the exposure period, concentrations of TCE in serum were below the limit of detection (1 µg/L) and were 280 and 20,000 ng per gram of fat in the 1 and 10 mg/day dose groups, respectively. Abbas and Fisher (1997) and Greenberg et al. (1999) measured tissue concentrations in the liver, lung, kidney, and fat of mice administered TCE by gavage (300–2,000 mg/kg) and by inhalation exposure (100 or 600 ppm for 4 hours). In a study to investigate the effects of TCE on neurological function, Simmons et al. (2002) conducted

1 pharmacokinetic experiments in rats exposed to 200, 2,000, or 4,000 ppm TCE vapors for 1 hour.
 2 Time-course data were collected on blood, liver, brain, and fat. The data were used to develop a
 3 PBPK model to explore the relationship between internal dose and neurological effect. Keys et
 4 al. (2003), exposed groups of rats to TCE vapors of 50 or 500 ppm for 2 hours and sacrificed at
 5 different time points during exposure. In addition to inhalation, this study also includes oral
 6 gavage and intra-arterial dosing, with the following time course measured: liver, fat, muscle,
 7 blood, GI, brain, kidney, heart, lung, and spleen. These pharmacokinetic data were presented
 8 with an updated PBPK model for all routes.

9
 10 **Table 3-7. Distribution of TCE to rat tissues^a following inhalation exposure**
 11 **(Savolainen et al., 1977)**
 12

Exposure on 5 th day	Tissue (concentration in nmol/gram tissue)					
	Cerebrum	Cerebellum	Lung	Liver	Perirenal fat	Blood
0 ^b	0	0	0.08	0.04	0.23 + 0.09	0.35 + 0.1
2	9.9 + 2.7	11.7 + 4.2	4.9 _ 0.3	3.6	65.9 + 1.2	7.5 + 1.6
3	7.3 + 2.2	8.8 + 2.1	5.5 + 1.4	5.5 + 1.7	69.3 + 3.3	6.6 + 0.9
4	7.2 + 1.7	7.6 + 0.5	5.8 + 1.1	2.5 + 1.4	69.5 + 6.3	6.0 + 0.2
6	7.4 + 2.1	9.5 + 2.5	5.6 + 0.5	2.4 + 0.2	75.4 + 14.9	6.8 + 1.2

13
 14 ^aData presented as mean of 2 determinations ± range.

15 ^bSample taken 17 hours following cessation of exposure on Day 4.
 16
 17

18 Besides the route of administration, another important factor contributing to body
 19 distribution is the individual solubility of the chemical in each organ, as measured by a partition
 20 coefficient. For volatile compounds, partition coefficients are measured *in vitro* using the vial
 21 equilibration technique to determine the ratio of concentrations between organ and air at
 22 equilibrium. Table 3-8 reports values developed by several investigators from mouse, rat, and
 23 human tissues. In humans, partition coefficients in the following tissues have been measured:
 24 brain, fat, kidney, liver, lung, and muscle; but the organ having the highest TCE partition
 25 coefficient is fat (63–70), while the lowest is the lung (0.5–1.7). The adipose tissue also has the
 26 highest measured value in rodents, and is one of the considerations needed to be accounted for
 27 when extrapolating across species. However, the rat adipose partition coefficient value is
 28 smaller (23–36), when compared to humans, that is, TCE is less lipophilic in rats than humans.
 29 For the mouse, the measured fat partition coefficient averages 36, ranging between rats and

This document is a draft for review purposes only and does not constitute Agency policy.

1 humans. The value of the partition coefficient plays a role in distribution for each organ and is
2 computationally described in computer simulations using a PBPK model. Due to its high
3 lipophilicity in fat, as compared to blood, the adipose tissue behaves as a storage compartment
4 for this chemical, affecting the slower component of the chemical's distribution. For example
5 Monster et al. (1979) reported that, following repeated inhalation exposures to TCE, TCE
6 concentrations in expired breath postexposure were highest for the subject with the greatest
7 amount of adipose tissue (adipose tissue mass ranged 3.5-fold among subjects). The intersubject
8 range in TCE concentration in exhaled breath increased from approximately 2-fold at 20 hours to
9 approximately 10-fold 140 hours postexposure. Notably, they reported that this difference was
10 not due to differences in uptake, as body weight and lean body mass were most closely
11 associated with TCE retention. Thus, adipose tissue may play an important role in postexposure
12 distribution, but does not affect its rapid absorption.

13 Mahle et al. (2007) reported age-dependent differences in partition coefficients in rats,
14 (see Table 3-9) that can have implications as to life-stage-dependent differences in tissue TCE
15 distribution. To investigate the potential impact of these differences, Rodriguez et al. (2007)
16 developed models for the postnatal Day 10 rat pup; the adult and the aged rat, including
17 age-specific tissue volumes and blood flows; and age-scaled metabolic constants. The models
18 predict similar uptake profiles for the adult and the aged rat during a 6-hour exposure to
19 500 ppm; uptake by the postnatal day (PND) 10 rat was higher (see Table 3-10). The effect was
20 heavily dependent on age-dependent changes in anatomical and physiological parameters
21 (alveolar ventilation rates and metabolic rates); age-dependent differences in partition coefficient
22 values had minimal impact on predicted differences in uptake.

23 Finally, TCE binding to tissues or cellular components within tissues can affect overall
24 pharmacokinetics. The binding of a chemical to plasma proteins, for example, affects the
25 availability of the chemical to other organs and the calculation of the total half-life. However,
26 most studies have evaluated binding using [¹⁴C]TCE, from which one cannot distinguish binding
27 of TCE from binding of TCE metabolites. Nonetheless, several studies have demonstrated
28 binding of TCE-derived radiolabel to cellular components (Moslen et al., 1977; Mazzullo et al.,
29 1992). Bolt and Filser (1977) examined the total amount irreversibly bound to tissues following
30 9-, 100-, and 1,000-ppm exposures via inhalation in closed chambers. The largest percent of *in*
31 *vivo* radioactivity taken up occurred in the liver; albumin is the protein favored for binding (see
32 Table 3-11). Bannerjee and van Duuren (1978) evaluated the *in vitro* binding of TCE to
33 microsomal proteins from the liver, lung, kidney, and stomachs in rats and mice. In both rats and
34 mice, radioactivity was similar in stomach and lung, but about 30% lower in kidney and liver.

This document is a draft for review purposes only and does not constitute Agency policy.

1
2

Table 3-8. Tissue:blood partition coefficient values for TCE

Species/ tissue	TCE partition coefficient		References
	Tissue:blood	Tissue:air	
Human			
Brain	2.62	21.2	Fiserova-Bergerova et al., 1984
Fat	63.8–70.2	583–674.4	Sato et al., 1977; Fiserova-Bergerova et al., 1984; Fisher et al., 1998
Kidney	1.3–1.8	12–14.7	Fiserova-Bergerova et al., 1984; Fisher et al., 1998
Liver	3.6–5.9	29.4–54	Fiserova-Bergerova et al., 1984; Fisher et al., 1998
Lung	0.48–1.7	4.4–13.6	Fiserova-Bergerova et al., 1984; Fisher et al., 1998
Muscle	1.7–2.4	15.3–19.2	Fiserova-Bergerova et al., 1984; Fisher et al., 1998
Rat			
Brain	0.71–1.29	14.6–33.3	Sato et al., 1977; Simmons et al., 2002; Rodriguez et al., 2007
Fat	22.7–36.1	447–661	Gargas et al., 1989; Sato et al., 1977; Simmons et al., 2002; Rodriguez et al. 2007; Fisher et al., 1989, Koizumi, 1989; Barton et al., 1995
Heart	1.1	28.4	Sato et al. 1977
Kidney	1.0–1.55	17.7–40	Sato et al., 1977; Barton et al., 1995; Rodriguez et al., 2007
Liver	1.03–2.43	20.5–62.7	Gargas et al., 1989; Sato et al., 1977; Simmons et al., 2002; Rodriguez et al., 2007; Fisher et al., 1989; Koizumi, 1989; Barton et al., 1995
Lung	1.03	26.6	Sato et al., 1977
Muscle	0.46–0.84	6.9–21.6	Gargas et al., 1989; Sato et al., 1977; Simmons et al., 2002; Rodriguez et al., 2007; Fisher et al., 1989; Koizumi, 1989; Barton et al., 1995
Spleen	1.15	29.7	Sato et al., 1977
Testis	0.71	18.3	Sato et al., 1977
Milk	7.10	N.R.	Fisher et al., 1990
Mouse			
Fat	36.4	578.8	Abbas and Fisher, 1997
Kidney	2.1	32.9	Abbas and Fisher, 1997
Liver	1.62	23.2	Fisher et al., 1991
Lung	2.6	41.5	Abbas and Fisher, 1997
Muscle	2.36	37.5	Abbas and Fisher, 1997

3
4

N.R. = not reported.

This document is a draft for review purposes only and does not constitute Agency policy.

Table 3-9. Age-dependence of tissue:air partition coefficients in rats

Age	Liver	Kidney	Fat	Muscle	Brain
PND10 male	22.1 ± 2.3	15.2 ± 1.3	398.7 ± 89.2	43.9 ± 11.0	11.0 ± 0.6
PND10 female	21.2 ± 1.7	15.0 ± 1.1	424.5 ± 67.5	48.6 ± 17.3	11.6 ± 1.2
Adult male	20.5 ± 4.0	17.6 ± 3.9 ^a	631.4 ± 43.1 ^a	12.6 ± 4.3	17.4 ± 2.6
Aged male	34.8 ± 8.7 ^{a,b}	19.9 ± 3.4 ^a	757.5 ± 48.3 ^{a,b}	26.4 ± 10.3 ^{a,b}	25.0 ± 2.0 ^{a,b}

^aStatistically significant ($p \leq 0.05$) difference between either the adult or aged partition coefficient and the PND10 male partition coefficient.

^bStatistically significant ($p \leq 0.05$) difference between aged and adult partition coefficient.

Data are mean ± standard deviation; $n = 10$, adult male and pooled male and female litters; 11, aged males. Source: Mahle et al. (2007).

Table 3-10. Predicted maximal concentrations of TCE in rat blood following a 6-hour inhalation exposure (Rodriguez et al., 2007)

Age	Exposure concentration					
	50 ppm			500 ppm		
	Predicted peak concentration (mg/L) in: ^a		Predicted time to reach 90% of steady state (hour) ^b	Predicted peak concentration (mg/L) in: ^a		Predicted time to reach 90% of steady state (hour) ^b
	Venous blood	Brain		Venous blood	Brain	
PND 10	3.0	2.6	4.1	33	28	4.2
Adult	0.8	1.0	3.5	22	23	11.9
Aged	0.8	1.2	6.7	21	26	23.3

^aDuring a 6 hour exposure.

^bUnder continuous exposure.

This document is a draft for review purposes only and does not constitute Agency policy.

1 **Table 3-11. Tissue distribution of TCE metabolites following inhalation**
 2 **exposure**
 3

Tissue*	Percent of radioactivity taken up/g tissue					
	TCE = 9 ppm, n = 4		TCE = 100 ppm, n = 4		TCE = 1,000 ppm, n = 3	
	Total metabolites	Irreversibly bound	Total metabolites	Irreversibly bound	Total metabolites	Irreversibly bound
Lung	0.23 ± 0.026	0.06 ± 0.002	0.24 ± 0.025	0.06 ± 0.006	0.22 ± 0.055	0.1 ± 0.003
Liver	0.77 ± 0.059	0.28 ± 0.027	0.68 ± 0.073	0.27 ± 0.019	0.88 ± 0.046	0.48 ± 0.020
Spleen	0.14 ± 0.015	0.05 ± 0.002	0.15 ± 0.001	0.05 ± 0.004	0.15 ± 0.006	0.08 ± 0.003
Kidney	0.37 ± 0.005	0.09 ± 0.007	0.40 ± 0.029	0.09 ± 0.007	0.39 ± 0.045	0.14 ± 0.016
Small intestine	0.41 ± 0.058	0.05 ± 0.010	0.38 ± 0.062	0.07 ± 0.008	0.28 ± 0.015	0.09 ± 0.015
Muscle	0.11 ± 0.005	0.014 ± 0.001	0.11 ± 0.013	0.012 ± 0.001	0.10 ± 0.011	0.027 ± 0.003

4 *Male Wistar rats, 250 g.

5
6
7 n = number of animals.

8 Values shown are means ± standard deviation.

9 Source: Bolt and Filser (1977).

10
11
12 Based on studies of the effects of metabolizing enzyme induction on binding, there is
 13 some evidence that a major contributor to the observed binding is from TCE metabolites rather
 14 than from TCE itself. Dekant et al. (1986a) studied the effect of enzyme modulation on the
 15 binding of radiolabel from [¹⁴C]TCE by comparing tissue binding after administration of
 16 200 mg/kg via oral gavage in corn oil between control (naïve) rats and rats pretreated with
 17 phenobarbital (a known inducer of CYP2B family) or arochlor 1254 (a known inducer of both
 18 CYP1A and CYP2B families of isoenzymes) (see Table 3-12). The results indicate that
 19 induction of total cytochromes P-450 content by 3- to 4-fold resulted in nearly 10-fold increase
 20 in radioactivity (decays per minute; DPM) bound in liver and kidney. By contrast, Mazzullo et
 21 al. (1992) reported that, phenobarbital pretreatment did not result in consistent or marked
 22 alterations of *in vivo* binding of radiolabel to DNA, RNA, or protein in rats and mice at 22 hours
 23 after an intraperitoneal (i.p.) injection of [¹⁴C]TCE. On the other hand, *in vitro* experiments by
 24 Mazzullo et al. (1992) reported reduction of TCE-radiolabel binding to calf thymus DNA with
 25 introduction of a CYP inhibitor into incubations containing rat liver microsomal protein.
 26 Moreover, increase/decrease of glutathione (GSH) levels in incubations containing lung

This document is a draft for review purposes only and does not constitute Agency policy.

1 cytosolic protein led to a parallel increase/decrease in TCE-radiolabel binding to calf thymus
2 DNA.

3
4 **Table 3-12. Binding of ¹⁴C from [¹⁴C]TCE in rat liver and kidney at 72 hours**
5 **after oral administration of 200 mg/kg [¹⁴C]TCE (Dekant et al., 1986a)**
6

Tissue	DPM/gram tissue		
	Untreated	Phenobarbital	Arochlor 1254
Liver	850 ± 100	9,300 ± 1,100	8,700 ± 1,000
Kidney	680 ± 100	5,700 ± 900	7,300 ± 800

7
8
9 **3.3. METABOLISM**

10 This section focuses on both *in vivo* and *in vitro* studies of the biotransformation of
11 trichloroethylene, identifying metabolites that are deemed significant for assessing toxicity and
12 carcinogenicity. In addition, metabolism studies may be used to evaluate the flux of parent
13 compound through the known metabolic pathways. Sex-, species-, and interindividual
14 differences in the metabolism of TCE are discussed, as are factors that possibly contribute to this
15 variability. Additional discussion of variability and susceptibility is presented in Section 4.10.

16
17 **3.3.1. Introduction**

18 The metabolism of TCE has been studied mostly in mice, rats, and humans and has been
19 extensively reviewed (U.S. EPA, 1985, 2001; Lash et al., 2000a; IARC, 1995). It is now well
20 accepted that TCE is metabolized in laboratory animals and in humans through at least two
21 distinct pathways: (1) oxidative metabolism via the cytochrome P450 mixed-function oxidase
22 system and (2) GSH conjugation followed by subsequent further biotransformation and
23 processing, either through the cysteine conjugate beta lyase pathway or by other enzymes (Lash
24 et al., 2000b). While the flux through the conjugative pathway is less, quantitatively, than the
25 flux through oxidation (Bloemen et al., 2001), GSH conjugation is an important route
26 toxicologically, giving rise to relatively potent toxic biotransformation products
27 (Elfarra et al., 1986a, b).

28 Information about metabolism is important because, as discussed extensively in
29 Chapter 4, certain metabolites are thought to cause one or more of the same acute and chronic
30 toxic effects, including carcinogenicity, as TCE. Thus, in many of these cases, the toxicity of

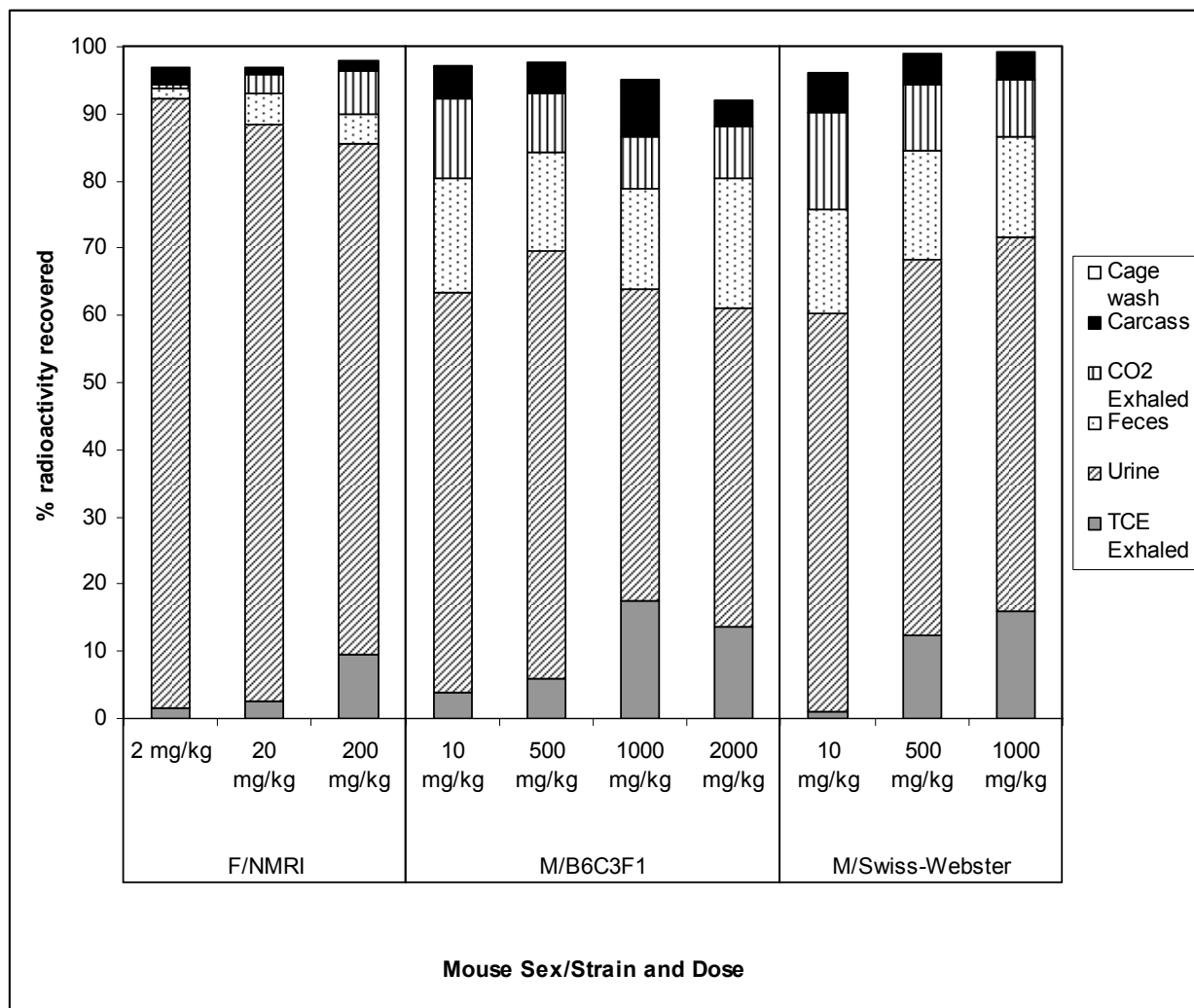
1 TCE is generally considered to reside primarily in its metabolites rather than in the parent
2 compound itself.

4 **3.3.2. Extent of Metabolism**

5 TCE is extensively metabolized in animals and humans. The most comprehensive
6 mass-balance studies are in mice and rats (Dekant et al., 1984; Dekant et al., 1986a, b; Green and
7 Prout, 1985; Prout et al., 1985) in which [¹⁴C]TCE is administered by oral gavage at doses of 2
8 to 2,000 mg/kg, the data from which are summarized in Figure 3-2 and Figure 3-3. In both mice
9 and rats, regardless of sex and strain, there is a general trend of increasing exhalation of
10 unchanged TCE with dose, suggesting saturation of a metabolic pathway. The increase is
11 smaller in mice (from 1–6% to 10–18%) than in rats (from 1–3% to 43–78%), suggesting
12 greater overall metabolic capacity in mice. The dose at which apparent saturation occurs appears
13 to be more sex- or strain-dependent in mice than in rats. In particular, the marked increase in
14 exhaled TCE occurred between 20 and 200 mg/kg in female NMRI mice, between 500 and
15 1,000 mg/kg in B6C3F1 mice, and between 10 and 500 mg/kg in male Swiss-Webster mice.
16 However, because only one study is available in each strain, interlot or interindividual variability
17 might also contribute to the observed differences. In rats, all three strains tested showed marked
18 increase in unchanged TCE exhaled between 20 and 200 mg/kg or 10 and 500 mg/kg.
19 Recovered urine, the other major source of excretion, had mainly trichloroacetic acid (TCA),
20 trichloroethanol (TCOH), and trichloroethanol-glucuronide conjugate (TCOG), but revealed no
21 detectable TCE. The source of radioactivity in feces was not analyzed, but it is presumed not to
22 include substantial TCE given the complete absorption expected from the corn oil vehicle.
23 Therefore, at all doses tested in mice, and at doses <200 mg/kg in rats, the majority of orally
24 administered TCE is metabolized. Pretreatment of rats with P450 inducers prior to a 200 mg/kg
25 dose did not change the pattern of recovery, but it did increase the amount recovered in urine by
26 10–15%, with a corresponding decrease in the amount of exhaled unchanged TCE (Dekant et al.,
27 1986a).

This document is a draft for review purposes only and does not constitute Agency policy.

1



2

3

4

Figure 3-2. Disposition of [¹⁴C]TCE administered by oral gavage in mice (Dekant et al., 1984, 1986a; Green and Prout, 1985; Prout et al., 1985).

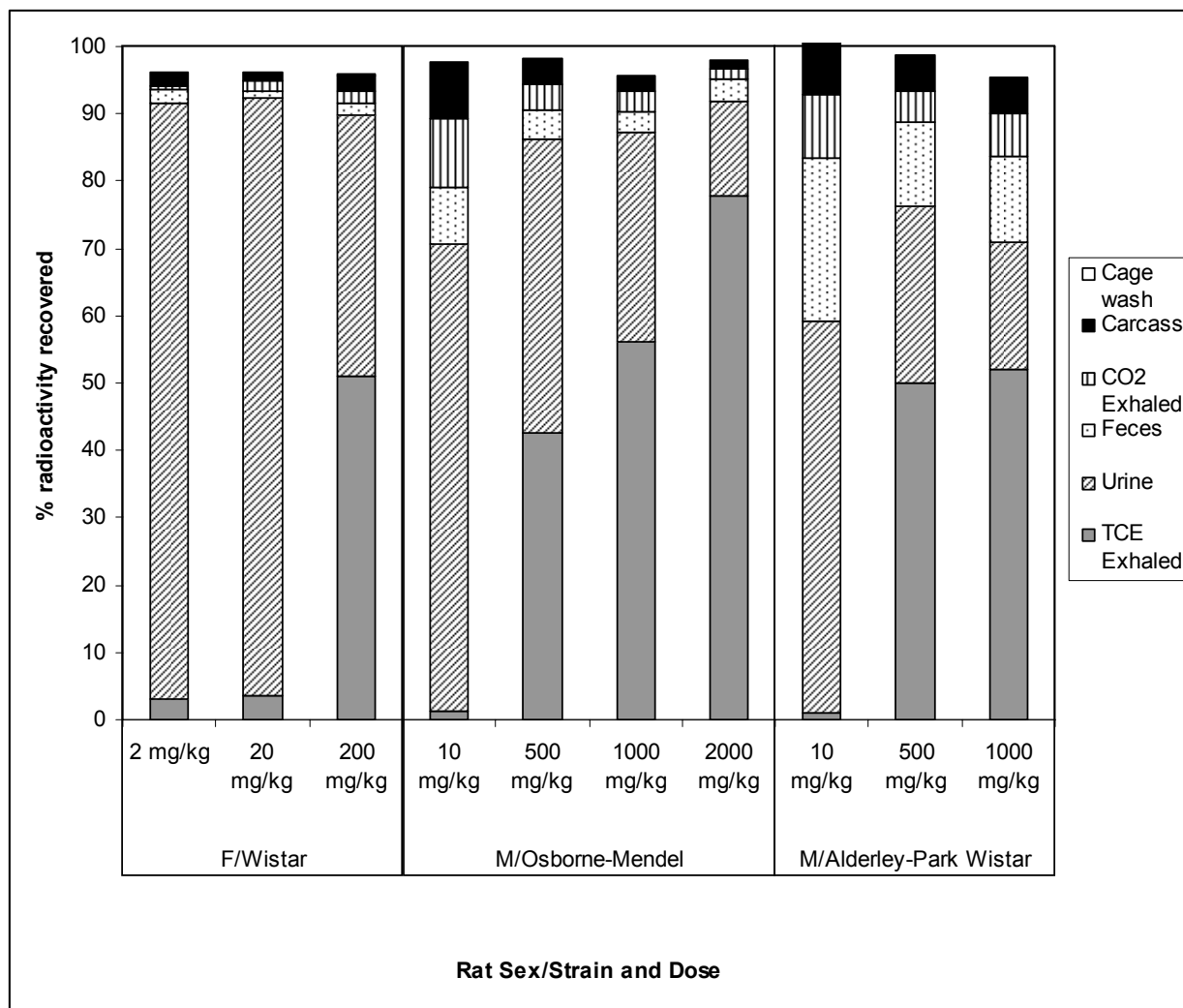


Figure 3-3. Disposition of [¹⁴C]TCE administered by oral gavage in rats (Dekant et al., 1984, 1986a; Green and Prout, 1985; Prout et al., 1985).

Comprehensive mass balance studies are not available in humans, but several studies have measured or estimated recovery of TCE in exhaled breath and/or TCA and TCOH in urine following controlled inhalation exposures to TCE (Monster et al., 1976; Opdam, 1989; Soucek and Vlachova, 1960). Opdam (1989) only measured exhaled breath, and estimated that, on average, 15–20% of TCE uptake (retained dose) was exhaled after exposure to 5.8–38 ppm for 29–62 minutes. Soucek and Vlachova (1960) and Bartonicek (1962) did not measure exhaled breath but did report 69–73% of the retained dose excreted in urine as TCA and TCOH following exposure to 93–194 ppm (500–1,043 mg/m³) for 5 hours. Soucek and Vlachova (1960) additionally reported 4% of the retained dose excreted in urine as monochloroacetic acid

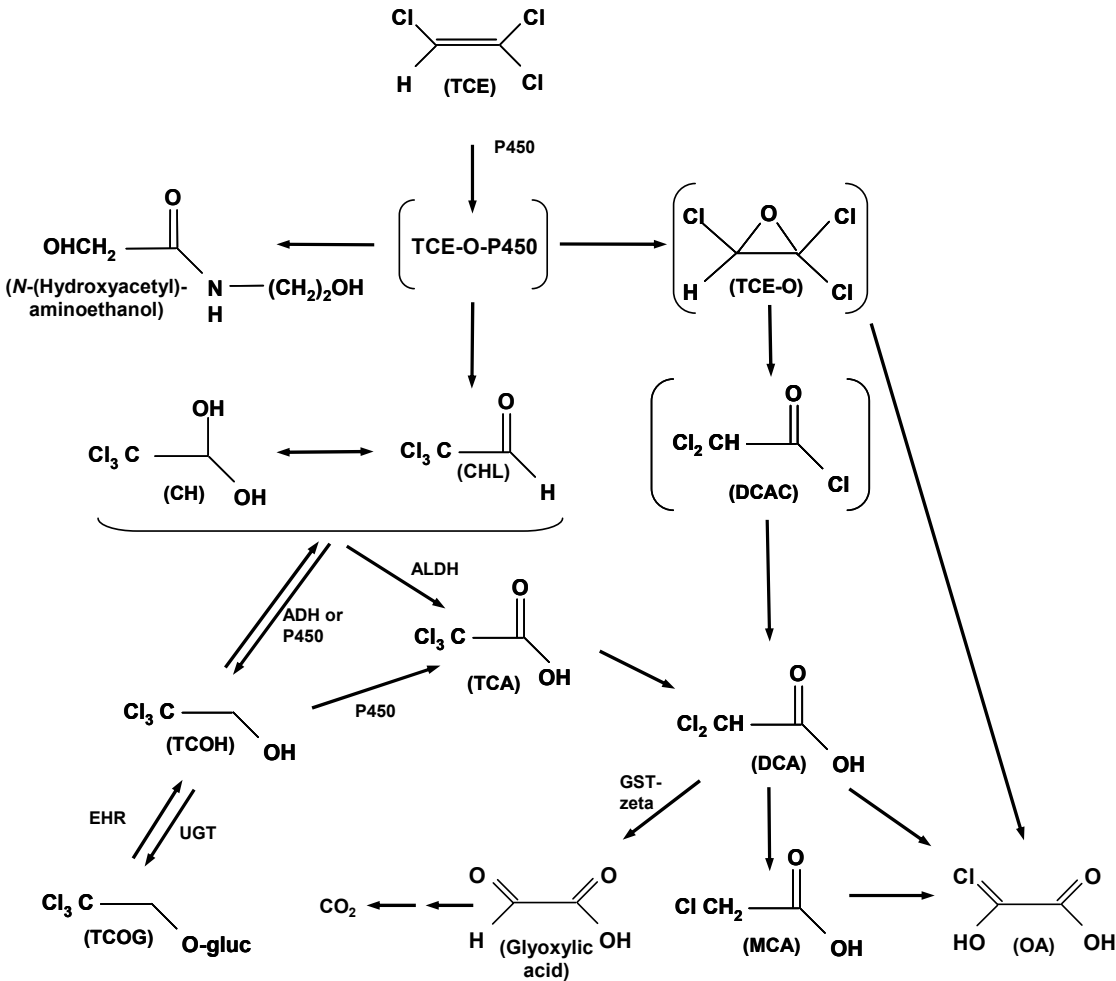
1 (MCA). Monster et al. (1976) reported that an average of 10% of the retained TCE dose was
2 eliminated unchanged following 6 hour exposures to 70–140 ppm (376–752 mg/m³) TCE, along
3 with an average of 57% of the retained dose excreted in urine as TCA and free or conjugated
4 TCOH. The differences among these studies may reflect a combination of interindividual
5 variability and errors due to the difficulty in precisely estimating dose in inhalation studies, but
6 in all cases less than 20% of the retained dose was exhaled unchanged and greater than 50% was
7 excreted in urine as TCA and TCOH. Therefore, it is clear that TCE is extensively metabolized
8 in humans. Unlike the rodent studies, no saturation was evident in any of these human recovery
9 studies even though the metabolic capacity may not have been saturated at the exposure levels
10 that were tested.

11 12 **3.3.3. Pathways of Metabolism**

13 As mentioned in Section 3.3.1, TCE metabolism in animals and humans has been
14 observed to occur via two major pathways: P450-mediated oxidation and GSH conjugation.
15 Products of the initial oxidation or conjugation step are further metabolized to a number of other
16 metabolites. For P450 oxidation, all steps of metabolism occur primarily in the liver, although
17 limited oxidation of TCE has been observed in the lungs of mice, as discussed below. The GSH
18 conjugation pathway also begins predominantly in the liver, but toxicologically significant
19 metabolic steps occur extrahepatically—particularly in the kidney (Lash et al., 1995, 1998,
20 1999b, 2006). The mass-balance studies cited above found that at exposures below the onset of
21 saturation, >50% of TCE intake is excreted in urine as oxidative metabolites (primarily as TCA
22 and TCOH), so TCE oxidation is generally greater than TCE conjugation. This is discussed in
23 detail in Section 3.3.3.3.

24 25 **3.3.3.1. Cytochrome P450-Dependent Oxidation**

26 Oxidative metabolism by the cytochrome P450, or CYP-dependent, pathway is
27 quantitatively the major route of TCE biotransformation (U.S. Environmental Protection Agency
28 [U.S. EPA], 1985; IARC, 1995; Lash et al., 2000a, b). The pathway is operative in humans and
29 rodents and leads to several metabolic products, some of which are known to cause toxicity and
30 carcinogenicity (U.S. EPA, 1985; IARC, 1995). Although several of the metabolites in this
31 pathway have been clearly identified, others are speculative or questionable. Figure 3-4 depicts
32 the overall scheme of TCE P450 metabolism.



2
3
4
5
6
7
8
9
10
11
12
13
14
15
16
Figure 3-4. Scheme for the oxidative metabolism of TCE.

Adapted from: Lash et al. (2000a, b), Clewell et al. (2000), Cummings et al. (2001), Forkert et al. (2006), and Tong et al. (1998).

In brief, TCE oxidation via P450, primarily CYP2E1 (Guengerich et al., 1991), yields an oxygenated TCE-P450 intermediate and TCE oxide. The TCE-P450 complex is a transition state that goes on to form chloral. In the presence of water, chloral rapidly equilibrates with chloral hydrate (CH), which undergoes reduction and oxidation by alcohol dehydrogenase and aldehyde dehydrogenase or aldehyde oxidase to form TCOH and TCA, respectively (Miller and Guengerich 1983; Green and Prout, 1985; Dekant et al., 1986a). Table 3-13 summarizes available *in vitro* measurements of TCE oxidation, as assessed by the formation of CH, TCOH, and TCA. Glucuronidation of TCOH forms TCOG, which is readily excreted in urine.

1 Alternatively, TCOG can be excreted in bile and passed to the small intestine where it is
2 hydrolyzed back to TCOH and reabsorbed (Bull, 2000). TCA is poorly metabolized but may
3 undergo dechlorination to form dichloroacetic acid (DCA). However, TCA is predominantly
4 excreted in urine, albeit at a relatively slow rate as compared to TCOG. Like the TCE-P450
5 complex, TCE oxide also seems to be a transient metabolite. Recent data suggest that it is
6 transformed to dichloroacetyl chloride, which subsequently decomposes to form DCA (Cai and
7 Guengerich, 1999). As shown in Figure 3-4, several other metabolites, including oxalic acid and
8 *N*-(hydroxyacetyl) aminoethanol, may form from the TCE oxide or the TCE-O-P450
9 intermediate and have been detected in the urine of rodents and humans following TCE
10 exposure. Pulmonary excretion of CO₂ has been identified in exhaled breath from rodents
11 exposed to ¹⁴C-labeled TCE and is thought to arise from metabolism of DCA. The following
12 sections provide details as to pathways of TCE oxidation, including discussion of inter- and
13 intraspecies differences in metabolism.

14
15 **3.3.3.1.1. Formation of trichloroethylene oxide.** In previous studies of halogenated alkene
16 metabolism, the initial step was the generation of a reactive epoxides (Anders and Jakobson,
17 1985). Early studies in anesthetized human patients (Powell, 1945), dogs (Butler, 1949), and
18 later reviews (e.g., Goeptar et al., 1995) suggest that the TCE epoxide may be the initial reaction
19 product of TCE oxidation.

20 Epoxides can form acyl chlorides or aldehydes, which can then form aldehydes,
21 carboxylic acids, or alcohols, respectively. Thus, the appearance of CH, TCA, and TCOH as the
22 primary metabolites was considered consistent with the oxidation of TCE to the epoxide
23 intermediate (Powell, 1945; Butler, 1949). Following *in vivo* exposures to 1,1-dichloroethylene,
24 a halocarbon very similar in structure to TCE, mouse liver cytosol and microsomes and lung
25 Clara cells exhibited extensive P450-mediated epoxide formation (Forkert, 1999a, b; Forkert et
26 al., 1999; Dowsley et al., 1996). Indeed, TCE oxide inhibits purified CYP2E1 activity (Cai and
27 Guengerich, 2001) similarly to TCE inhibition of CYP2E1 in human liver microsomes
28 (Lipscomb et al., 1997).

1
2
3

Table 3-13. *In vitro* TCE oxidative metabolism in hepatocytes and microsomal fractions

<i>In vitro</i> system	K_M	V_{MAX}	$1,000 \times V_{MAX}/K_M$	Source
	μM in medium	nmol TCE oxidized/min/mg MSP* or 10^6 hepatocytes		
Human hepatocytes	210 \pm 159 (45–403)	0.268 \pm 0.215 (0.101–0.691)	2.45 \pm 2.28 (0.46–5.57)	Lipscomb et al., 1998a
Human liver microsomal protein	16.7 \pm 2.45 (13.3–19.7)	1.246 \pm 0.805 (0.490–3.309)	74.1 \pm 44.1 (38.9–176)	Lipscomb et al., 1997 (Low K_M)
	30.9 \pm 3.3 (27.0–36.3)	1.442 \pm 0.464 (0.890–2.353)	47.0 \pm 16.0 (30.1–81.4)	Lipscomb et al., 1997 (Mid K_M)
	51.1 \pm 3.77 (46.7–55.7)	2.773 \pm 0.577 (2.078–3.455)	54.9 \pm 14.1 (37.3–69.1)	Lipscomb et al., 1997 (High K_M)
	24.6	1.44	58.5	Lipscomb et al., 1998b (pooled)
	12 \pm 3 (9–14)	0.52 \pm 0.17 (0.37–0.79)	48 \pm 23 (26–79)	Elfarra et al., 1998 (males, high affinity)
	26 \pm 17 (13–45)	0.33 \pm 0.15 (0.19–0.48)	15 \pm 10 (11–29)	Elfarra et al., 1998 (females, high affinity)
Rat liver microsomal protein	55.5	4.826	87.0	Lipscomb et al., 1998b (pooled)
	72 \pm 82	0.96 \pm 0.65	24 \pm 21	Elfarra et al., 1998 (males, high affinity)
	42 \pm 21	2.91 \pm 0.71	80 \pm 34	Elfarra et al., 1998 (females, high affinity)
Rat kidney microsomal protein	940	0.154	0.164	Cummings et al., 2001
Mouse liver microsomal protein	35.4	5.425	153	Lipscomb et al., 1998b (pooled)
	378 \pm 414	8.6 \pm 4.5	42 \pm 29	Elfarra et al., 1998 (males)
	161 \pm 29	26.06 \pm 7.29	163 \pm 37	Elfarra et al., 1998 (females)

4
5
6
7
8
9
10

* MSP = Microsomal protein.

Notes: Results presented as mean \pm standard deviation (minimum–maximum). K_M for human hepatocytes converted from ppm in headspace to μM in medium using reported hepatocyte:air partition coefficient (Lipscomb et al., 1998a).

1 or the other of these enzymes. For instance, Ni et al. (1996) reported that CYP2E1 expression
2 was necessary for metabolism of CH to mutagenic metabolites in a human lymphoblastoid cell
3 line, suggesting a role for CYP2E1. Furthermore, Ni et al. (1996) reported that cotreatment of
4 mice with CH and pyrazole, a specific CYP2E1 inducer, resulted in enhanced liver microsomal
5 lipid peroxidation, while treatment with DPEA, an inhibitor of CYP2E1, suppressed lipid
6 peroxidation, suggesting CYP2E1 as a primary enzyme for CH metabolism in this system.
7 Lipscomb et al. (1996) suggested that two enzymes are likely responsible for CH reduction to
8 TCOH based on observation of bi-phasic metabolism for this pathway in mouse liver
9 microsomes. This behavior has also been observed in mouse liver cytosol, but was not observed
10 in rat or human liver microsomes. Moreover, CH metabolism to TCOH increased significantly
11 both in the presence of NADH in the 700× g supernatant of mouse, rat, and human liver
12 homogenate as well as with the addition of NADPH in human samples, suggesting two enzymes
13 may be involved (Lipscomb et al., 1996).

14 TCOH formed from CH is available for oxidation to TCA (see below) or glucuronidation
15 via UDP-glucuronyltransferase to TCOG, which is excreted in urine or in bile (Stenner et al.,
16 1997). Biliary TCOG is hydrolyzed in the gut and available for reabsorption to the liver as
17 TCOH, where it can be glucuronidated again or metabolized to TCA. This enterohepatic
18 circulation appears to play a significant role in the generation of TCA from TCOH and in the
19 observed lengthy residence time of this metabolite, compared to TCE. Using jugular-, duodenal-
20 , and bile duct-cannulated rats, Stenner et al. (1997) showed that enterohepatic circulation of
21 TCOH from the gut back to the liver and subsequent oxidation to TCA was responsible for 76%
22 of TCA measured in the systemic blood.

23 Both CH and TCOH can be oxidized to TCA, and has been demonstrated *in vivo* in mice
24 (Larson and Bull, 1992a; Dekant et al., 1986a; Green and Prout, 1985), rats (Stenner et al., 1997;
25 Pravecek et al., 1996; Templin et al., 1995b; Larson and Bull, 1992a; Dekant et al., 1986a; Green
26 and Prout, 1985), dogs (Templin et al., 1995a), and humans (Sellers et al., 1978). Urinary
27 metabolite data in mice and rats exposed to 200 mg/kg TCE (Larson and Bull, 1992a;
28 Dekant et al., 1986a) and humans following oral CH exposure (Sellers et al., 1978) show greater
29 TCOH production relative to TCA production. However, because of the much longer urinary
30 half-life in humans of TCA relative to TCOH, the total amount of TCA excreted may be similar
31 to TCOH (Monster et al., 1976; Fisher et al., 1998). This is thought to be primarily due to
32 conversion of TCOH to TCA, either directly or via “back-conversion” of TCOH to CH, rather
33 than due to the initial formation of TCA from CH (Marshall and Owens, 1955).

34 *In vitro* data are also consistent with CH oxidation to TCA being much less than CH
35 reduction to TCOH. For instance, Lipscomb et al. (1996) reported 1,832-fold differences in K_M

1 values and 10–195-fold differences in clearance efficiency (V_{MAX}/K_M) for TCOH and TCA in all
 2 three species (see Table 3-14). Clearance efficiency of CH to TCA in mice is very similar to
 3 humans but is 13-fold higher than rats. Interestingly, Bronley-DeLancey et al. (2006) recently
 4 reported that similar amounts of TCOH and TCA were generated from CH using cryopreserved
 5 human hepatocytes. However, the intersample variation was extremely high, with measured
 6 V_{MAX} ranging from 8-fold greater TCOH to 5-fold greater TCA and clearance (V_{MAX}/K_M)
 7 ranging from 13-fold greater TCOH to 17-fold greater TCA. Moreover, because a comparison
 8 with fresh hepatocytes or microsomal protein was not made, it is not clear to what extent these
 9 differences are due to population heterogeneity or experimental procedures.

10
 11 **Table 3-14. *In vitro* kinetics of trichloroethanol and trichloroacetic acid**
 12 **formation from chloral hydrate in rat, mouse, and human liver homogenates**
 13

Species	TCOH			TCA		
	K_m^a	V_{max}^b	V_{MAX}/K_m^c	K_m^a	V_{max}^b	V_{MAX}/K_m^c
Rat	0.52	24.3	46.7	16.4	4	0.24
Mouse ^d	0.19	11.3	59.5	3.5	10.6	3.0
High affinity	0.12	6.3	52.5	na ^e	na	na
Low affinity	0.51	6.1	12.0	na	na	na
Human	1.34	34.7	25.9	23.9	65.2	2.7

14 ^a K_m presented as mM CH in solution.

15 ^b V_{max} presented as nmoles/mg supernatant protein/min.

16 ^cClearance efficiency represented by V_{MAX}/K_M .

17 ^dMouse kinetic parameters derived for observations over the entire range of CH exposure as well as discrete, bi-
 18 phasic regions for CH concentrations below (high affinity) and above (low affinity) 1.0 mM.

19 ^ena = not applicable.
 20

21
 22 Source: Lipscomb et al. (1996).
 23
 24

25 The metabolism of CH to TCA and TCOH involves several enzymes including CYP2E1,
 26 alcohol dehydrogenase, and aldehyde dehydrogenase enzymes (Guengerich et al., 1991; Miller
 27 and Guengerich, 1983; Ni et al., 1996; Shultz and Weiner, 1979; Wang et al., 1993). Because
 28 these enzymes have preferred cofactors (NADPH, NADH, and NAD⁺), cellular cofactor ratio
 29 and redox status of the liver may have an impact on the preferred pathway
 30 (Kawamoto et al., 1988; Lipscomb et al., 1996).
 31

1 **3.3.3.1.3. Formation of dichloroacetic acid (DCA) and other products.** As discussed above,
2 DCA could hypothetically be formed via multiple pathways. The work reviewed by Guengerich
3 (2004) has suggested that one source of DCA may be through a TCE oxide intermediary. Miller
4 and Guengerich (1983) report evidence of formation of the epoxide, and Cai and Guengerich
5 (1999) report that a significant amount (about 35%) of DCA is formed from aqueous
6 decomposition of TCE oxide via hydrolysis in an almost pH-independent manner. Because this
7 reaction forming DCA from TCE oxide is a chemical process rather than a process mediated by
8 enzymes, and because evidence suggests that some epoxide was formed from TCE oxidation,
9 Guengerich (2004) notes that DCA would be an expected product of TCE oxidation (see also
10 Yoshioka et al. [2002]). Alternatively, dechlorination of TCA and oxidation of TCOH have been
11 proposed as sources of DCA (Lash et al., 2000a). Merdink et al. (2000) investigated
12 dechlorination of TCA and reported trapping a DCA radical with the spin-trapping agent phenyl-
13 tert-butyl nitroxide, identified by gas chromatography/mass spectroscopy, in both a chemical
14 Fenton system and rodent microsomal incubations with TCA as substrate. Dose-dependent
15 catalysis of TCA to DCA was observed in cultured microflora from B6C3F1 mice (Moghaddam
16 et al., 1996). However, while antibiotic-treated mice lost the ability to produce DCA in the gut,
17 plasma DCA levels were unaffected by antibiotic treatment, suggesting that the primary site of
18 murine DCA production is other than the gut (Moghaddam et al., 1997).

19 However, direct evidence for DCA formation from TCE exposure remains equivocal. *In*
20 *vitro* studies in human and animal systems have demonstrated very little DCA production in the
21 liver (James et al., 1997). *In vivo*, DCA was detected in the blood of mice (Templin et al., 1993;
22 Larson and Bull, 1992a) and humans (Fisher et al., 1998) and in the urine of rats and mice
23 (Larson and Bull, 1992b) exposed to TCE by aqueous oral gavage. However, the use of strong
24 acids in the analytical methodology produces *ex vivo* conversion of TCA to DCA in mouse blood
25 (Ketcha et al., 1996). This method may have resulted in the appearance of DCA as an artifact in
26 human plasma (Fisher et al., 1998) and mouse blood *in vivo* (Templin et al., 1995b). Evidence
27 for the artifact is suggested by DCA AUCs that were larger than would be expected from the
28 available TCA (Templin et al., 1995a). After the discovery of these analytical issues, Merdink et
29 al. (1998) reevaluated the formation of DCA from TCE, TCOH, and TCA in mice, with
30 particular focus on the hypothesis that DCA is formed from dechlorination of TCA. They were
31 unable to detect blood DCA in naive mice after administration of TCE, TCOH, or TCA. Low
32 levels of DCA were detected in the blood of children administered therapeutic doses of CH
33 (Henderson et al., 1997), suggesting TCA or TCOH as the source of DCA. Oral TCE exposure
34 in rats and dogs failed to produce detectable levels of DCA (Templin et al., 1995a).

This document is a draft for review purposes only and does not constitute Agency policy.

1 Another difficulty in assessing the formation of DCA is its rapid metabolism at low
 2 exposure levels. Degradation of DCA is mediated by glutathione-S-transferase (GST)-zeta
 3 (Saghir and Schultz, 2002; Tong et al., 1998), apparently occurring primarily in the hepatic
 4 cytosol. DCA metabolism results in suicide inhibition of the enzyme, evidenced by decreased
 5 DCA metabolism in DCA-treated animals (Gonzalez-Leon et al., 1999) and humans (Shroads et
 6 al., 2008) and loss of DCA metabolic activity and enzymatic protein in liver samples from
 7 treated animals (Schultz et al., 2002). This effect has been noted in young mice exposed to DCA
 8 in drinking water at doses approximating 120 mg/kg/d (Schultz et al., 2002). The experimental
 9 data and pharmacokinetic model simulations of several investigators (Jia et al., 2006; Keys et al.,
 10 2004; Li et al., 2008; Merdink et al., 1998; Shroads et al., 2008) suggest that several factors
 11 prevent the accumulation of measurable amounts of DCA: (1) its formation as a short-lived
 12 intermediate metabolite, and (2) its rapid elimination relative to its formation from TCA. While
 13 DCA elimination rates appear approximately one order of magnitude higher in rats and mice than
 14 in humans (James et al., 1997) (see Table 3-15), they still may be rapid enough so that even if
 15 DCA were formed in humans, it would be metabolized too quickly to appear in detectable
 16 quantities in blood.

17
 18 **Table 3-15. *In vitro* kinetics of DCA metabolism in hepatic cytosol**
 19 **of mice, rats, and humans**
 20

Species	V _{MAX} (nmol/min/mg protein)	K _M (μM)	V _{MAX} /K _M
Mouse	13.1	350	37.4
Rat	11.6	280	41.4
Human	0.37	71	5.2

21 Source: James et al. (1997).
 22
 23
 24

25 A number of other metabolites, such as oxalic acid, MCA, glycolic acid, and glyoxylic
 26 acid, are formed from DCA (Lash et al., 2000a; Saghir and Schultz, 2002). Unlike other
 27 oxidative metabolites of TCE, DCA appears to be metabolized primarily via hepatic cytosolic
 28 proteins. Since P450 activity resides almost exclusively in the microsomal and mitochondrial
 29 cell fractions, DCA metabolism appears to be independent of P450. Rodent microsomal and
 30 mitochondrial metabolism of DCA was measured to be ≤10% of cytosolic metabolism
 31 (Lipscomb et al., 1995). DCA in the liver cytosol from rats and humans is transformed to
 32 glyoxylic acid via a GSH-dependent pathway (James et al., 1997). In rats, the K_M for GSH was

This document is a draft for review purposes only and does not constitute Agency policy.

1 0.075 mM with a V_{MAX} for glyoxylic acid formation of 1.7 nmol/mg protein/minute. While this
2 pathway may not involve GST (as evidenced by very low GST activity in this study), Tong et al.
3 (1998) showed GST-zeta, purified from rat liver, to be involved in metabolizing DCA to
4 glyoxylic acid, with a V_{MAX} of 1,334 nmol/mg protein/minute and K_M of 71.4 μ M for glyoxylic
5 acid formation and a GSH K_M of 59 μ M.

6
7 **3.3.3.1.4. Tissue distribution of oxidative metabolism and metabolites.** Oxidative metabolism
8 of TCE, irrespective of the route of administration, occurs predominantly in the liver, but TCE
9 metabolism via the P450 (CYP) system also occurs at other sites because CYP isoforms are
10 present to some degree in most tissues of the body. For example, both the lung and kidneys
11 exhibit cytochrome P450 enzyme activities (Green et al., 1997a, b; Forkert et al., 2005;
12 Cummings et al., 2001). Green et al. (1997b) detected TCE oxidation to chloral in microsomal
13 fractions of whole-lung homogenates from mice, rats, and humans, with the activity in mice the
14 greatest and in humans the least. The rates were slower than in the liver (which also has a higher
15 microsomal protein content as well as greater tissue mass) by 1.8-, 10-, and >10-fold in mice,
16 rats, and humans, respectively. While qualitatively informative, these rates were determined at a
17 single concentration of about 1 mM TCE. A full kinetic analysis was not performed, so
18 clearance and maximal rates of metabolism could not be determined. With the kidney,
19 Cummings et al. (2001) performed a full kinetic analysis using kidney microsomes, and found
20 clearance rates (V_{MAX}/K_M) for oxidation were more than 100-fold smaller than average rates that
21 were found in the liver (see Table 3-13). In human kidney microsomes, Amet et al. (1997)
22 reported that CYP2E1 activity was weak and near detection limits, with no CYP2E1 detectable
23 using immunoblot analysis. Cummings and Lash (2000) reported detecting oxidation of TCE in
24 only one of 4 kidney microsome samples, and only at the highest tested concentration of 2 mM,
25 with a rate of 0.13 nmol/minute/mg protein. This rate contrasts with the V_{MAX} values for human
26 liver microsomal protein of 0.19–3.5 nmol/minute/mg protein reported in various experiments
27 (see Table 3-13, above). Extrahepatic oxidation of TCE may play an important role for
28 generation of toxic metabolites in situ. The roles of local metabolism in kidney and lung toxicity
29 are discussed in detail in Sections 4.4 and 4.7, respectively.

30 With respect to further metabolism beyond oxidation of TCE, CH has been shown to be
31 metabolized to TCA and TCOH in lysed whole blood of mice and rats and fractionated human
32 blood (Lipscomb et al., 1996) (see Table 3-16). TCOH production is similar in mice and rats and
33 is approximately 2-fold higher in rodents than in human blood. However, TCA formation in
34 human blood is 2- or 3-fold higher than in mouse or rat blood, respectively. In human blood,
35 TCA is formed only in the erythrocytes. TCOH formation occurs in both plasma and

1 erythrocytes, but 4-fold more TCOH is found in plasma than in an equal volume of packed
 2 erythrocytes. While blood metabolism of CH may contribute further to its low circulating levels
 3 *in vivo.*, the metabolic capacity of blood (and kidney) may be substantially lower than liver.
 4 Regardless, any CH reaching the blood may be rapidly metabolized to TCA and TCOH.
 5

6 **Table 3-16. TCOH and TCA formed from CH *in vitro* in lysed whole blood**
 7 **of rats and mice or fractionated blood of humans (nmoles formed in 400 μ L**
 8 **samples over 30 minutes)**
 9

	Rat	Mouse	Human	
			Erythrocytes	Plasma
TCOH	45.4 \pm 4.9	46.7 \pm 1.0	15.7 \pm 1.4	4.48 \pm 0.2
TCA	0.14 \pm 0.2	0.21 \pm 0.3	0.42 \pm 0.0	not detected

10
 11 Source: Lipscomb et al. (1996).
 12
 13

14 DCA and TCA are known to bind to plasma proteins. Schultz et al. (1999) measured
 15 DCA binding in rats at a single concentration of about 100 μ M and found a binding fraction of
 16 less than 10%. However, these data are not greatly informative for TCE exposure in which DCA
 17 levels are significantly lower, and limitation to a single concentration precludes fitting to
 18 standard binding equations from which the binding at low concentrations could be extrapolated.
 19 Templin et al. (1993, 1995a, b), Schultz et al. (1999), Lumpkin et al. (2003), and Yu et al. (2003)
 20 all measured TCA binding in various species and at various concentration ranges. Of these,
 21 Templin et al. (1995a, b) and Lumpkin et al. (2003) measured levels in humans, mice, and rats.
 22 Lumpkin et al. (2003) studied the widest concentration range, spanning reported TCA plasma
 23 concentrations from experimental studies. Table 3-17 shows derived binding parameters.
 24 However, these data are not entirely consistent among researchers; 2- to 5-fold differences in
 25 B_{MAX} and K_d are noted in some cases, although some differences existed in the rodent strains and
 26 experimental protocols used. In general, however, at lower concentrations, the bound fraction
 27 appears greater in humans than in rats and mice. Typical human TCE exposures, even in
 28 controlled experiments with volunteers, lead to TCA blood concentrations well below the
 29 reported K_d (see Table 3-17, below), so the TCA binding fraction should be relatively constant.
 30 However, in rats and mice, experimental exposures may lead to peak concentrations similar to,
 31 or above, the reported K_d (e.g., Templin et al., 1993; Yu et al., 2000), meaning that the bound
 32 fraction should temporarily decrease following such exposures.
 33

1
2

Table 3-17. Reported TCA plasma binding parameters

	A	B _{MAX} (μM)	K _d (μM)	A+ B _{MAX} /K _d	Concentration range (μM bound+free)
Human					
Templin et al., 1995a	–	1,020	190	5.37	3–1,224
Lumpkin et al., 2003	–	708.9	174.6	4.06	0.06–3,065
Rat					
Templin et al., 1995a	–	540	400	1.35	3–1,224
Yu et al., 2000	0.602	312	136	2.90	3.8–1,530
Lumpkin et al., 2003	–	283.3	383.6	0.739	0.06–3,065
Mouse					
Templin et al., 1993	–	310	248	1.25	3–1,224
Lumpkin et al., 2003	–	28.7	46.1	0.623	0.06–1,226

3
4
5
6
7
8

Notes: Binding parameters based on the equation $C_{\text{bound}} = A \times C_{\text{free}} + B_{\text{MAX}} \times C_{\text{free}} / (K_d + C_{\text{free}})$, where C_{bound} is the bound concentration, C_{free} is the free concentration, and $A = 0$ for Templin et al. (1993, 1995a) and Lumpkin et al. (2003). The quantity $A + B_{\text{MAX}}/K_d$ is the ratio of bound-to-free at low concentrations.

9
10
11
12
13
14
15
16

Limited data are available on tissue:blood partitioning of the oxidative metabolites CH₂TCA, TCOH and DCA, as shown in Table 3-18. As these chemicals are all water soluble and not lipophilic, it is not surprising that their partition coefficients are close to 1 (within about 2-fold). It should be noted that the TCA tissue:blood partition coefficients reported in Table 3-18 were measured at concentrations 1.6–3.3 M, over 1,000-fold higher than the reported K_d. Therefore, these partition coefficients should reflect the equilibrium between tissue and free blood concentrations. In addition, only one *in vitro* measurement has been reported of blood:plasma concentration ratios for TCA: Schultz et al. (1999) reported a value of 0.76 in rats.

1 **Table 3-18. Partition coefficients for TCE oxidative metabolites**
 2

Species/tissue	Tissue:blood partition coefficient			
	CH	TCA	TCOH	DCA
Human^a				
Kidney	–	0.66	2.15	-
Liver	–	0.66	0.59	-
Lung	–	0.47	0.66	-
Muscle	–	0.52	0.91	-
Mouse^b				
Kidney	0.98	0.74	1.02	0.74
Liver	1.42	1.18	1.3	1.08
Lung	1.65	0.54	0.78	1.23
Muscle	1.35	0.88	1.11	0.37

3
 4 ^a Fisher et al. (1998).

5 ^b Abbas and Fisher (1997).

6 Note: TCA and TCOH partition coefficients have not been reported for rats.
 7
 8

9 **3.3.3.1.5. Species-, sex-, and age-dependent differences of oxidative metabolism.** The ability
 10 to describe species- and sex-dependent variations in TCE metabolism is important for species
 11 extrapolation of bioassay data and identification of human populations that are particularly
 12 susceptible to TCE toxicity. In particular, information on the variation in the initial oxidative
 13 step of CH formation from TCE is desirable, because this is the rate-limiting step in the eventual
 14 formation and distribution of the putative toxic metabolites TCA and DCA (Lipscomb et al.,
 15 1997).

16 Inter- and intraspecies differences in TCE oxidation have been investigated *in vitro* using
 17 cellular or subcellular fractions, primarily of the liver. The available *in vitro* metabolism data on
 18 TCE oxidation in the liver (see Table 3-13) show substantial inter and intraspecies variability.
 19 Across species, microsomal data show that mice apparently have greater capacity (V_{MAX}) than
 20 rat or humans, but the variability within species can be 2- to 10-fold. Part of the explanation may
 21 be related to CYP2E1 content. Although liver P450 content is similar across species, mice and
 22 rats exhibit higher levels of CYP2E1 content (0.85 and 0.89 nmol/mg protein, respectively)
 23 (Nakajima et al., 1993; Davis et al., 2002) than humans (approximately 0.25–0.30 nmol/mg
 24 protein) (Elfarrar et al., 1998; Davis et al., 2002). Thus, the data suggest that rodents would have
 25 a higher capacity than humans to metabolize TCE, but this is difficult to verify *in vivo* because

This document is a draft for review purposes only and does not constitute Agency policy.

1 very high exposure concentrations in humans would be necessary to assess the maximum
2 capacity of TCE oxidation.

3 With respect to the K_M of liver microsomal TCE oxidative metabolism, where K_M is
4 indicative of affinity (the lower the numerical value of K_M , the higher the affinity), the trend
5 appears to be mice and rats have higher K_M values (i.e., lower affinity) than humans, but with
6 substantial overlap due to interindividual variability. Note that, as shown in Table 3-13, the
7 ranking of rat and mouse liver microsomal K_M values between the two reports by Lipscomb et al.
8 (1998b) and Elfarra et al. (1998) is not consistent. However, both studies clearly show that K_M is
9 the lowest (i.e., affinity is highest) in humans. Because clearance at lower concentrations is
10 determined by the ratio V_{MAX} to K_M , the lower apparent K_M in humans may partially offset the
11 lower human V_{MAX} , and lead to similar oxidative clearances in the liver at environmentally
12 relevant doses. However, differences in activity measured *in vitro* may not translate into *in vivo*
13 differences in metabolite production, as the rate of metabolism *in vivo* depends also on the rate of
14 delivery to the tissue via blood flow (e.g., Lipscomb et al., 2003). The interaction of enzyme
15 activity and blood flow is best investigated using PBPK models and is discussed, along with
16 descriptions of *in vivo* data, in Section 3.5.

17 Data on sex- and age-dependence in oxidative TCE metabolism are limited but suggest
18 relatively modest differences in humans and animals. In an extensive evaluation of
19 CYP-dependent activities in human liver microsomal protein and cryopreserved hepatocytes,
20 Parkinson et al. (2004) identified no age or gender-related differences in CYP2E1 activity. In
21 liver microsomes from 23 humans, the K_M values for females was lower than males, but V_{MAX}
22 values were very similar (Lipscomb et al., 1997). Appearance of total trichloro compounds in
23 urine following intraperitoneal dosing with TCE was 28% higher in female rats than in males
24 (Verma and Rana, 2003). The oxidation of TCE in male and female rat liver microsomes was
25 not significantly different; however, pregnancy resulted in a decrease of 27–39% in the rate of
26 CH production in treated microsomes from females (Nakajima et al., 1992b). Formation of CH
27 in liver microsomes in the presence of 0.2 or 5.9 mM TCE exhibited some dependency on age of
28 rats, with formation rates in both sexes of 1.1–1.7 nmol/mg protein/minute in 3-week-old
29 animals and 0.5–1.0 nmol/mg protein/minute in 18-week-old animals (Nakajima et al., 1992b).

30 Fisher et al. (1991) reviewed data available at that time on urinary metabolites to
31 characterize species differences in the amount of urinary metabolism accounted for by TCA (see
32 Table 3-19). They concluded that TCA seemed to represent a higher percentage of urinary
33 metabolites in primates than in other mammalian species, indicating a greater proportion of
34 oxidation leading ultimately to TCA relative to TCOG.

This document is a draft for review purposes only and does not constitute Agency policy.

1 **Table 3-19. Urinary excretion of trichloroacetic acid by various species**
 2 **exposed to trichloroethylene (based on data reviewed in Fisher et al., 1991)**
 3

Species	Percentage of urinary excretion of TCA		Dose route	TCE dose (mg TCE/kg)	References, comments
	Male	Female			
Baboon ^{a,c}	16	—	Intramuscular injection	50	Mueller et al., 1982
Chimpanzee ^a	24	22	Intramuscular injection	50	Mueller et al., 1982
Monkey, Rhesus ^{a,c}	19	—	Intramuscular injection	50	Mueller et al., 1982
Mice, NMRI ^b	—	8–20	Oral intubation	2–200	Dekant et al., 1986a
Mice, B6C3F1 ^a	7–12	—	Oral intubation	10–2,000	Green and Prout, 1985
Rabbit, Japanese White ^{a,c}	0.5	—	Intraperitoneal injection	200	Nomiyama and Nomiyama, 1979
Rat, Wistar ^b	—	14–17	Oral intubation	2–200	Dekant et al., 1986a
Rat, Osborne-Mendel ^a	6–7	—	Oral intubation	10–2,000	Green and Prout, 1985
Rat, Holtzman ^a	7	—	Intraperitoneal injection	10 mg TCE/rat	Nomiyama and Nomiyama, 1979

4
 5 ^aPercentage urinary excretion determined from accumulated amounts of TCOH and TCA in urine 3 to 6 days
 6 postexposure.

7 ^bPercentage urinary excretion determined from accumulated amounts of TCOH, dichloroacetic acid, oxalic acid, and
 8 *N*-(hydroxyacetyl)aminoethanol in urine 3 days postexposure.

9 ^cSex is not specified.

10
 11 Note: Human data tabulated in Fisher et al. (1991) from Nomiyama and Nomiyama (1971) was not included here
 12 because it was relative to urinary excretion of total trichloro-compounds, not as fraction of intake as was the case for
 13 the other data included here.

1 **3.3.3.1.6. CYP isoforms and genetic polymorphisms.** A number of studies have identified
 2 multiple P450 isozymes as having a role in the oxidative metabolism of TCE. These isozymes
 3 include CYP2E1 (Nakajima et al., 1992a, 1990, 1988; Guengerich and Shimada, 1991;
 4 Guengerich et al., 1991), CYP3A4 (Shimada et al., 1994), CYP1A1/2, CYP2C11/6
 5 (Nakajima et al., 1993, 1992a), CYP2F, and CYP2B1 (Forkert et al., 2005). Recent studies in
 6 CYP2E1-knockout mice have shown that in the absence of CYP2E1, mice still have substantial
 7 capacity for TCE oxidation (Kim and Ghanayem, 2006; Forkert et al., 2006). However,
 8 CYP2E1 appears to be the predominant (i.e., higher affinity) isoform involved in oxidizing TCE
 9 (Nakajima et al., 1992a; Guengerich and Shimada, 1991; Guengerich et al., 1991; Forkert et al.,
 10 2005). In rat liver, CYP2E1 catalyzed TCE oxidation more than CYP2C11/6 (Nakajima et al.,
 11 1992a). In rat recombinant-derived P450s, the CYP2E1 had a lower K_M (higher affinity) and
 12 higher V_{MAX}/K_M ratio (intrinsic clearance) than CYP2B1 or CYP2F4 (Forkert et al., 2005).
 13 Interestingly, there was substantial differences in K_M between rat and human CYP2E1s and
 14 between rat CYP2F4 and mouse CYP2F2, suggesting that species-specific isoforms have
 15 different kinetic behavior (see Table 3-20).

16
 17 **Table 3-20. P450 isoform kinetics for metabolism of TCE to CH in human,**
 18 **rat, and mouse recombinant P450s**
 19

Experiment	K_M μM	V_{MAX} pmol/min/pmol P450	V_{MAX}/K_M
Human rCYP2E1	196 ± 40	4 ± 0.2	0.02
Rat rCYP2E1	14 ± 3	11 ± 0.3	0.79
Rat rCYP2B1	131 ± 36	9 ± 0.5	0.07
Rat rCYP2F4	64 ± 9	17 ± 0.5	0.27
Mouse rCYP2F2	114 ± 17	13 ± 0.4	0.11

20
 21 Source: Forkert et al. (2005)
 22
 23

24 The presence of multiple P450 isoforms in human populations affects the variability in
 25 individuals' ability to metabolize TCE. Studies using microsomes from human liver or from
 26 human lymphoblastoid cell lines expressing CYP2E1, CYP1A1, CYP1A2, or CYP3A4 have
 27 shown that CYP2E1 is responsible for greater than 60% of oxidative TCE metabolism
 28 (Lipscomb et al., 1997). Similarities between metabolism of chlorzoxazone (a CYP2E1
 29 substrate) in liver microsomes from 28 individuals (Peter et al., 1990) and TCE metabolism

1 helped identify CYP2E1 as the predominant (high affinity) isoform for TCE oxidation.
 2 Additionally, Lash et al. (2000a) suggested that, at concentrations above the K_M value for
 3 CYP2E1, CYP1A2 and CYP2A4 may also metabolize TCE in humans; however, their
 4 contribution to the overall TCE metabolism was considered low compared to that of CYP2E1.
 5 Given the difference in expression of known TCE-metabolizing P450 isoforms (see Table 3-21)
 6 and the variability in P450-mediated TCE oxidation (Lipscomb et al., 1997), significant
 7 variability may exist in individual human susceptibility to TCE toxicity.

8
 9 **Table 3-21. P450 isoform activities in human liver microsomes exhibiting**
 10 **different affinities for TCE**
 11

Affinity group	CYP isoform activity (pmol/min/mg protein)		
	CYP2E1	CYP1A2	CYP3A4
Low K_M	520 ± 295	241 ± 146	2.7 ± 2.7
Mid K_M	820 ± 372	545 ± 200	2.9 ± 2.8
High K_M	1,317 ± 592	806 ± 442	1.8 ± 1.1

12 Activities of CYP1A2, CYP2E1, and CYP3A4 were measured with phenacetin, chlorzoxazone, and testosterone as
 13 substrates, respectively. Data are means ± standard deviation from 10, 9, and 4 samples for the low-, mid-, and
 14 high- K_M groups, respectively. Only CYP3A4 activities are not significantly different ($p < 0.05$) from one another
 15 by Kruskal-Wallis one-way analysis of variance.
 16 Source: Lash et al. (2000a).
 17
 18
 19

20 Differences in content and/or intrinsic catalytic properties (K_M , V_{MAX}) of specific
 21 enzymes among species, strains, and individuals may play an important role in the observed
 22 differences in TCE metabolism and resulting toxicities. Lipscomb et al. (1997) reported
 23 observing three statistically distinct groups of K_M values for TCE oxidation using human
 24 microsomes. The mean ± standard deviation [SD] (μM TCE) for each of the three groups was
 25 16.7 ± 2.5 ($n = 10$), 30.9 ± 3.3 ($n = 9$), and 51.1 ± 3.8 ($n = 4$). Within each group, there were no
 26 significant differences in sex or ethnicity. However, the overall observed K_M values in female
 27 microsomes ($21.9 \pm 3.5 \mu\text{M}$, $n = 10$) were significantly lower than males ($33.1 \pm 3.5 \mu\text{M}$,
 28 $n = 13$). Interestingly, in human liver microsomes, different groups of individuals with different
 29 affinities for TCE oxidation appeared to also have different activities for other substrates not
 30 only with respect to CYP2E1 but also CYP1A2 (Lash et al., 2000a) (see Table 3-21). Genetic
 31 polymorphisms in humans have been identified in the CYP isozymes thought to be responsible
 32 for TCE metabolism (Pastino et al., 2000), but no data exist correlating these polymorphisms
 33 with enzyme activity. It is relevant to note that repeat polymorphism (Hu et al., 1999) or

This document is a draft for review purposes only and does not constitute Agency policy.

1 polymorphism in the regulatory sequence (McCarver et al., 1998) were not involved in the
2 constitutive expression of human CYP2E1; however, it is unknown if these types of
3 polymorphisms may play a role in the inducibility of the respective gene.

4 Individual susceptibilities to TCE toxicity may also result from variations in enzyme
5 content, either at baseline or due to enzyme induction/inhibition, which can lead to alterations in
6 the amounts of metabolites formed. Certain physiological and pathological conditions or
7 exposure to other chemicals (e.g., ethanol and acetaminophen) can induce, inhibit, or compete
8 for enzymatic activity. Given the well established (or characterized) role of the liver to
9 oxidatively metabolize TCE (by CYP2E1), increasing the CYP2E1 content or activity (e.g., by
10 enzyme induction) may not result in further increases in TCE oxidation. Indeed, Kaneko et al.
11 (1994) reported that enzyme induction by ethanol consumption in humans increased TCE
12 metabolism only at high concentrations (500 ppm, 2,687 mg/m³) in inspired air. However, other
13 interactions between ethanol and the enzymes that oxidatively metabolize TCE metabolites can
14 result in altered metabolic fate of TCE metabolites. In addition, enzyme inhibition or
15 competition can decrease TCE oxidation and subsequently alter the TCE toxic response via, for
16 instance, increasing the proportion undergoing GSH conjugation (Lash et al., 2000a). TCE itself
17 is a competitive inhibitor of CYP2E1 activity (Lipscomb et al., 1997), as shown by reduced
18 *p*-nitrophenol hydroxylase activity in human liver microsomes, and so may alter the toxicity of
19 other chemicals metabolized through that pathway. On the other hand, suicidal CYP heme
20 destruction by the TCE-oxygenated CYP intermediate has also been shown (Miller and
21 Guengerich, 1983).

22 23 **3.3.3.2. Glutathione (GSH) Conjugation Pathway**

24 Historically, the conjugative metabolic pathways have been associated with xenobiotic
25 detoxification. This is true for GSH conjugation of many compounds. However, several
26 halogenated alkanes and alkenes, including TCE, are bioactivated to cytotoxic metabolites by the
27 GSH conjugate processing pathway (mercapturic acid) pathways (Elfarra et al., 1986a, b). In the
28 case of TCE, production of reactive species several steps downstream from the initial GSH
29 conjugation is believed to cause cytotoxicity and carcinogenicity, particularly in the kidney.
30 Since the GSH conjugation pathway is in competition with the P450 oxidative pathway for TCE
31 biotransformation, it is important to understand the role of various factors in determining the flux
32 of TCE through each pathway. Figure 3-5 depicts the present understanding of TCE metabolism
33 via GSH conjugation.

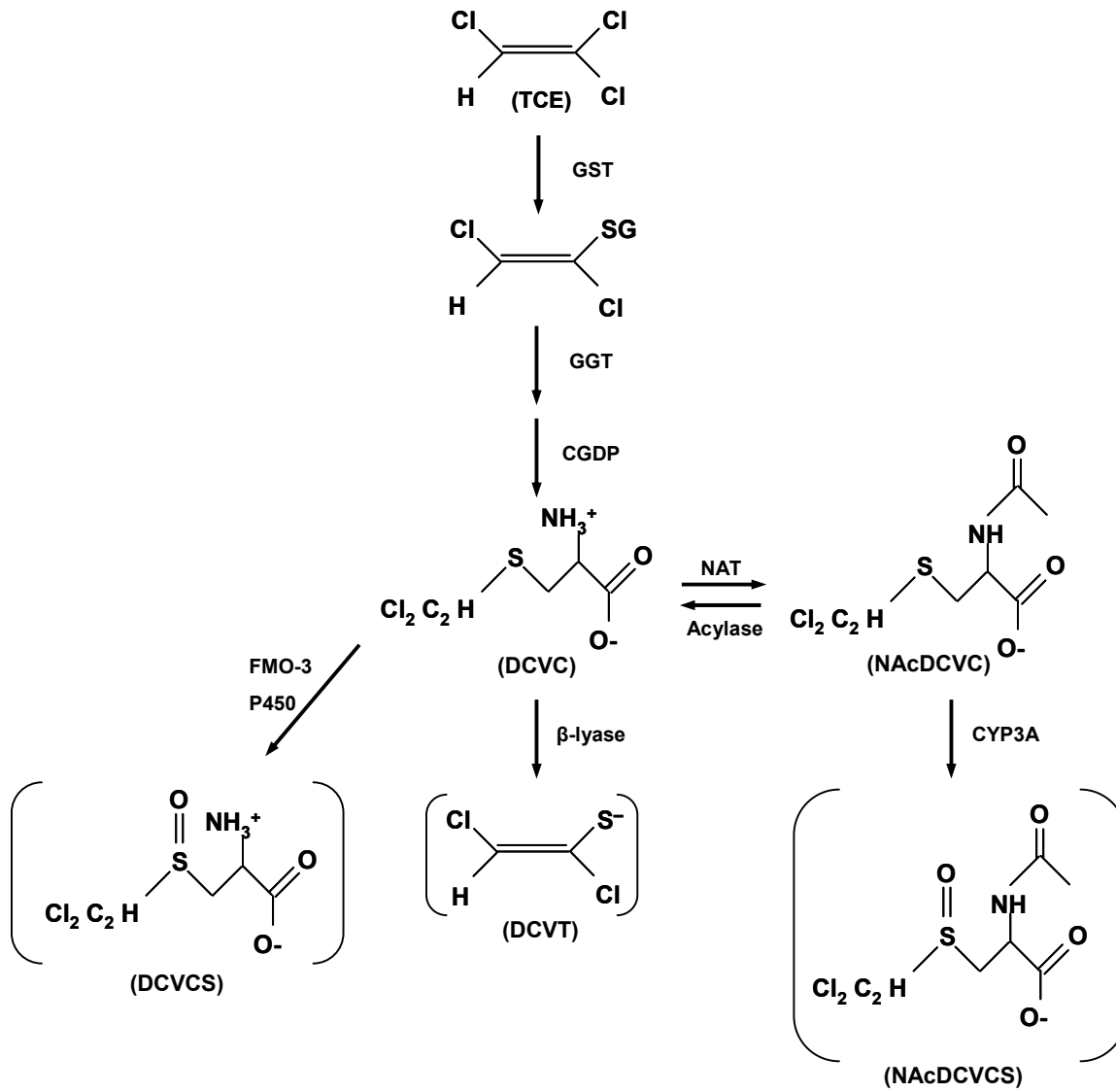


Figure 3-5. Scheme for GSH-dependent metabolism of TCE.

Adapted from: Lash et al. (2000a); Cummings and Lash (2000); NRC (2006).

3.3.3.2.1. Formation of *S*-(1,2-dichlorovinyl)glutathione or *S*-(2,2-dichlorovinyl)glutathione

(*DCVG*). The conjugation of TCE to GSH produces *S*-(1,2-dichlorovinyl)glutathione or its isomer *S*-(2,2-dichlorovinyl)glutathione (*DCVG*). There is some uncertainty as to which GST isoforms mediate TCE conjugation. Lash and colleagues studied TCE conjugation in renal tissue preparations, isolated renal tubule cells from male F344 rats and purified GST alpha-class isoforms 1-1, 1-2 and 2-2 (Cummings et al., 2000a; Cummings and Lash, 2000; Lash et al., 2000b). The results demonstrated high conjugative activity in renal cortex and in proximal

1 tubule cells. Although the isoforms studied had similar V_{MAX} values, the K_M value for GST 2-2
2 was significantly lower than the other forms, indicating that this form will catalyze TCE
3 conjugation at lower (more physiologically relevant) substrate concentrations. In contrast, using
4 purified rat and human enzymes, Hissink et al. (2002) reported *in vitro* activity for DCVG
5 formation only for mu- and pi-class GST isoforms, and none towards alpha-class isoforms;
6 however, the rat mu-class GST 3-3 was several folds more active than the human mu-class
7 GST M1-1. Although GSTs are present in tissues throughout the body, the majority of TCE
8 GSH conjugation is thought to occur in the liver (Lash et al., 2000a). Using *in vitro* studies with
9 renal preparations, it has been demonstrated that GST catalyzed conjugation of TCE is increased
10 following the inhibition of CYP-mediated oxidation (Cummings et al., 2000b).

11 In F344 rats, following gavage doses of 263–1,971 mg/kg TCE in 2 mL corn oil, DCVG
12 was observed in the liver and kidney of females only, in blood of both sexes (Lash et al., 2006),
13 and in bile of males (Dekant et al., 1990). The data from Lash et al. (2006) are difficult to
14 interpret because the time courses seem extremely erratic, even for the oxidative metabolites
15 TCOH and TCA. Moreover, a comparison of blood levels of TCA and TCOH with other studies
16 in rats at similar doses reveals differences of over 1,000-fold in reported concentrations. For
17 instance, at the lowest dose of 263 mg/kg, the peak blood levels of TCE and TCA in male F344
18 rats were 10.5 and 1.6 $\mu\text{g/L}$, respectively (Lash et al., 2006). By contrast, Larson and Bull
19 (1992a) reported peak blood TCE and TCA levels in male Sprague-Dawley rats over 1,000-fold
20 higher—around 10 and 13 mg/L, respectively—following oral doses of 197 mg/kg as a
21 suspension in 1% aqueous Tween 80[®]. The results of Larson and Bull (1992a) are similar to Lee
22 et al. (2000a), who reported peak blood TCE levels of 20–50 mg/L after male Sprague-Dawley
23 rats received oral doses of 144–432 mg/kg in a 5% aqueous Alkamus emulsion (polyethoxylated
24 vegetable oil), and to Stenner et al. (1997), who reported peak blood levels of TCA in male F344
25 rats of about 5 mg/L at a slightly lower TCE oral dose of 100 mg/kg administered to fasted
26 animals in 2% Tween 80[®]. Thus, while useful qualitatively as an indicator of the presence of
27 DCVG in rats, the quantitative reliability of reported concentrations, for metabolites of either
28 oxidation or GSH conjugation, may be questionable.

29 In humans, DCVG was readily detected at in human blood following onset of a 4-hour
30 TCE inhalation exposure to 50 or 100 ppm (269 or 537 mg/m³; Lash et al., 1999a). At 50 ppm,
31 peak blood levels ranged from 2.5 to 30 μM , while at 100 ppm, the mean (\pm SE, $n = 8$) peak
32 blood levels were $46.1 \pm 14.2 \mu\text{M}$ in males and $13.4 \pm 6.6 \mu\text{M}$ in females. Although on average,
33 male subjects had 3-fold higher peak blood levels of DCVG than females, DCVG blood levels
34 in half of the male subjects were similar to or lower than those of female subjects. This suggests
35 a polymorphism in GSH conjugation of TCE rather than a true gender difference (Lash et al.,

1 1999a) as also has been indicated by Hissink et al. (2002) for the human mu-class GST M1-1
 2 enzyme. Interestingly, as shown in Table 3-22, the peak blood levels of DCVG are similar on a
 3 molar basis to peak levels of TCE, TCA, and TCOH in the same subjects, as reported in
 4 Fisher et al. (1998).

5
 6 **Table 3-22. Comparison of peak blood concentrations in humans exposed to**
 7 **100 ppm (537 mg/m³) TCE for 4 hours (Fisher et al., 1998; Lash et al., 1999a)**
 8

Chemical species	Peak blood concentration (mean \pm SD, μ M)	
	Males	Females
TCE	23 \pm 11	14 \pm 4.7
TCA	56 \pm 9.8	59 \pm 12
TCOH	21 \pm 5.0	15 \pm 5.6
DCVG	46.1 \pm 14.2	13.4 \pm 6.6

9
 10
 11 Tables 3-23 and 3-24 summarize DCVG formation from TCE conjugation from *in vitro*
 12 studies of liver and kidney cellular and subcellular fractions in mouse, rat, and human. Tissue-
 13 distribution and species-and gender-differences in DCVG formation are discussed below.

14
 15 **3.3.3.2.2. Formation of S-(1,2-dichlorovinyl) cysteine or S-(2,2-dichlorovinyl) cysteine**
 16 **(DCVC).** The cysteine conjugate, isomers S-(1,2-dichlorovinyl) cysteine (1,2-DCVC) or
 17 S-(2,2-dichlorovinyl) cysteine (2,2-DCVC), is formed from DCVG in a two-step sequence.
 18 DCVG is first converted to the cysteinylglycine conjugate
 19 S-(1,2-dichlorovinyl)-L-cysteinylglycine or its isomer S-(2,2-dichlorovinyl)-L-cysteinylglycine
 20 by γ -glutamyl transpeptidase (GGT) in the renal brush border (Elfarra and Anders, 1984; Lash et
 21 al., 1988).

22 Cysteinylglycine dipeptidases in the renal brush border and basolateral membrane
 23 convert DCVG to DCVC via glycine cleavage (Goeptar et al., 1995; Lash et al., 1998). This
 24 reaction can also occur in the bile or gut, as DCVG excreted into the bile is converted to DCVC
 25 and reabsorbed into the liver where it may undergo further acetylation.

1
2
3

Table 3-23. GSH conjugation of TCE (at 1–2 mM) in liver and kidney cellular fractions in humans, male F344 rats, and male B6C3F1 mice

Species and cellular/subcellular fraction (TCE concentration)	DCVG formation (nmol/hour/mg protein or 10 ⁶ cells)	
	Male	Female
Human		
Hepatocytes (0.9 mM) [pooled]	11 ± 3	
Liver cytosol (1 mM) [individual samples]	156 ± 16	174 ± 13
Liver cytosol (2 mM) [pooled]	346	
Liver microsomes (1 mM) [individual samples]	108 ± 24	83 ± 11
Liver microsomes (1 mM) [pooled]	146	
Kidney cytosol (2 mM) [pooled]	42	
Kidney microsomes (1 mM) [pooled]	320	
Rat		
Liver cytosol (2 mM)	7.30 ± 2.8	4.86 ± 0.14
Liver microsomes (2 mM)	10.3 ± 2.8	7.24 ± 0.24
Kidney cortical cells (2 mM)	0.48 ± 0.02	0.65 ± 0.15
Kidney cytosol (2 mM)	0.45 ± 0.22	0.32 ± 0.02
Kidney microsomes (2 mM)	not detected	0.61 ± 0.06
Mouse		
Liver cytosol (2 mM)	24.5 ± 2.4	21.7 ± 0.9
Liver microsomes (2 mM)	40.0 ± 3.1	25.6 ± 0.8
Kidney cytosol (2 mM)	5.6 ± 0.24	3.7 ± 0.48
Kidney microsomes (2 mM)	5.47 ± 1.41	16.7 ± 4.7

4
5

Mean ± SE. Source: Lash et al. (1999a, 1998, 1995); Cummings and Lash (2000); Cummings et al. (2000b).

1 **Table 3-24. Kinetics of TCE metabolism via GSH conjugation in male F344**
 2 **rat kidney and human liver and kidney cellular and subcellular fractions**
 3

Tissue and cellular fraction	K_M ($\mu\text{M TCE}$)	V_{MAX} (nmol DCVG/min/mg protein or 10^6 hepatocytes)	$1,000 \times$ V_{MAX}/K_M
Rat			
Kidney proximal tubular cells: low affinity	2,910	0.65	0.22
Kidney proximal tubular cells: high affinity	460	0.47	1.0
Human			
Liver hepatocytes*	37~106	0.16~0.26	2.4~4.5
Liver cytosol: low affinity	333	8.77	2.6
Liver cytosol: high affinity	22.7	4.27	190
Liver microsomes: low affinity	250	3.1	12
Liver microsomes: high affinity	29.4	1.42	48
Kidney proximal tubular cells: low affinity	29,400	1.35	0.046
Kidney proximal tubular cells: high affinity	580	0.11	0.19
Kidney cytosol	26.3	0.81	31
Kidney microsomes	167	6.29	38

4
 5 *Kinetic analyses of first 6 to 9 (out of 10) data points from Figure 1 from Lash et al. (1999a) using Lineweaver-
 6 Burk or Eadie-Hofstee plots and linear regression ($R^2 = 0.50\sim 0.95$). Regression with best R^2 used first 6 data
 7 points and Eadie-Hofstee plot, with resulting K_M and V_{MAX} of 106 and 0.26, respectively.
 8

9 Source: Lash et al. (1999a); Cummings and Lash (2000); Cummings et al. (2000b).
 10

11
 12 **3.3.3.2.3. Formation of NAcDCVC.** N-acetylation of DCVC can either occur in the kidney, as
 13 demonstrated in rat kidney microsomes (Duffel and Jakoby, 1982), or in the liver (Birner et al.,
 14 1997). Subsequent release of DCVC from the liver to blood may result in distribution to the
 15 kidney resulting in increased internal kidney exposure to the acetylated metabolite over and
 16 above what the kidney already is capable of generating. In the kidney, NAcDCVC may undergo
 17 deacetylation, which is considered a rate-limiting-step in the production of proximal tubule
 18 damage (Wolfgang et al., 1989; Zhang and Stevens, 1989). As a polar mercapturtae, NAcDCVC
 19 may be excreted in the urine as evidenced by findings in mice (Birner et al., 1993), rats

1 (Bernauer et al., 1996; Commandeur and Vermeulen, 1990), and humans who were exposed to
2 TCE (Bernauer et al., 1996; Birner et al., 1993), suggesting a common glutathione-mediated
3 metabolic pathway for DCVC among species.

4
5 **3.3.3.2.4. *Beta lyase metabolism of S-(1,2-dichlorovinyl) cysteine (DCVC).*** The enzyme
6 cysteine conjugate β -lyase catalyzes the breakdown of DCVC to reactive nephrotoxic
7 metabolites (Goeptar et al., 1995). This reaction involves removal of pyruvate and ammonia and
8 production of S-(1,2-dichlorovinyl) thiol (DCVT), an unstable intermediate, which rearranges to
9 other reactive alkylation metabolites that form covalent bonds with cellular nucleophiles
10 (Goeptar et al., 1995; Dekant et al., 1988). The rearrangement of DCVT to enethiols and their
11 acetylating agents has been described in trapping experiments (Dekant et al., 1988) and proposed
12 to be responsible for nucleophilic adduction and toxicity in the kidney. The quantification of
13 acid-labile adducts was proposed as a metric for TCE flux through the GSH pathway. However,
14 the presence of analytical artifacts precluded such analysis. In fact, measurement of acid-labile
15 adduct products resulted in higher values in mice than in rats (Eyre et al., 1995a, b).

16 DCVC metabolism to reactive species via a β -lyase pathway has not been directly
17 observed *in vivo* in animals or humans. However, β -lyase activity in humans and rats (reaction
18 rates were not reported) was demonstrated *in vivo* using a surrogate substrate,
19 2-(fluoromethoxy)-1,1,3,3,3-pentafluoro-1-propene (Iyer et al., 1998). β -lyase-mediated
20 reactive adducts have been described in several extrarenal tissues, including rat and human liver
21 and intestinal microflora (Larsen and Stevens, 1986; Tomisawa et al., 1984, 1986; Stevens,
22 1985a; Stevens and Jakoby, 1983; Dohn and Anders, 1982; Tateishi et al., 1978) and rat brain
23 (Alberati-Giani et al., 1995; Malherbe et al., 1995).

24 In the kidneys, glutamine transaminase K appears to be primarily responsible for β -lyase
25 metabolism of DCVC (Perry et al., 1993; Lash et al., 1990a, 1986; Jones et al., 1988;
26 Stevens et al., 1988, 1986). β -lyase transformation of DCVC appears to be regulated by 2-keto
27 acids. DCVC toxicity in isolated rat proximal tubular cells was significantly increased with the
28 addition of α -keto- γ -methiolbutyrate or phenylpyruvate (Elfarra et al., 1986b). The presence of
29 α -keto acid cofactors is necessary to convert the inactive form of the β -lyase enzyme (containing
30 pyridoxamine phosphate) to the active form (containing pyridoxal phosphate) (Goeptar et al.,
31 1995).

32 Both low- and high-molecular-weight enzymes with β -lyase activities have been
33 identified in rat kidney cytosol and mitochondria (Abraham et al., 1995a, b; Stevens et al., 1988;
34 Lash et al., 1986). While glutamine transaminase K and kynureninase-associated β -lyase
35 activities have been identified in rat liver (Alberati-Giani et al., 1995; Stevens, 1985a), they are

This document is a draft for review purposes only and does not constitute Agency policy.

1 quite low compared to renal glutamine transaminase K activity and do not result in
2 hepatotoxicity in DCVG- or DCVC-treated rats (Elfarra and Anders, 1984). Similar isoforms of
3 β -lyase have also been reported in mitochondrial fractions of brain tissue (Cooper, 2004).

4 The kidney enzyme L- α -hydroxy (L-amino) acid oxidase is capable of forming an
5 iminium intermediate and keto acid analogues (pyruvate or S-(1,2-dichlorovinyl)-2-oxo-
6 3-mercaptopropionate) of DCVC, which decomposes to dichlorovinylthiol (Lash et al., 1990b;
7 Stevens et al., 1989). In rat kidney homogenates, this enzyme activity resulted in as much as
8 35% of GSH pathway-mediated bioactivation. However, this enzyme is not present in humans,
9 an important consideration for extrapolation of renal effects across species.

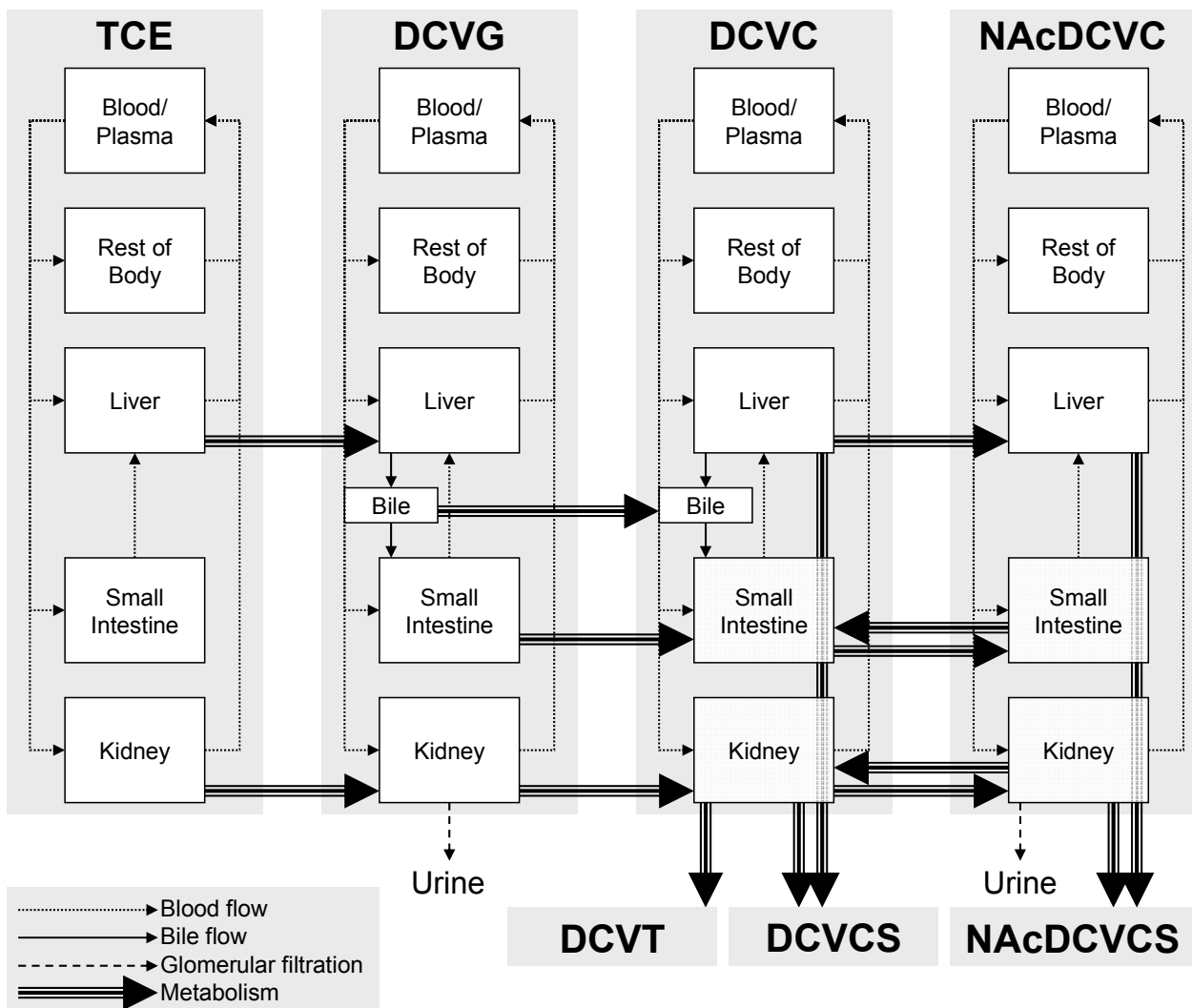
10
11 **3.3.3.2.5. Sulfoxidation of S-(1,2-dichlorovinyl) cysteine (DCVC) and NAcDCVC.** A second
12 pathway for bioactivation of TCE S-conjugates involves sulfoxidation of either the cysteine or
13 mercapturic acid conjugates (Sausen and Elfarra, 1990; Park et al., 1992; Lash et al., 1994, 2003;
14 Werner et al., 1995a, b, 1996; Birner et al., 1998; Krause et al., 2003). Sulfoxidation of DCVC
15 was mediated mainly by flavin monooxygenase 3 (FMO3), rather than CYP, in rabbit liver
16 microsomes (Ripp et al., 1997) and human liver microsomes (Krause et al., 2003). Krause et al.,
17 (2003) also reported DCVC sulfoxidation by human cDNA-expressed FMO3, as well as
18 detection of FMO3 protein in human kidney samples. While Krause et al. (2003) were not able
19 to detect sulfoxidation in human kidney microsomes, the authors noted FMO3 expression in the
20 kidney was lower and more variable than that in the liver.

21 Sulfoxidation of NAcDCVC, by contrast, was found to be catalyzed predominantly, if not
22 exclusively, by CYP3A enzymes (Werner et al., 1996), whose expressions are highly
23 polymorphic in humans. Sulfoxidation of other haloalkyl mercapturic acid conjugates has also
24 been shown to be catalyzed by CYP3A (Werner et al., 1995a, b; Altuntas et al., 2004). While
25 Lash et al. (2000a) suggested that this pathway would be quantitatively minor because of the
26 relatively low CYP3A levels in the kidney, no direct data exist to establish the relative
27 toxicological importance of this pathway relative to bioactivation of DCVC by β -lyase or FMO3.
28 However, the contribution of CYP3A in S-conjugate sulfoxidation to nephrotoxicity *in vivo* was
29 recently demonstrated by Sheffels et al. (2004) with fluoromethyl-2,2-difluoro-
30 1-(trifluoromethyl)vinyl ether (FDVE). In particular, *in vivo* production and urinary excretion of
31 FDVE-mercapturic acid sulfoxide metabolites were unambiguously established by mass
32 spectrometry, and CYP inducers/inhibitors increased/decreased nephrotoxicity *in vivo* while
33 having no effect on urinary excretion of metabolites produced through β -lyase (Sheffels et al.,
34 2004). These data suggest that, by analogy, sulfoxidation of NAcDCVC may be an important
35 bioactivating pathway.

This document is a draft for review purposes only and does not constitute Agency policy.

1 **3.3.3.2.6. Tissue distribution of glutathione (GSH) metabolism.** The sites of enzymatic
 2 metabolism of TCE to the various GSH pathway-mediated metabolites are significant in
 3 determining target tissue toxicity along this pathway. Figure 3-6 presents a schematic of
 4 interorgan transport and metabolism of TCE along the glutathione pathway. TCE is taken up
 5 either by the liver or kidney and conjugated to DCVG. The primary factors affecting TCE flux
 6 via this pathway include high hepatic GST activity, efficient transport of DCVG from the liver to
 7 the plasma or bile, high renal brush border and low hepatic GGT activities, and the capability for
 8 GSH conjugate uptake into the renal basolateral membranes with limited or no uptake into liver
 9 cell plasma membranes.

10



11
 12
 13
 14

Figure 3-6. Interorgan TCE transport and metabolism via the GSH pathway. See Figure 3-5 for enzymes involved in metabolic steps. Source: Lash et al. (2000a, b); NRC (2006).

1 As discussed previously, GST activity is present in many different cell types. However,
2 the liver is the major tissue for GSH conjugation. GST activities in rat and mouse cytosolic
3 fractions were measured using 1-chloro-2,4-dinitrobenzene, a GST substrate that is nonspecific
4 for particular isoforms (Lash et al., 1998). Specific activities (normalized for protein content) in
5 whole kidney cytosol were slightly less than those in the liver (0.64 compared to 0.52 mU/mg
6 protein for males and females). However, the much larger mass of the liver compared to the
7 kidney indicates that far more total GST activity resides in the liver. This is consistent with *in*
8 *vitro* data on TCE conjugation to DCVG, discussed previously (see Tables 3-23 and 3-24). For
9 instance, in humans, rats, and mice, liver cytosol exhibits greater DCVG production than kidney
10 cytosol. Distinct high- and low-affinity metabolic profiles were observed in the liver but not in
11 the kidney (see Table 3-24). In microsomes, human liver and kidney had similar rates of DCVG
12 production, while for rats and mice, the production in the liver was substantially greater.

13 According to studies by Lash et al. (1998, 1999b), the activity of GGT, the first step in
14 the conversion of DCVG to DCVC, is much higher in the kidney than the liver of mice, rats, and
15 humans, with most of the activity being concentrated in the microsomal, rather than the
16 cytosolic, fraction of the cell (see Table 3-25). In rats, this activity is quite high in the kidney but
17 is below the level of detection in the liver while the relative kidney to liver levels in humans and
18 mice were higher by 18- and up to 2,300-fold, respectively. Similar qualitative findings were
19 also reported in another study (Hinchman and Ballatori, 1990) when total organ GGT levels were
20 compared in several species (see Table 3-26). Cysteinylglycine dipeptidase was also
21 preferentially higher in the kidney than the liver of all tested species although the interorgan
22 differences in this activity (1–9-folds) seemed to be less dramatic than for GGT (see Table 3-26).
23 High levels of both GGT and dipeptidases have also been reported in the small intestine of rat
24 (Kozak and Tate, 1982) and mouse (Habib et al., 1996, 1998), as well as GGT in the human
25 jejunum (Fairman et al., 1977). No specific human intestinal cysteinylglycine dipeptidase has
26 been identified; however, a related enzyme (EC 3.4.13.11) from human kidney microsomes has
27 been purified and studied (Adachi et al., 1989) while several human intestinal dipeptidases have
28 been characterized including a membrane dipeptidase (EC 3.4.13.19) which has a wide dipeptide
29 substrate specificity including cysteinylglycine (Hooper et al., 1994; Ristoff and Larsson, 2007).

This document is a draft for review purposes only and does not constitute Agency policy.

1
2
3

Table 3-25. GGT activity in liver and kidney subcellular fractions of mice, rats, and humans

Species	Sex	Tissue	Cellular fraction	Activity (mU/mg)
Mouse	Male	Liver	Cytosol	0.07 ± 0.04
			Microsomes	0.05 ± 0.04
		Kidney	Cytosol	1.63 ± 0.85
			Microsomes	92.6 ± 15.6
	Female	Liver	Cytosol	0.10 ± 0.10
			Microsomes	0.03 ± 0.03
		Kidney	Cytosol	0.79 ± 0.79
			Microsomes	69.3 ± 14.0
Rat	Male	Liver	Cytosol	<0.02
			Microsomes	<0.02
		Kidney	Cytosol	<0.02
			Microsomes	1,570 ± 100
	Female	Liver	Cytosol	<0.02
			Microsomes	<0.02
		Kidney	Cytosol	<0.02
			Microsomes	1,840 ± 40
Human	Male	Liver	Cytosol	8.89 ± 3.58
			Microsomes	29
		Kidney	Cytosol	13.2 ± 1.0
			Microsomes	960 ± 77

4
5

Source: Lash et al. (1998, 1999b).

1 **Table 3-26. Multispecies comparison of whole-organ activity levels of GGT**
 2 **and dispeptidase**
 3

Species	Whole organ enzyme activity ($\mu\text{mol substrate/organ}$)			
	Kidney		Liver	
	GGT	Dispeptidase	GGT	Dispeptidase
Rat	1,010 \pm 41	20.2 \pm 1.1	7.1 \pm 1.4	6.1 \pm 0.4
Mouse	60.0 \pm 4.2	3.0 \pm 0.3	0.47 \pm 0.05	1.7 \pm 0.2
Rabbit	1,119 \pm 186	112 \pm 17	71.0 \pm 9.1	12.6 \pm 1.0
Guinea pig	148 \pm 13	77 \pm 10	46.5 \pm 4.2	13.2 \pm 1.5
Pig	3,800 \pm 769	2,428 \pm 203	1,600 \pm 255	2,178 \pm 490
Macaque	988	136	181	71

4
 5 Source: Hinchman and Ballatori (1990).
 6
 7

8 **3.3.3.2.7. Sex- and species-dependent differences in glutathione (GSH) metabolism.** Diverse
 9 sex and species differences appear to exist in TCE metabolism via the glutathione pathway. In
 10 rodents, rates of TCE conjugation to GSH in male rats and mice are higher than females (see
 11 Table 3-23). Verma and Rana (2003) reported 2-fold higher GST activity values in liver cytosol
 12 of female rats, compared to males, given 15 intraperitoneal injections of TCE over 30 days
 13 period. This effect may be due to sex-dependent variation in induction, as GST activities in male
 14 and female controls were similar. DCVG formation rates by liver and kidney subcellular
 15 fractions were much higher in both sexes of mice than in rats and, except for mouse kidney
 16 microsomes, the rates were generally higher in males than in females of the same species(see
 17 Table 3-23).

18 In terms of species differences, comparisons at 1–2 mM TCE concentrations (see
 19 Table 3-23) suggest that, in liver and kidney cytosol, the greatest DCVG production rate was in
 20 humans, followed by mice and then rats. However, different investigators have reported
 21 considerably different rates for TCE conjugation in human liver and kidney cell fractions. For
 22 instance, values in Table 3-23 from Lash et al. (1999a) are between two and five orders of
 23 magnitude higher than those reported by Green et al. (1997a). (The rates of DCVG formation by
 24 liver cytosol from male F344 rat, male B6C3F1 mouse, and human were 1.62, 2.5, and
 25 0.19 pmol/minute/mg protein, respectively, while there were no measurable activity in liver
 26 microsomes or subcellular kidney fractions [Green et al., 1997a]). The reasons for such

1 discrepancies are unclear but may be related to different analytical methods employed such as
2 detection of radiolabeled substrate vs. derivatized analytes (Lash et al., 2000a).

3 Expression of GGT activity does not appear to be influenced by sex (see Table 3-25); but
4 species differences in kidney GGT activity are notable with rat subcellular fractions exhibiting
5 the highest levels and mice and humans exhibiting about 4–6% and 50%, respectively, of rat
6 levels (Lash et al., 1999a, 1998). Table 3-26 shows measures of whole-organ GGT and
7 dipeptidase activities in rats, mice, guinea pigs, rabbits, pigs, and monkeys. These data show
8 that the whole kidney possesses higher activities than liver for these enzymes, despite the
9 relatively larger mass of the liver.

10 As discussed above, the three potential bioactivating pathways subsequent to the
11 formation of DCVC are catalyzed by β -lyase, FMO3 or CYP3A. Lash et al. (2000a) compared
12 *in vitro* β -lyase activities and kinetic constants (when available) for kidney of rats, mice, and
13 humans. They reported that variability of these values spans up to two orders of magnitude
14 depending on substrate, analytical method used, and research group. Measurements of rat,
15 mouse, and human β -lyase activities collected by the same researchers following
16 tetrachloroethylene exposure (Green et al., 1990) resulted in higher K_M and lower V_{MAX} values
17 for mice and humans than rats. Further, female rats exhibited higher K_M and lower V_{MAX} values
18 than males

19 With respect to FMO3, Ripp et al. (1999) found that this enzyme appeared catalytically
20 similar across multiple species, including humans, rats, dogs, and rabbits, with respect to several
21 substrates, including DCVC, but that there were species differences in expression. Specifically,
22 in male liver microsomes, rabbits had 3-fold higher methionine S-oxidase activity than mice and
23 dogs had 1.5-fold higher activity than humans and rats. Species differences were also noted in
24 male and female kidney microsomes; rats exhibited 2- to 6-fold higher methionine S-oxidase
25 activity than the other species. Krause et al. (2003) detected DCVC sulfoxidation in incubations
26 with human liver microsomes but did not in an incubation with a single sample of human kidney
27 microsomes. However, FMO3 expression in the 26 human kidney samples was found to be
28 highly variable, with a range of 5–6-fold (Krause et al., 2003).

29 No data on species differences in CYP3A-mediated sulfoxidation of NAcDCVC are
30 available. However, Altuntas et al. (2004) examined sulfoxidation of cysteine and mercapturic
31 acid conjugates of FDVE (fluoromethyl-2,2-difluoro-1-(trifluoromethyl)vinyl ether) in rat and
32 human liver and kidney microsomes. They reported that the formation of sulfoxides from the
33 mercapturates *N*-Ac-FFVC and (*Z*)-*N*-Ac-FFVC (FFVC is (*E,Z*)-S-(1-fluoro-2-fluoromethoxy-
34 2-(trifluoromethyl)vinyl-Lcysteine) were greatest in rat liver microsomes, and 2- to 30-fold
35 higher than in human liver microsomes (which had high variability). Sulfoxidation of

1 *N*-Ac-FFVC could not be detected in neither rat nor human kidney microsomes, but
2 sulfoxidation of (*Z*)-*N*-Ac-FFVC was detected in both rat and human kidney microsomes at rates
3 comparable to human liver microsomes. Using human- and rat-expressed CYP3A, Altuntas et
4 al. (2004) reported that rates of sulfoxidation of (*Z*)-*N*-Ac-FFVC were comparable in human
5 CYP3A4 and rat CYP3A1 and CYP3A2., but that only rat CYP3A1 and A2 catalyzed
6 sulfoxidation of *N*-Ac-FFVC. As the presence or absence of the species differences in
7 mercapturate sulfoxidation appear to be highly chemical-specific, no clear inferences can be
8 made as to whether species differences exist for sulfoxidation of NAcDCVC

9 Also relevant to assess the flux through the various pathways are the rates of
10 *N*-acetylation and de-acetylation of DCVC. This is demonstrated by the results of Elfarra and
11 Hwang (1990) using S-(2-benzothiazolyl)-L-cysteine as a marker for β -lyase metabolism in rats,
12 mice, hamsters, and guinea pigs. Guinea pigs exhibited about 2-fold greater flux through the
13 β -lyase pathway, but this was not attributable to higher β -lyase activity. Rather, guinea pigs
14 have relatively low *N*-acetylation and high deacetylation activities, leading to a high level of
15 substrate recirculation (Lau et al., 1995). Thus, a high *N*-deacetylase:*N*-acetylase activity ratio
16 may favor DCVC recirculation and subsequent metabolism to reactive species. In human,
17 Wistar rat, Fischer rat, and mouse cytosol, deacetylation rates for NAcDCVC varied less than
18 3-fold (0.35, 0.41, 0.61, and 0.94 nmol DCVC formed/minute/mg protein in humans, rats, and
19 mice) (Birner et al., 1993). However, similar experiments have not been carried out for
20 *N*-acetylation of DCVC, so the balance between its *N*-acetylation and de-acetylation has not been
21 established.

22
23 **3.3.3.2.8. Human variability and susceptibility in glutathione (GSH) conjugation.** Knowledge
24 of human variability in metabolizing TCE through the glutathione pathway is limited to *in vitro*
25 comparisons of variance in GST activity rates. Unlike CYP-mediated oxidation, quantitative
26 differences in the polymorphic distribution or activity levels of GST isoforms in humans are not
27 presently known. However, the available data (Lash et al., 1999a, b) do suggest that significant
28 variation in GST-mediated conjugation of TCE exists in humans. In particular, at a single
29 substrate concentration of 1 mM, the rate of GSH conjugation of TCE in human liver cytosol
30 from 9 male and 11 females spanned a range of 2.4-fold (34.7–83.6 nmol DCVG
31 formed/20-minute/mg protein) (Lash et al., 1999b). In liver microsomes from 5 males and
32 15-females, the variation in activity was 6.5-fold (9.9–64.6 nmol DCVG formed/20 minute/mg
33 protein). No sex-dependent variation was identified. Despite being less pronounced than the
34 known variability in human CYP-mediated oxidation, the impact on risk assessment of the
35 variability in GSH conjugation to TCE is currently unknown especially in the absence of data on

1 variability for N-acetylation and bioactivation via β -lyase, FMO3, or CYP3A in the human
2 kidney.

3 4 **3.3.3.3. Relative Roles of the Cytochrome P450 (CYP) and Glutathione (GSH) Pathways**

5 *In vivo* mass balance studies in rats and mice, discussed above, have shown
6 unequivocally that in these species, CYP oxidation of TCE predominates over GSH conjugation.
7 In these species, at doses from 2 to 2,000 mg/kg of [¹⁴C]TCE, the sum of radioactivity in exhaled
8 TCE, urine, and exhaled CO₂ constitutes 69–94% of the dose, with the vast majority of the
9 radioactivity in urine (95–99%) attributable to oxidative metabolites (Dekant et al., 1986a, 1984;
10 Green and Prout, 1985; Prout et al., 1995). The rest of the radioactivity was found mostly in
11 feces and the carcass. More rigorous quantitative limits on the amount of GSH conjugation
12 based on *in vivo* data such as these can be obtained using PBPK models, discussed in
13 Section 3.5.

14 Comprehensive mass-balance studies are unavailable in humans. DCVG and DCVC in
15 urine have not been detected in any species, while the amount of urinary NAcDCVC from
16 human exposures is either below detection limits or very small from a total mass balance point of
17 view (Birner et al., 1993; Bernauer et al., 1996; Lash et al., 1999b; Bloemen et al., 2001). For
18 instance, the ratio of primary oxidative metabolites (TCA + TCOH) to NAcDCVC in urine of
19 rats and humans exposed to 40–160 ppm (215 to 860 mg/m³) TCE heavily favored oxidation,
20 resulting in ratios of 986–2,562:1 in rats and 3,292–7,163:1 in humans (Bernauer et al., 1996).
21 Bloemen et al. (2001) reported that at most 0.05% of an inhaled TCE dose would be excreted as
22 NAcDCVC, and concluded that this suggested TCE metabolism by GSH conjugation was of
23 minor importance. While it is a useful biomarker of exposure and an indicator of GSH
24 conjugation, NAcDCVC may capture only a small fraction of TCE flux through the GSH
25 conjugation pathway due to the dominance of bioactivating pathways (Lash et al., 2000a).

26 A number of lines of evidence suggest that the amount of TCE conjugation to GSH in
27 humans, while likely smaller than the amount of oxidation, may be much more substantial than
28 analysis of urinary mercapturates would suggest. In Table 3-27, *in vitro* estimates of the V_{MAX},
29 K_M, and clearance (V_{MAX}/K_M) for hepatic oxidation and conjugation of TCE are compared in a
30 manner that accounts for differences in cytosolic and microsomal partitioning and protein
31 content. Surprisingly, the range of *in vitro* kinetic estimates for oxidation and conjugation of
32 TCE substantially overlap, suggesting similar flux through each pathway, though with high
33 interindividual variation. The microsomal and cytosolic protein measurements of GSH
34 conjugation should be caveated by the observation by Lash et al. (1999a) that GSH conjugation
35 of TCE was inhibited by ~50% in the presence of oxidation. Note that this comparison cannot be

This document is a draft for review purposes only and does not constitute Agency policy.

1 made in rats and mice because *in vitro* kinetic parameters for GSH conjugation in the liver are
 2 not available in those species (only activity at 1 or 2 mM have been measured).

3
 4 **Table 3-27. Comparison of hepatic *in vitro* oxidation and conjugation of**
 5 **TCE**
 6

Cellular or subcellular fraction	V_{MAX} (nmol TCE metabolized/min/g tissue)		K_M (μ M in blood)		V_{MAX}/K_M (mL/min/g tissue)	
	Oxidation	GSH conjugation	Oxidation	GSH conjugation	Oxidation	GSH conjugation
Hepatocytes	10.0–68.4	16~25	22.1–198	16~47	0.087–1.12	0.55~1.0
Liver microsomes	6.1–111	45	2.66–11.1 ^a	5.9 ^a	1.71–28.2 ^a	7.6 ^a
			71.0–297 ^b	157 ^b	0.064–1.06 ^b	0.29 ^b
Liver cytosol	–	380	–	4.5 ^a	–	84 ^a
	–		–	22.7 ^b	–	16.7 ^b

7
 8 Note: When biphasic metabolism was reported, only high affinity pathway is shown here.

9 Conversion assumptions for V_{MAX} :

10 Hepatocellularity of 99 million cells/g liver (Barter et al., 2007);

11 Liver microsomal protein content of 32 mg protein/g tissue (Barter et al., 2007); and

12 Liver cytosolic protein content of 89 mg protein/g tissue (based on rats: Prasanna et al., 1989;
 13 van Bree et al., 1990).

14 Conversion assumptions for K_M :

15 For hepatocytes, K_M in headspace converted to K_M in blood using blood:air partition coefficient of 9.5
 16 (reported range of measured values 6.5–12.1, Table 3-1);

17 For microsomal protein, option (a) assumes K_M in medium is equal to K_M in tissue, and converts to
 18 K_M in blood by using a liver:blood partition coefficient of 5 (reported ranges of measured values
 19 3.6–5.9, Table 3-8), and option (b) converts K_M in medium to K_M in air using the measured
 20 microsomal protein:air partition coefficient of 1.78 (Lipscomb et al., 1997), and then converts to
 21 K_M in blood by using the blood:air partition coefficient of 9.5; and

22 For cytosolic protein, option (a) assumes K_M in medium is equal to K_M in tissue, and converts to K_M
 23 in blood by using a liver:blood partition coefficient of 5 (reported ranges of measured values
 24 3.6–5.9, Table 3-8), and option (b) assumes K_M in medium is equal to K_M in blood, so no
 25 conversion is necessary.

26
 27
 28 Furthermore, as shown earlier in Table 3-22, the human *in vivo* data of Lash et al.
 29 (1999a) show blood concentrations of DCVG similar, on a molar basis, to that of TCE, TCA, or
 30 TCOH, suggesting substantial conjugation of TCE. In addition, these data give a lower limit as
 31 to the amount of TCE conjugated. In particular, by multiplying the peak blood concentration of
 32 DCVG by the blood volume, a minimum amount of DCVG in the body at that time can be

This document is a draft for review purposes only and does not constitute Agency policy.

1 derived (i.e., assuming the minimal empirical distribution volume equal to the blood volume).
 2 As shown in Table 3-28, this lower limit amounts to about 0.4–3.7% of the inhaled TCE dose.
 3 Since this is the minimum amount of DCVG in the body at a single time point, the total amount
 4 of DCVG formed is likely to be substantially greater owing to possible distribution outside of the
 5 blood as well as the metabolism and/or excretion of DCVG. Lash et al. (1999) found levels of
 6 urinary mercapturates were near or below the level of detection of 0.19 uM, results that are
 7 consistent with those of Bloemen et al. (2001), who reported urinary concentrations below
 8 0.04 uM at 2- to 4-fold lower cumulative exposures. Taken together, these results confirm the
 9 suggestion by Lash et al. (2000a) that NAcDCVC is a poor quantitative marker for the flux
 10 through the GSH pathway.

11

12 **Table 3-28. Estimates of DCVG in blood relative to inhaled TCE dose in**
 13 **humans exposed to 50 and 100 ppm (269 and 537 mg/m³; Fisher et al., 1998;**
 14 **Lash et al., 1999)**

15

Sex exposure	Estimated inhaled TCE dose (mmol) ^a	Estimated peak amount of DCVG in blood (mmol) ^b
Males		
50 ppm × 4 hours	3.53	0.11 ± 0.08
100 ppm × 4 hours	7.07	0.26 ± 0.08
Females		
50 ppm × 4 hours	2.36	0.010 ± 0
100 ppm × 4 hours	4.71	0.055 ± 0.027

16

17 ^aInhaled dose estimated by (50 or 100 ppm)/(24,450 ppm/mM) × (240 min) × Q_p, where alveolar ventilation rate Q_p
 18 is 7.2 L/min for males and 4.8 L/min for females. Q_p is calculated as (V_T - V_D) × f_R with the following
 19 respiratory parameters: tidal volume V_T (0.75 L for males, 0.46 L for females), dead space V_D (0.15 L for males,
 20 0.12 L for females), and respiration frequency f_R (12 min⁻¹ for males, 14 min⁻¹ for females) (assumed sitting,
 21 awake from The International Commission on Radiological Protection [ICRP], 2002).

22 ^bPeak amount of DCVG in blood estimated by multiplying the peak blood concentration by the estimated blood
 23 volume: 5.6 L in males and 4.1 L in females (ICRP, 2002).

24

25

26 In summary, TCE oxidation is likely to be greater quantitatively than conjugation with
 27 GSH in mice, rats, and humans. However, the flux through the GSH pathway, particularly in
 28 humans, may be greater by an order of magnitude or more than the <0.1% typically excreted of
 29 NAcDCVC in urine. This is evidenced both by a direct comparison of *in vitro* rates of oxidation
 30 and conjugation, as well as by *in vivo* data on the amount of DCVG in blood. PBPK models can

This document is a draft for review purposes only and does not constitute Agency policy.

1 be used to more quantitatively synthesize these data and put more rigorous limits on relative
2 amount TCE oxidation and conjugation with GSH. Such analyses are discussed in Section 3.5.

3 4 **3.4. TRICHLOROETHYLENE (TCE) EXCRETION**

5 This section discusses the major routes of excretion of TCE and its metabolites in exhaled
6 air, urine, and feces. Unmetabolized TCE is eliminated primarily via exhaled air. As discussed
7 in Section 3.3, the majority of TCE absorbed into the body is eliminated by metabolism. With
8 the exception of CO₂, which is eliminated solely via exhalation, most TCE metabolites have low
9 volatility and, therefore, are excreted primarily in urine and feces. Though trace amounts of TCE
10 metabolites have also been detected in sweat and saliva (Bartonicek et al., 1962), these excretion
11 routes are likely to be relatively minor.

12 13 **3.4.1. Exhaled Air**

14 In humans, pulmonary elimination of unchanged trichloroethylene and other volatile
15 compounds is related to ventilation rate, cardiac output, and the solubility of the compound in
16 blood and tissue, which contribute to final exhaled air concentration of TCE. In their study of
17 the impact of workload on TCE absorption and elimination, Astrand and Ovrum (1976)
18 characterized the postexposure elimination of TCE in expired breath. TCE exposure (540 or
19 1,080 mg/m³; 100 or 200 ppm) was for a total of 2 hours, at workloads from 0 to 150 Watts.
20 Elimination profiles were roughly equivalent among groups, demonstrating a rapid decline in
21 TCE concentrations in expired breath postexposure (see Table 3-29).

22 The lung clearance of TCE represents the volume of air from which all TCE can be
23 removed per unit time, and is a measure of the rate of excretion via the lungs. Monster et al.
24 (1976) reported lung clearances ranging from 3.8 to 4.9 L/minute in four adults exposed at rest to
25 70 ppm and 140 ppm of trichloroethylene for four hours. Pulmonary ventilation rates in these
26 individuals at rest ranged from 7.7–12.3 L/minute. During exercise, when ventilation rates
27 increased to 29–30 L/minute, lung clearance was correspondingly higher, 7.7–12.3 L/minute.
28 Under single and repeated exposure conditions, Monster et al. (1976, 1979) reported from
29 7–17% of absorbed TCE excreted in exhaled breath.

1 **Table 3-29. Concentrations of TCE in expired breath from inhalation-**
 2 **exposed humans (Astrand and Ovrum, 1976)**
 3

Time postexposure	Alveolar air		
	I*	II	III
0	459 ± 44	244 ± 16	651 ± 53
30	70 ± 5	51 ± 3	105 ± 18
60	40 ± 4	28 ± 2	69 ± 8
90	35 ± 9	21 ± 1	55 ± 2
120	31 ± 8	16 ± 1	45 ± 1
300	8 ± 1	9 ± 2	14 ± 2
420	5 ± 0.5	4 ± 0.5	8 ± 1.3
19 hours	2 ± 0.3	2 ± 0.2	4 ± 0.5

4 * Roman numerals refer to groups assigned different workloads.

5 Concentrations are in mg/m³ for expired air.
 6
 7
 8
 9

10 Pulmonary elimination of unchanged trichloroethylene at the end of exposure is a
 11 first-order diffusion process across the lungs from blood into alveolar air, and it can be thought
 12 of as the reversed equivalent of its uptake from the lungs. Exhaled pulmonary excretion occurs
 13 in several distinct (delayed) phases corresponding to release from different tissue groups, at
 14 different times. Sato et al. (1977) detected 3 first-order phases of pulmonary excretion in the
 15 first 10 hours after exposure to 100 ppm for 4 hours, with fitted half-times of pulmonary
 16 elimination of 0.04 hour, 0.67 hour, and 5.6 hours, respectively. Opdam (1989) sampled alveolar
 17 air up to 20–310 hours after 29–62 minute exposures to 6–38 ppm, and reported terminal half-
 18 lives of 8–44 hours at rest. Chiu et al. (2007) sampled alveolar air up to 100 hours after 6-hour
 19 exposures to 1 ppm and reported terminal half-lives of 14–23 hours. The long terminal half-time
 20 of TCE pulmonary excretion indicates that a considerable time is necessary to completely
 21 eliminate the compound, primarily due to the high partitioning to adipose tissues (see
 22 Section 3.2).

23 As discussed above, several studies (Dekant et al., 1986a, 1984; Green and Prout, 1985;
 24 Prout et al., 1985) have investigated the disposition of [¹⁴C]TCE in rats and mice following
 25 gavage administrations (see Section 3.3.2). These studies have reported CO₂ as an exhalation
 26 excretion product in addition to unchanged TCE. With low doses, the amount of TCE excreted

This document is a draft for review purposes only and does not constitute Agency policy.

1 unchanged in exhaled breath is relatively low. With increasing dose in rats, a disproportionately
2 increased amount of radiolabel is expired as unchanged TCE. This may indicate saturation of
3 metabolic activities in rats at doses 200 mg/kg and above, which is perhaps only minimally
4 apparent in the data from mice. In addition, exhaled air TCE concentration has been measured
5 after constant inhalation exposure for 2 hours to 50 or 500 ppm in rats (Dallas et al., 1991), and
6 after dermal exposure in rats and humans (Poet, 2000). Exhaled TCE data from rodents and
7 humans have been integrated into the PBPK model presented in Section 3.5.

8 Finally, TCOH is also excreted in exhaled breath, though at a rate about 10,000-fold
9 lower than unmetabolized TCE (Monster et al., 1976, 1979).

11 3.4.2. Urine

12 Urinary excretion after TCE exposure consists predominantly of the metabolites TCA
13 and TCOH, with minor contributions from other oxidative metabolites and GSH conjugates.
14 Measurements of unchanged TCE in urine have been at or below detection limits (e.g.,
15 Fisher et al., 1998; Chiu et al., 2007). The recovery of urinary oxidative metabolites in mice,
16 rats, and humans was addressed earlier (see Section 3.3.2) and will not be discussed here.

17 Because of their relatively long elimination half-life, urinary oxidative metabolites have
18 been used as an occupational biomarker of TCE exposure for many decades
19 (Ikeda and Imamura, 1973; Carrieri, 2007). Ikeda and Imamura (1973) measured total trichloro
20 compounds (TTC), TCOH and TCA, in urine over three consecutive postexposure days for
21 4 exposure groups totaling 24 adult males and one exposure group comprising 6 adult females.
22 The elimination half-life for TTC ranged 26.1 to 48.8 hours in males and was 50.7 hours in
23 females. The elimination half-life for TCOH was 15.3 hours in the only group of males studied
24 and was 42.7 hours in females. The elimination half-life for TCA was 39.7 hours in the only
25 group of males studied and was 57.6 hours in females. These authors compared their results to
26 previously published elimination half-lives for TTC, TCOH, and TCA. Following experimental
27 exposures of groups of 2 to 5 adults, elimination half-lives ranged 31–50 hours for TTC;
28 19–29 hours for TCOH; and 36–55 hours for TCA (Bartonicek, 1962; Stewart et al., 1970;
29 Nomiyama and Nomiyama, 1971; Ogata et al., 1971). The urinary elimination half-life of TCE
30 metabolites in a subject who worked with and was addicted to sniffing TCE for 6–8 years
31 approximated 49.7 hours for TCOH, 72.6 hours for TCA, and 72.6 hours for TTC (Ikeda et al.,
32 1971).

33 The quantitative relationship between urinary concentrations of oxidative metabolites and
34 exposure in an occupational setting was investigated by Ikeda (1977). This study examined the
35 urinary elimination of TCE and metabolites in urine of 51 workers from 10 workshops. The

1 concentration of TCA and TCOH in urine demonstrated a marked concentration-dependence,
2 with concentrations of TCOH being approximately twice as high as those for TCA. Urinary
3 half-life values were calculated for 6 males and 6 females from 5 workshops; males were
4 intermittently exposed to 200 ppm and females were intermittently exposed to 50 ppm
5 (269 mg/m³). Urinary elimination half-lives for TTC, TCOH and TCA were 26.1, 15.3, and
6 39.7 hours; and 50.7, 42.7 and 57.6 hours in males and females, respectively, which were similar
7 to the range of values previously reported. These authors estimated that urinary elimination of
8 parent TCE during exposure might account for one-third of the systemically absorbed dose.
9 Importantly, urinary TCA exhibited marked saturation at exposures higher than 50 ppm.
10 Because neither TTC nor urinary TCOH (in the form of the glucuronide TCOG) showed such an
11 effect, this saturation cannot be due to TCE oxidation itself, but must rather be from one of the
12 metabolic processes forming TCA from TCOH. Unfortunately, since biological monitoring
13 programs usually measure only urinary TCA, rather than TTC, urinary TCA levels above around
14 150 mg/L cannot distinguish between exposures at 50 ppm and at much higher concentrations.

15 It is interesting to attempt to extrapolate on a cumulative exposure basis the Ikeda (1977)
16 results for urinary metabolites obtained after occupational exposures at 50 ppm to the controlled
17 exposure study by Chiu et al. (2007) at 1.2 ppm for 6 hours (the only controlled exposure study
18 for which urinary concentrations, rather than only cumulative excretion, are available). Ikeda
19 (1977) reported that measurements were made during the second half of the week, so one can
20 postulate a cumulative exposure duration of 20~40 hours. At 50 ppm, Ikeda (1977) report a
21 urinary TCOH concentration of about 290 mg/L, so that per ppm-hour, the expected urinary
22 concentration would be $290/(50 \times 20\sim40) = 0.145\sim0.29$ mg/L-ppm-hour. The cumulative
23 exposure in Chiu et al. (2007) is $1.2 \times 6 = 7.2$ ppm-hour, so the expected urinary TCOH
24 concentration would be $7.2 \times (0.145\sim0.29) = 1.0\sim2.1$ mg/L. This estimate is somewhat
25 surprisingly consistent with the actual measurements of Chiu et al. (2007) during the first day
26 postexposure, which ranged from 0.8~1.2 mg/L TCOH in urine.

27 On the other hand, extrapolation of TCA concentrations was less consistent. At 50 ppm,
28 Ikeda (1977) report a urinary TCA concentration of about 140 mg/L, so that per ppm-hour, the
29 expected urinary concentration would be $140/(50 \times 20\sim40) = 0.07\sim0.14$ mg/L-ppm-hour. The
30 cumulative exposure in Chiu et al. (2007) is $1.2 \times 6 = 7.2$ ppm-hour, so the expected urinary
31 TCA concentration would be $7.2 \times (0.07\sim0.14) = 0.5\sim1.0$ mg/L, whereas Chiu et al. (2007)
32 reported urinary TCA concentrations on the first day after exposure of 0.03~0.12 mg/L.
33 However, as noted in Chiu et al. (2007), relative urinary excretion of TCA was 3- to 10-fold
34 lower in Chiu et al. (2007) than other studies at exposures 50~140 ppm, which may explain part
35 of the discrepancies. However, this may be due in part to saturation of many urinary TCA

This document is a draft for review purposes only and does not constitute Agency policy.

1 measurements, and, furthermore, interindividual variance, observed to be substantial in Fisher et
2 al. (1998), cannot be ruled out.

3 Urinary elimination kinetics have been reported to be much faster in rodents than in
4 humans. For instance, adult rats were exposed to 50, 100, or 250 ppm (269, 537, or
5 1,344 mg/m³) via inhalation for 8 hours or were administered an i.p. injection (1.47 g/kg) and the
6 urinary elimination of total trichloro compounds was followed for several days (Ikeda and
7 Imamura, 1973). These authors calculated urinary elimination half-lives of 14.3–15.6 hours for
8 female rats and 15.5–16.6 hours for male rats; the route of administration did not appear to
9 influence half-life value. In other rodent experiments using orally administered radiolabeled
10 TCE, urinary elimination was complete within one or two days after exposure (Dekant et al.,
11 1986a, 1984; Green and Prout, 1985; Prout et al., 1985).

12 13 **3.4.3. Feces**

14 Fecal elimination accounts for a small percentage of TCE as shown by limited
15 information in the available literature. Bartonicek (1962) exposed 7 human volunteers to
16 1.042 mg TCE/L air for 5 hours and examined TCOH and TCA in feces on the third and seventh
17 day following exposure. The mean amount of TCE retained during exposure was 1,107 mg,
18 representing 51–64% (mean 58%) of administered dose. On the third day following TCE
19 exposure, TCOH and TCA in feces demonstrated mean concentrations of 17.1 and
20 18.5 mg/100 grams feces, similar to concentrations in urine. However, because of the 10-fold
21 smaller daily rate of excretion of feces relative to urine, this indicates fecal excretion of these
22 metabolites is much less significant than urinary excretion. Neither TCOH nor TCA was
23 detected in feces on the seventh day following exposure.

24 In rats and mice, total radioactivity has been used to measure excretion in feces after oral
25 gavage TCE administration in corn oil, but since the radiolabel was not characterized it is not
26 possible to determine whether the fecal radiolabel in feces represented unabsorbed parent
27 compound, excreted parent compound, and/or excreted metabolites. Dekant et al. (1984)
28 reported mice eliminated 5% of the total administered TCE, while rats eliminated 2% after oral
29 gavage. Dekant et al. (1986a) reported a dose response related increase in fecal elimination with
30 dose, ranging between 0.8–1.9% in rats and 1.6–5% in mice after oral gavage in corn oil. Due to
31 the relevant role of CYP2E1 in the metabolism of TCE (see Section 3.3.3.1.6), Kim and
32 Ghanayem (2006) compared fecal elimination in both wild-type and CYP2E1 knockouts mice
33 and reported fecal elimination ranging between 4.1–5.2% in wild-type and 2.1–3.8% in
34 knockout mice exposed by oral gavage in aqueous solution.

1 3.5. PHYSIOLOGICALLY BASED PHARMACOKINETIC (PBPK) MODELING OF 2 TRICHLOROETHYLENE (TCE) AND ITS METABOLITES

3 3.5.1. Introduction

4 PBPK models are extremely useful tools for quantifying the relationship between
5 external measures of exposure and internal measures of toxicologically relevant dose. In
6 particular, for the purposes of this assessment, PBPK models are evaluated for the following:
7 (1) providing additional quantitative insights into the ADME of TCE and metabolites described
8 in the sections above; (2) cross-species pharmacokinetic extrapolation of rodent studies of both
9 cancer and noncancer effects, (3) exposure-route extrapolation; and (4) characterization of
10 human pharmacokinetic variability. The following sections first describe and evaluate previous
11 and current TCE PBPK modeling efforts, then discuss the insights into ADME (1, above), and
12 finally present conclusions as to the utility of the model to predict internal doses for use in dose-
13 response assessment (2–4, above).

15 3.5.2. Previous Physiologically Based Pharmacokinetic (PBPK) Modeling of 16 Trichloroethylene (TCE) for Risk Assessment Application

17 TCE has an extensive number of both *in vivo* pharmacokinetic and PBPK modeling
18 studies (see Chiu et al., 2006, supplementary material, for a review). Models previously
19 developed for occupational or industrial hygiene applications are not discussed here but are
20 reviewed briefly in Clewell et al. (2000). Models designed for risk assessment applications have
21 focused on descriptions of TCE and its major oxidative metabolites TCA, TCOH, and TCOG.
22 Most of these models were extensions of the “first generation” of models developed by Fisher
23 and coworkers (Allen and Fisher, 1993; Fisher et al., 1991) in rats, mice, and humans. These
24 models, in turn, are based on a Ramsey and Andersen (1984) structure with flow-limited tissue
25 compartments and equilibrium gas exchange, saturable Michaelis-Menten kinetics for oxidative
26 metabolism, and lumped volumes for the major circulating oxidative metabolites TCA and
27 TCOH. Fisher and coworkers updated their models with new *in vivo* and *in vitro* experiments
28 performed in mice (Abbas and Fisher, 1997; Greenberg et al., 1999) and human volunteers
29 (Fisher et al., 1998) and summarized their findings in Fisher (2000). Clewell et al. (2000) added
30 enterohepatic recirculation of TCOG and pathways for local oxidative metabolism in the lung
31 and GST metabolism in the liver. While Clewell et al. (2000) does not include the updated
32 Fisher data, they have used a wider set of *in vivo* and *in vitro* mouse, rat, and human data than
33 previous models. Finally, Bois (2000a, b) performed re-estimations of PBPK model parameters
34 for the Fisher and Clewell models using a Bayesian population approach (Gelman et al., 1996,
35 and discussed further below).

This document is a draft for review purposes only and does not constitute Agency policy.

1 As discussed in Rhomberg (2000), the choice as to whether to use the Fisher, Clewell,
2 and Bois models for cross-species extrapolation of rodent cancer bioassays led to quantitative
3 results that differed by as much as an order of magnitude. There are a number of differences in
4 modeling approaches that can explain their differing results. First, the Clewell et al. (2000)
5 model differed structurally in its use of single-compartment volume-of-distribution models for
6 metabolites as opposed to the Fisher (2000) models' use of multiple physiologic compartments.
7 Also, the Clewell et al. (2000) model, but not the Fisher models, includes enterohepatic
8 recirculation of TCOH/TCOG (although reabsorption was set to zero in some cases). In addition
9 to structural differences in the models, the input parameter values for these various models were
10 calibrated using different subsets of the overall *in vivo* database (see Chiu et al., 2006,
11 supplementary material, for a review). The Clewell et al. (2000) model is based primarily on a
12 variety of data published before 1995; the Fisher (2000) models were based primarily on new
13 studies conducted by Fisher and coworkers (after 1997); and the Bois (2000a, b) re-estimations
14 of the parameters for the Clewell et al. (2000) and Fisher (2000) models used slightly different
15 data sets than the original authors. The Bois (2000a, b) re-analyses also led to somewhat
16 different parameter estimates than the original authors, both because of the different data sets
17 used as well as because the methodology used by Bois allowed many more parameters to be
18 estimated simultaneously than were estimated in the original analyses.

19 Given all these methodological differences, it is not altogether surprising that the
20 different models led to different quantitative results. Even among the Fisher models themselves,
21 Fisher (2000) noted some inconsistencies, including differing estimates for metabolic parameters
22 between mouse gavage and inhalation experiments. These authors included possible
23 explanations for these inconsistencies: the impact of corn oil vehicle use during gavage
24 (Staats et al., 1991) and the impact of a decrease in ventilation rate in mice due to sensory
25 irritation during the inhalation of solvents (e.g., Stadler and Kennedy, 1996).

26 As discussed in a report by the National Research Council (NRC, 2006), several
27 additional PBPK models relevant to TCE pharmacokinetics have been published since 2000 and
28 are reviewed briefly here. Poet et al. (2000) incorporated dermal exposure to TCE in PBPK
29 models in rats and humans, and published *in vivo* data in both species from dermal exposure
30 (Thrall et al., 2000; Poet et al., 2000). Albanese et al. (2002) published a series of models with
31 more complex descriptions of TCE distribution in adipose tissue but did not show comparisons
32 with experimental data. Simmons et al. (2002) developed a PBPK model for TCE in the
33 Long-Evans rat that focused on neurotoxicity endpoints and compared model predictions with
34 experimentally determined TCE concentrations in several tissues—including the brain. Keys et
35 al. (2003) investigated the lumping and unlumping of various tissue compartments in a series of

This document is a draft for review purposes only and does not constitute Agency policy.

1 PBPK models in the rat and compared model predictions with TCE tissue concentrations in a
2 multitude of tissues. Although none of these TCE models included metabolite descriptions, the
3 experimental data was available for either model or evaluation. Finally, Keys et al. (2004)
4 developed a model for DCA in the mouse that included a description of suicide inhibition of
5 GST-zeta, but this model was not been linked to TCE.

7 **3.5.3. Development and Evaluation of an Interim “Harmonized” Trichloroethylene (TCE)** 8 **Physiologically Based Pharmacokinetic (PBPK) Model**

9 Throughout 2004, U.S. EPA and the U.S. Air Force jointly sponsored an integration of
10 the Fisher, Clewell, and Bois modeling efforts (Hack et al., 2006). In brief, a single interim
11 PBPK model structure combining features from both the Fisher and Clewell models was
12 developed and used for all 3 species of interest (mice, rats, and humans). An effort was made to
13 combine structures in as simple a manner as possible; the evaluation of most alternative
14 structures was left for future work. The one level of increased complexity introduced was
15 inclusion of species- and dose-dependent TCA plasma binding, although only a single *in vitro*
16 study of Lumpkin et al. (2003) was used as parameter inputs. As part of this joint effort, a
17 hierarchical Bayesian population analysis using Markov chain Monte Carlo (MCMC) sampling
18 (similar to the Bois [2000a, b] analyses) was performed on the revised model with a
19 cross-section of the combined database of kinetic data to provide estimates of parameter
20 uncertainty and variability (Hack et al., 2006). Particular attention was given to using data from
21 each of the different efforts, but owing to time and resource constraints, a combined analysis of
22 all data was not performed. The results from this effort suggested that a single model structure
23 could provide reasonable fits to a variety of data evaluated for TCE and its major oxidative
24 metabolites TCA, TCOH, and TCOG. However, in many cases, different parameter values—
25 particularly for metabolism—were required for different studies, indicating significant
26 interindividual or interexperimental variability. In addition, these authors concluded that
27 dosimetry of DCA, conjugative metabolites, and metabolism in the lung remained highly
28 uncertain (Hack et al., 2006).

29 Subsequently, U.S. EPA conducted a detailed evaluation of the Hack et al. (2006) model
30 that included (1) additional model runs to improve convergence; (2) evaluation of posterior
31 distributions for population parameters; and (3) comparison of model predictions both with the
32 data used in the Hack et al. (2006) analysis as well as with additional data sets identified in the
33 literature. Appendix A provides the details and conclusions of this evaluation, briefly
34 summarized in Table 3-30, along with their pharmacokinetic implications.

This document is a draft for review purposes only and does not constitute Agency policy.

Table 3-30. Conclusions from evaluation of Hack et al. (2006), and implications for PBPK model development

Conclusion from evaluation of Hack et al. (2006) model	Implications for PBPK model parameters, structure, or data
<p>For some model parameters, posterior distributions were somewhat inconsistent with the prior distributions.</p> <ul style="list-style-type: none"> • For parameters with strongly informative priors (e.g., tissue volumes and flows), this may indicate errors in the model. • For many parameters, the prior distributions were based on visual fits to the same data. If the posteriors are inconsistent, then that means they priors were “inappropriately” informative, and, thus, the same data was used twice. 	<p>Re-evaluation of all prior distributions</p> <ul style="list-style-type: none"> • Update priors for parameters with independent data (physiological parameters, partition coefficients, <i>in vitro</i> metabolism), looking across all available data sets. • For priors without independent data (e.g., many metabolism parameters), use less informative priors (e.g., log-uniform distributions with wide bounds) so as prevent bias. <p>Evaluate modifications to the model structure, as discussed below.</p>
<p>A number of data sets involve TCE (i.a., portal vein), TCA (oral, i.v.), and TCOH (oral, i.v.) dosing routes that are not currently in the model, but could be useful for calibration.</p>	<ul style="list-style-type: none"> • Additional dosing routes can be added easily.
<p>TCE concentrations in blood, air, and tissues well-predicted only in rats, not in mice and humans. Specifically:</p> <ul style="list-style-type: none"> • In mice, the oral uptake model could not account for the time-course of several data sets. Blood TCE concentrations after inhalation consistently over-predicted. • In rats, tissue concentrations measured in data not used for calibration were accurately predicted. • In humans, blood and air TCE concentrations were consistently over-predicted in the majority of (but not all) data sets. 	<ul style="list-style-type: none"> • In mice, uptake from the stomach compartment (currently zero), but previously included in Abbas and Fisher (1997), may improve the model fit. • In mice and humans, additional extrahepatic metabolism, either presystemic (e.g., in the lung) or postsystemic (e.g., in the kidney) and/or a wash-in/wash-out effect may improve the model fit.
<p>Total metabolism appears well-predicted in rats and mice based on closed chamber data, but required significantly different V_{MAX} values between dose groups. Total recovery in humans (60–70%) is less than the model would predict. In all three species, the ultimate disposition of metabolism is uncertain. In particular, there are uncertainties in attributing the “missing” metabolism to</p> <ul style="list-style-type: none"> • GSH pathway (e.g., urinary mercapturates may only capture a fraction of the total flux; moreover, in Bernauer et al. (1996), excretion was still ongoing at end of collection period; model does not accurately depict time-course of mercapturate excretion). • Other hepatic oxidation (currently attributed to DCA). • Extrahepatic systemic metabolism (e.g., kidney). • Presystemic metabolism in the lung. • Additional metabolism of TCOH or TCA (see below). 	<ul style="list-style-type: none"> • Calibration of GSH pathway may be improved by utilizing <i>in vitro</i> data on liver and kidney GSH metabolism, adding a DCVG compartment to improve the prediction of the time-course for mercapturate excretion, and/or using the Lash et al. (1999b) blood DCVG in humans (necessitating the addition of a DCVG compartment). • Presystemic lung metabolism can only be evaluated if added to the model (<i>in vitro</i> data exists to estimate the V_{MAX} for such metabolism). In addition, a wash-in/wash-out effect (e.g., suggested by Greenberg et al., 1999) can be evaluated using a continuous breathing model that separately tracks inhaled and exhaled air, with adsorption/desorption in the respiratory tract. • Additional elimination pathways for TCOH and TCA can be added for evaluation.

Table 3-30. Conclusions from evaluation of Hack et al. (2006), and implications for PBPK model development (continued)

Conclusion from evaluation of Hack et al. (2006) model	Implications for PBPK model parameters, structure, or data
<p>TCA blood/plasma concentrations well predicted following TCE exposures in all species. However, there may be inaccuracies in the total flux of TCA production, as well as its disposition.</p> <ul style="list-style-type: none"> • In TCA dosing studies, the majority (>50%), but substantially <100%, was recovered in urine, suggesting significant metabolism of TCA. Although urinary TCA was well predicted in mice and humans (but not in rats), if TCA metabolism is significant, then this means that the current model underestimates the flux of TCE metabolism to TCA. • An improved TCOH/TCOG model may also provide better estimates of TCA kinetics (see below). <p>TCOH/TCOG concentrations and excretion were inconsistently predicted, particularly after TCOH dosing.</p> <ul style="list-style-type: none"> • In mice and rats, first-order clearance for TCOH glucuronidation was predicted to be greater than hepatic blood flow, which is consistent with a first pass effect that is not currently accounted for. • In humans, the estimated clearance rate for TCOH glucuronidation was substantially smaller than hepatic blood flow. However, the presence of substantial TCOG in blood (as opposed to free TCOH) in the Chiu et al. (2007) data are consistent with greater glucuronidation than predicted by the model. • In TCOH dosing studies, substantially <100% was recovered in urine as TCOG and TCA, suggesting another metabolism or elimination pathway. 	<ul style="list-style-type: none"> • Additional elimination pathways for TCOH and TCA can be added for evaluation. • The addition of a liver compartment for TCOH and TCOG would permit hepatic first-pass effects to be accounted for, as appears necessary for mice and rats.

i.a. = intra-arterial, i.v. = intravenous.

1 **3.5.4. Physiologically Based Pharmacokinetic (PBPK) Model for Trichloroethylene (TCE)**
2 **and Metabolites Used for This Assessment**

3 **3.5.4.1. Introduction**

4 Based on the recommendations of the NRC (2006) as well as additional analysis and
5 evaluation of the Hack et al. (2006) PBPK model, an updated PBPK model for TCE and
6 metabolites was developed for use in this risk assessment. The updated model is reported in
7 Evans et al. (2009) and Chiu et al. (2009), and the discussion below provides some details in
8 additional to the information in the published articles.

9 This updated model included modification of some of aspects of the Hack et al. (2006)
10 PBPK model structure, incorporation of additional *in vitro* and *in vivo* data for estimating model
11 parameters, and an updated hierarchical Bayesian population analysis of PBPK model
12 uncertainty and variability. In the subsections below, the updated PBPK model, and baseline
13 parameter values are described, and the approach and results of the analysis of PBPK model
14 uncertainty and variability. Appendix A provides more detailed descriptions of the model and
15 parameters, including background on hierarchical Bayesian analyses, model equations, statistical
16 distributions for parameter uncertainty and variability, data sources for these parameter values,
17 and the PBPK model code. Additional computer codes containing input files to the MCSim
18 program are available electronically.

19
20 **3.5.4.2. Updated Physiologically Based Pharmacokinetic (PBPK) Model Structure**

21 The updated TCE PBPK model is illustrated in Figure 3-7, with the major changes from
22 the Hack et al. (2006) model described here. The TCE submodel was augmented by the addition
23 of kidney and venous blood compartments, and an updated respiratory tract model that included
24 both metabolism and the possibility of local storage in the respiratory tissue. In particular, in the
25 updated lung, separate processes describing inhalation and exhalation allowed for adsorption and
26 desorption from tracheobronchial epithelium (wash-in/wash-out), with the possibility of local
27 metabolism as well. In addition, conjugative metabolism in the kidney was added, motivated by
28 the *in vitro* data on TCE conjugation described in Sections 3.3.3.2–3.3.3.3. With respect to
29 oxidation, a portion of the lung metabolism was assumed to produce systemically available
30 oxidative metabolites, including TCOH and TCA, with the remaining fraction assumed to be
31 locally cleared. This is clearly a lumping of a multistep process, but the lack of data precludes
32 the development of a more sequential model. TCE oxidation in the kidney was not included
33 because it was not likely to constitute a substantial flux of total TCE oxidation given the much
34 lower CYP activity in the kidney relative to the liver (Cummings et al., 1999, 2000) and the

1 greater tissue mass of the liver.¹ In addition, liver compartments were added to the TCOH and
2 TCOG submodels to account properly for first-pass hepatic metabolism, which is important for
3 consistency across routes of exposure. Furthermore, additional clearance pathways of TCOH
4 and TCA was added to their respective submodels. With respect to TCE conjugation, in humans,
5 an additional DCVG compartment was added between TCE conjugation and production of
6 DCVC. In addition, it should be noted that the urinary clearance of DCVC represents a lumping
7 of *N*-acetylation of DCVC, deacetylation of NAcDCVC, and urinary excretion NAcDCVC, and
8 that the bioactivation of DCVC represents a lumping of thiol production from DCVC by beta-
9 lyase, sulfoxidation of DCVC by FMO3, and sulfoxidation of NAcDCVC by CYP3A. Such
10 lumping was used because these processes are not individually identifiable given the available
11 data.

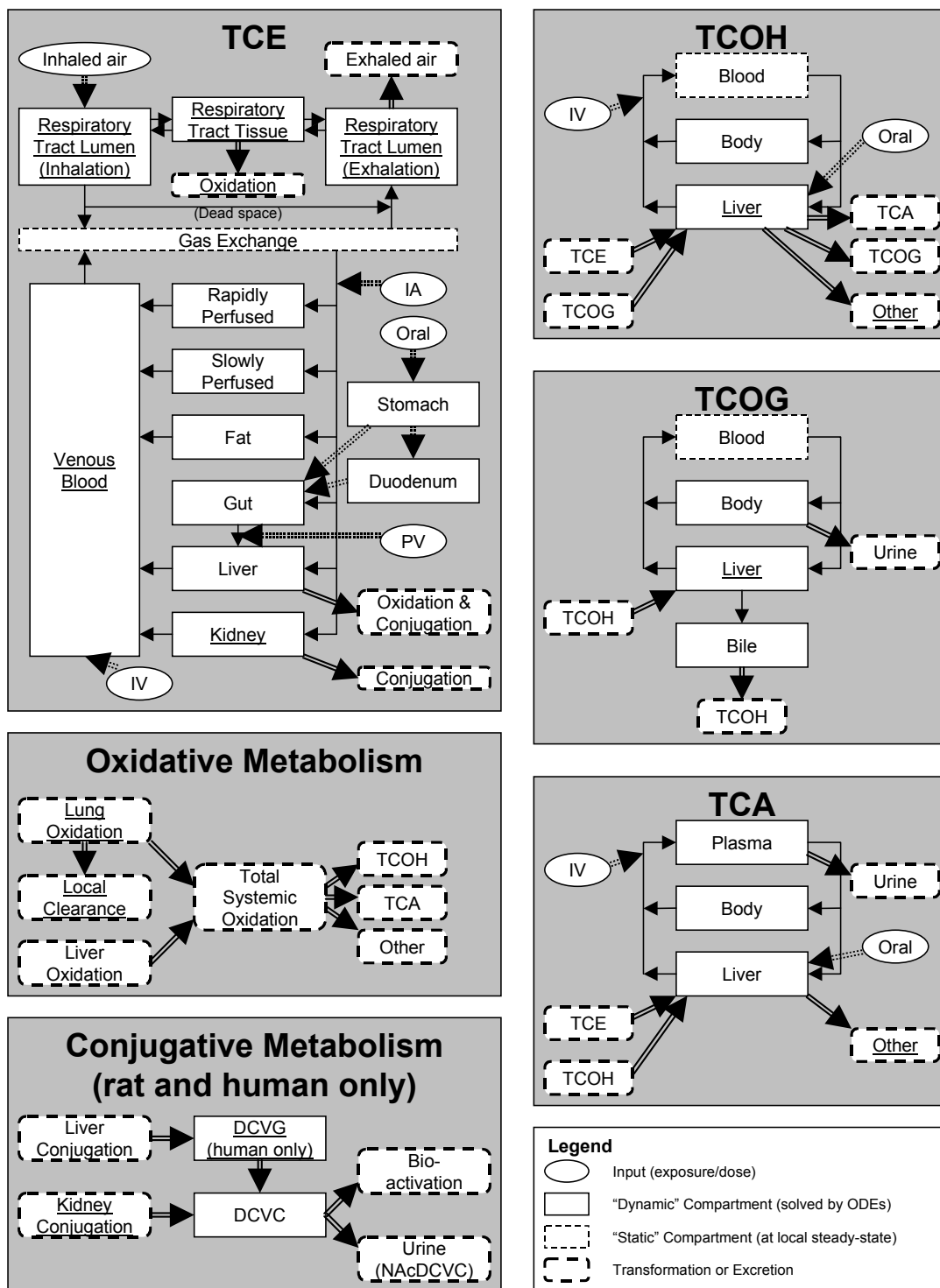
12

13 **3.5.4.3. *Specification of Physiologically Based Pharmacokinetic (PBPK) Model Parameter*** 14 ***Prior Distributions***

15 Point estimates for PBPK model parameters (“baseline values”), used as central estimates
16 in the prior distributions for population mean parameters in the hierarchical Bayesian statistical
17 model (see Appendix A), were developed using standard methodologies to ensure biological
18 plausibility, and were a refinement of those used in Hack et al. (2006). Because the Bayesian
19 parameter estimation methodology utilizes the majority of the useable *in vivo* data on TCE
20 pharmacokinetics, all baseline parameter estimates were based solely on measurements
21 independent of the *in vivo* data. This avoids using the same data in both the prior and the
22 likelihood. These parameters were, in turn, given truncated normal or lognormal distributions
23 for the uncertainty in the population mean. If no independent data were available, as is the case
24 for many “downstream” metabolism parameters, then no baseline value was specified, and a
25 noninformative prior was used. Section 3.5.5.4, below, discusses the updating of these
26 noninformative priors using interspecies scaling.

¹ The extraction ratio for kidney oxidation is likely to be very low, as shown by the following calculation in rats and humans. In rats, the *in vitro* kidney oxidative clearance (V_{MAX}/K_M) rate (Table 3-13, converting units) is 1.64×10^{-7} L/min/mg microsomal protein. Converting units using 16 mg microsomal protein to g tissue (Bong et al., 1985) gives a clearance rate per unit tissue mass of 2.6×10^{-6} L/min/g kidney. This is more than a 1000-fold smaller than the kidney specific blood flow rate of 6.3×10^{-3} L/min/g kidney (Brown et al., 1997). In humans, an *in vitro* clearance rate of 6.5×10^{-8} L/min/mg microsomal protein is derived from the only detectable *in vitro* oxidation rate from Cummings and Lash (2000) of 0.13 nmol/minute/mg protein at 2 mM. Using the same conversion from microsomal protein to tissue mass gives a clearance rate of 1.0×10^{-6} L/min/g kidney, more than 1000-fold smaller than the kidney specific blood flow of 3.25×10^{-3} L/min/g kidney (Brown et al., 1997). No data on kidney metabolism are available in mice, but the results are likely to be similar. Therefore, even accounting for uncertainties of up to an order of magnitude in the *in vitro*-to-*in vivo* conversion, kidney oxidation should contribute negligibly to total metabolism of TCE.

This document is a draft for review purposes only and does not constitute Agency policy.



1
2
3
4

Figure 3-7. Overall structure of PBPK model for TCE and metabolites used in this assessment. Boxes with underlined labels are additions or modifications of the Hack et al. (2006) model, which are discussed in Table 3-31.

This document is a draft for review purposes only and does not constitute Agency policy.

1
2
3

Table 3-31. Discussion of changes to the Hack et al. (2006) PBPK model implemented for this assessment

Change to Hack et al. (2006) PBPK model	Discussion
TCE respiratory tract compartments and metabolism	<p><i>In vitro</i> data indicate that the lung (at least in the mouse) has a significant capacity for oxidizing TCE. However, in the Hack et al. (2006) model, respiratory metabolism was blood flow-limited. The model structure used was inconsistent with other PBPK models in which the same mechanism for respiratory metabolism is assumed (e.g., styrene, Sarangapani et al. [2003]). In these models, the main source of exposure in the respiratory tract tissue is from the respiratory lumen—not from the tracheobronchial blood flow. In addition, a wash-in/wash-out effect has also been postulated. The current structure, which invokes a “continuous breathing” model with separate “inhaled” and “exhaled” respiratory lumens, can accommodate both respiratory metabolism due to exposure from the respiratory lumen as well as a wash-in/wash-out effect in which there is temporary storage in the respiratory tract tissue.</p> <p>Moreover, preliminary analyses indicated that these changes to the model structure allowed for a substantially better fit to mouse closed chamber data under the requirement that all the dose levels are modeled using the same set of parameters.</p>
TCE kidney compartment	<p><i>In vitro</i> data indicate that the kidney has a significant capacity for conjugating TCE with GSH.</p>
TCE venous blood compartment	<p>Many PBPK models have used a separate blood compartment. It was believed to be potentially important and feasible to implement here because (1) TCE blood concentrations were often not well predicted by the Hack et al. (2006) model; (2) the TCA submodel has a plasma compartment, which is a fraction of the blood volume based on the blood volume; (3) adequate independent information on blood volume is available; and (4) the updated model was to include the intravenous route of exposure.</p>
TCOH and TCOG liver compartments	<p>In mice and rats, the Hack et al. (2006) model estimated a rate of TCOH glucuronidation that exceeded hepatic blood flow (all glucuronidation is assumed to occur in the liver), indicated a significant first-pass effect. Therefore, a separate liver compartment is necessary to account properly for hepatic first-pass.</p>
TCOH and TCA “other” elimination pathways	<p>Mass-balance studies with TCOH and TCA dosing indicated that, although the majority of TCOH and TCA are excreted in urine, the amount is still substantially less than 100%. Therefore, additional elimination of TCOH and TCA must exist and should be accounted for.</p>
DCVG compartment (human model only)	<p>Blood DCVG data in humans exist as part of the Fisher et al. (1998) experiments, reported in Lash et al. (1999b), and a DCVG compartment is necessary in order to utilize those data.</p>

4
5

1 In keeping with standard practice, many of the PBPK model parameters were “scaled” by
2 body or organ weights, cardiac output, or allometrically by an assumed (fixed) power of body
3 weight. Metabolic capacity and cardiac output were scaled by the $\frac{3}{4}$ power of body weight and
4 rate coefficients were scaled by the $\frac{1}{4}$ power of body weight, in keeping with general
5 expectations as to the relationship between metabolic rates and body size (U.S. EPA, 1992; West
6 et al., 2002) So as to ensure a consistent model structure across species as well as improve the
7 performance of the MCMC algorithm, parameters were further scaled to the baseline point-
8 estimates where available, as was done by Hack et al. (2006). For example, to obtain the actual
9 liver volume in liters, a point estimate is first obtained by multiplying the fixed, species-specific
10 baseline point estimate for the fractional liver volume by a fixed body weight (measured or
11 species-specific default) with density of 1 kg per liter assumed to convert from kg to liters.
12 Then, any deviation from this point estimate is represented by multiplying by a separate “scaled”
13 parameter VLivC that has a value of 1 if there is no deviation from the point estimate. These
14 “scaled” parameters are those estimated by the MCMC algorithm, and for which population
15 means and variances are estimated.

16 Baseline physiological parameters were re-estimated based on the updated tissue lumping
17 (e.g., separate blood and kidney compartments) using the standard references ICRP (2002) and
18 Brown et al. (1997). For a few of these parameters, such as hematocrit and respiratory tract
19 volumes in rodents, additional published sources were used as available, but no attempt was
20 made to compile a comprehensive review of available measurements. In addition, a few
21 parameters, such as the slowly perfused volume, were calculated rather than sampled in order to
22 preserve total mass or flow balances.

23 For chemical-specific distribution and metabolism parameters, *in vitro* data from various
24 sources were used. Where multiple measurements had been made, as was the case for many
25 partition coefficients, TCA plasma protein binding parameters, and TCE metabolism, different
26 results were pooled together, with their uncertainty reflected appropriately in the prior
27 distribution. Such *in vitro* measurements were available for most chemical partition coefficients,
28 except for those for TCOG (TCOH used as a proxy) and DCVG. There were also such data to
29 develop baseline values for the oxidative metabolism of TCE in the liver (V_{MAX} and K_M), the
30 relative split in TCE oxidation between formation of TCA and TCOH, and the V_{MAX} for TCE
31 oxidation in the lung. All other metabolism parameters were not given baseline values and
32 needed to be estimated from the *in vivo* data.

1 **3.5.4.4. Dose Metric Predictions**

2 The purpose of this PBPK model is to make predictions of internal dose in rodents used
3 in toxicity studies or in humans in the general population, and not in the groups or individuals for
4 which pharmacokinetic data exist. Therefore, to evaluate its predictive utility for risk
5 assessment, a number of dose metrics were selected for simulation in a “generic” mouse, rat, or
6 human, summarized in Table 3-32. The parent dose metric was AUC in blood. TCE metabolism
7 dose metrics (i.e., related to the amount metabolized) included both total metabolism,
8 metabolism splits between oxidation versus conjugation, oxidation in the liver versus the lung,
9 the amount of oxidation in the liver to products *other* than TCOH and TCA, and the amount of
10 TCA produced. These metabolism rate dose metrics are scaled by body weight in the case of
11 TCA produced, by the metabolizing tissue volume and by body weight to the $\frac{3}{4}$ power in the
12 cases of the lung and “other” oxidation in the liver, and by body weight to the $\frac{3}{4}$ power only in
13 other cases. With respect to the oxidative metabolites, liver concentrations of TCA and blood
14 concentrations of free TCOH were used. With respect to conjugative metabolites, the dose
15 metrics considered were total GSH metabolism scaled by body weight to the $\frac{3}{4}$ power, and the
16 amount of DCVC bioactivated (rather than excreted in urine) per unit body weight to the $\frac{3}{4}$
17 power and per unit kidney mass.

18 All dose metrics are converted to daily or weekly averages based on simulations lasting
19 10 weeks for rats and mice and 100 weeks for humans. These simulation times were the shortest
20 for which additional simulation length did not add substantially to the average (i.e., less than a
21 few percent change with a doubling of simulation time).

22 23 **3.5.5. Bayesian Estimation of Physiologically Based Pharmacokinetic (PBPK) Model** 24 **Parameters, and Their Uncertainty and Variability**

25 **3.5.5.1. Updated Pharmacokinetic Database**

26 An extensive search was made for data not previously considered in the PBPK modeling
27 of TCE and metabolites, with a few studies identified or published subsequent to the review by
28 Chiu et al. (2006). The studies considered for analysis are listed in Tables 3-33–3-34, along with
29 an indication of whether and how they were used.²

² Additional in vivo data on TCE or metabolites published after the PBPK modeling was completed (reported in Sweeney et al., 2009; Liu et al., 2009; and Kim et al., 2009) was evaluated separately, and discussed in Appendix A.

This document is a draft for review purposes only and does not constitute Agency policy.

1
2

Table 3-32. PBPK model-based dose metrics

Abbreviation	Description
ABioactDCVCBW34	Amount of DCVC bioactivated in the kidney (mg) per unit body weight ^{3/4} (kg ^{3/4})
ABioactDCVCKid	Amount of DCVC bioactivated in the kidney (mg) per unit kidney mass (kg)
AMetGSHBW34	Amount of TCE conjugated with GSH (mg) per unit body weight ^{3/4} (kg ^{3/4})
AMetLiv1BW34	Amount of TCE oxidized in the liver per unit body weight ^{3/4} (kg ^{3/4})
AMetLivOtherBW34	Amount of TCE oxidized to metabolites other than TCA and TCOH in the liver (mg) per unit body weight ^{3/4} (kg ^{3/4})
AMetLivOtherLiv	Amount of TCE oxidized to metabolites other than TCA and TCOH in the liver (mg) per unit liver mass (kg)
AMetLngBW34	Amount of TCE oxidized in the respiratory tract (mg) per unit body weight ^{3/4} (kg ^{3/4})
AMetLngResp	Amount of TCE oxidized in the respiratory tract (mg) per unit respiratory tract tissue mass (kg)
AUCCBld	Area under the curve of the venous blood concentration of TCE (mg-h/L)
AUCCTCOH	Area under the curve of the blood concentration of TCOH (mg-h/L)
AUCLivTCA	Area under the curve of the liver concentration of TCA (mg-h/L)
TotMetabBW34	Total amount of TCE metabolized (mg) per unit body weight ^{3/4} (kg ^{3/4})
TotOxMetabBW34	Total amount of TCE oxidized (mg) per unit body weight ^{3/4} (kg ^{3/4})
TotTCAInBW	Total amount of TCA produced (mg) per unit body weight (kg)

3

This document is a draft for review purposes only and does not constitute Agency policy.

Table 3-33. Rodent studies with pharmacokinetic data considered for analysis

Reference	Species (strain)	Sex	TCE exposures	Other exposures	Calibration	Validation	Not used	Comments
Mouse studies								
Abbas et al., 1996	Mouse (B6C3F1)	M	--	CH i.v.			√	CH not in model.
Abbas and Fisher, 1997	Mouse (B6C3F1)	M	Oral (corn oil)	--	√*			
Abbas et al., 1997	Mouse (B6C3F1)	M	--	TCOH, TCA i.v.	√			
Barton et al., 1999	Mouse (B6C3F1)	M	--	DCA i.v. and oral (aqueous)			√	DCA not in model.
Birmer et al., 1993	Mouse (NMRI)	M+F	Gavage	--			√	Only urine concentrations available, not amount.
Fisher and Allen, 1993	Mouse (B6C3F1)	M+F	Gavage (corn oil)	--	√			
Fisher et al., 1991	Mouse (B6C3F1)	M+F	Inhalation	--	√*			
Green and Prout, 1985	Mouse (B6C3F1)	M	Gavage (corn oil)	TCA i.v.	√			
Greenberg et al., 1999	Mouse (B6C3F1)	M	Inhalation	--	√*			
Larson and Bull, 1992a	Mouse (B6C3F1)	M	--	DCA, TCA oral (aqueous)	√			Only data on TCA dosing was used, since DCA is not in the model.
Larson and Bull, 1992b	Mouse (B6C3F1)	M	Oral (aqueous)	--	√			
Merdink et al., 1998	Mouse (B6C3F1)	M	i.v.	CH i.v.	√			Only data on TCE dosing was used, since CH is not in the model.

Table 3-33. Rodent studies with pharmacokinetic data considered for analysis (continued)

Reference	Species (strain)	Sex	TCE exposures	Other exposures	Calibration	Validation	Not used	Comments
Prout et al., 1985	Mouse (B6C3F1, Swiss)	M	Gavage (corn oil)	--	√*			
Templin et al., 1993	Mouse (B6C3F1)	M	Oral (aqueous)	TCA oral	√*			
Rat studies								
Andersen et al., 1987	Rat (F344)	M	Inhalation	--		√*		
Barton et al., 1995	Rat (S-D)	M	Inhalation	--			√	Initial chamber concentrations unavailable, so not used.
Bernauer et al., 1996	Rat (Wistar)	M	Inhalation	--	√*			
Birner et al., 1993	Rat (Wistar, F344)	M+F	Gavage (ns)	--			√	Only urine concentrations available, not amount.
Birner et al., 1997	Rat (Wistar)	M+F	--	DCVC i.v.			√	Single dose, route does not recapitulate how DCVC is formed from TCE, excreted NAcDCVC ~100-fold greater than that from relevant TCE exposures (Bernauer et al., 1996).
Bruckner et al., unpublished	Rat (S-D)	M	Inhalation	--		√		Not published, so not used for calibration. Similar to Keys et al. (2003) data.
Dallas et al., 1991	Rat (S-D)	M	Inhalation	--	√			

Table 3-33. Rodent studies with pharmacokinetic data considered for analysis (continued)

Reference	Species (strain)	Sex	TCE exposures	Other exposures	Calibration	Validation	Not used	Comments
D'Souza et al., 1985	Rat (S-D)	M	i.v., oral (aqueous)	--			√	Only TCE blood measurements, and ≥10-fold greater than other similar studies.
Fisher et al., 1989	Rat (F344)	F	Inhalation	--	√			
Fisher et al., 1991	Rat (F344)	M+F	Inhalation	--	√*	√		Experiment with blood only data not used for calibration.
Green and Prout, 1985	Rat (Osborne-Mendel)	M	Gavage (corn oil)	TCA gavage (aqueous)	√			
Hissink et al., 2002	Rat (Wistar)	M	Gavage (corn oil), i.v.	--	√			
Jakobson et al., 1986	Rat (S-D)	F	Inhalation	Various pretreatments (oral)		√		Pretreatments not included. Only blood TCE data available.
Kaneko et al., 1994	Rat (Wistar)	M	Inhalation	Ethanol pretreatment (oral)	√			Pretreatments not included.
Keys et al., 2003	Rat (S-D)	M	Inhalation, oral (aqueous), i.a.	--	√			
Kimmerle and Eben, 1973a	Rat (Wistar)	M	Inhalation	--	√			
Larson and Bull, 1992a	Rat (F344)	M	--	DCA, TCA oral (aqueous)	√			Only TCA dosing data used, since DCA is not in the model.
Larson and Bull, 1992b	Rat (S-D)	M	Oral (aqueous)	--	√*			
Lash et al., 2006	Rat (F344)	M+F	Gavage (corn oil)	--			√	Highly inconsistent with other studies.

Table 3-33. Rodent studies with pharmacokinetic data considered for analysis (continued)

Reference	Species (strain)	Sex	TCE exposures	Other exposures	Calibration	Validation	Not used	Comments
Lee et al., 1996	Rat (S-D)	M	Arterial, venous, portal, stomach injections	--		√		Only blood TCE data available.
Lee et al., 2000a, b	Rat (S-D)	M	Stomach injection, i.v., p.v.	p-nitrophenol pretreatment (i.a.)	√	√		Pretreatments not included. Only experiments with blood and liver data used for calibration.
Merdink et al., 1999	Rat (F344)	M	--	CH, TCOH i.v.	√			TCOH dosing used; CH not in model.
Poet et al., 2000	Rat (F344)	M	Dermal	--			√	Dermal exposure not in model.
Prout et al., 1985	Rat (Osborne-Mendel, Wistar)	M	Gavage (corn oil)	--	√*			
Saghir et al., 2002	Rat (F344)	M	--	DCA i.v., oral (aqueous)			√	DCA not in model
Simmons et al., 2002	Rat (Long-Evans)	M	Inhalation	--	√			
Stenner et al., 1997	Rat (F344)	M	intraduodenal	TCOH, TCA i.v.	√			
Templin et al., 1995	Rat (F344)	M	Oral (aqueous)	--	√*			
Thrall et al., 2000	Rat (F344)	M	i.v., i.p.	with toluene			√	Only exhaled breath data available from i.v. study. i.p. dosing not in model.
Yu et al., 2000	Rat (F344)	M	--	TCA i.v.	√			

*Part or all of the data in the study was used for calibration in Hack et al. (2006).

i.a. = intra-arterial, i.p. = intraperitoneal, i.v. = intravenous, p.v. = intraperivenous.

Table 3-34. Human studies with pharmacokinetic data considered for analysis

Reference	Species (number of individuals)	Sex	TCE exposures	Other exposures	Calibration	Validation	Not used	Comments
Bartonicek, 1962	Human (n = 8)	M+F	Inhalation	--		√		Sparse data, so not included for calibration to conserve computational resources.
Bernaer et al., 1996	Human	M	Inhalation	--	√ ^a			Grouped data, but unique in that includes NAcDCVC urine data.
Bloemen et al., 2001	Human (n = 4)	M	Inhalation	--		√		Sparse data, so not included for calibration to conserve computational resources.
Chiu et al., 2007	Human (n = 6)	M	Inhalation	--	√			
Ertle et al., 1972	Human	M	Inhalation	CH oral			√	Very similar to Muller data.
Fernandez et al., 1977	Human	M	Inhalation	--		√		
Fisher et al., 1998	Human (n = 17)	M+F	Inhalation	--	√ ^a			
Kimmerle and Eben, 1973b	Human (n = 12)	M+F	Inhalation	--	√			
Lapare et al., 1995	Human (n = 4)	M+F	Inhalation	--		√ ^b		Complex exposure patterns, and only grouped data available for urine, so used for validation.
Lash et al., 1999b	Human	M+F	Inhalation	--	√			Grouped only, but unique in that DCVG blood data available (same individuals as Fisher et al. [1998]),
Monster et al., 1976	Human (n = 4)	M	Inhalation	--	√ ^b			Experiments with exercise not included.
Monster et al., 1979	Human	M	Inhalation	--		√ ^a		Grouped data only.
Muller et al., 1972	Human	ns	Inhalation	--			√	Same data also included in Muller et al. (1975).

Table 3-34. Human studies with pharmacokinetic data considered for analysis (continued)

Reference	Species (number of individuals)	Sex	TCE exposures	Other exposures	Calibration	Validation	Not used	Comments
Muller et al., 1974	Human	M	Inhalation	CH, TCA, TCOH oral	√	√ ^a		TCA and TCOH dosing data used for calibration, since it is rare to have metabolite dosing data. TCE dosing data used for validation, since only grouped data available. CH not in model.
Muller et al., 1975	Human	M	Inhalation	Ethanol oral		√ ^a		Grouped data only.
Paycok et al., 1945	Human (n = 3)	ns	--	TCA i.v.	√			
Poet et al., 2000	Human	M+F	Dermal	--				Dermal exposure not in model.
Sato et al., 1977	Human	M	Inhalation	--		√		
Stewart et al., 1970	Human	ns	Inhalation	--		√ ^a		
Treibig et al., 1976	Human	ns	Inhalation	--		√ ^a		
Vesterberg and Astrand, 1976	Human	M	Inhalation	--			√	All experiments included exercise, so were not included.

^aPart or all of the data in the study was used for calibration in Hack et al. (2006).

^bGrouped data from this study was used for calibration in Hack et al. (2006), but individual data was used here.

1 The least amount of data was available for mice, so an effort was made to include as
2 many studies as feasible for use in calibrating the PBPK model parameters. Exceptions include
3 mouse studies with CH or DCA dosing, since those metabolites are not included in the PBPK
4 model. In addition, the Birner et al. (1993) data only reported urine concentrations, not the
5 amount excreted in urine. Because there is uncertainty as to total volume of urine excreted, and
6 over what time period, these data were not used. Moreover, many other studies had urinary
7 excretion data, so this exclusion should have minimal impact. Several data sets not included by
8 Hack et al. (2006) were used here. Of particular importance was the inclusion of TCA and
9 TCOH dosing data from Abbas et al. (1997), Green and Prout (1985), Larson and Bull (1992a),
10 and Templin et al. (1993).

11 A substantial amount of data are available in rats, so some data that appeared to be
12 redundant was excluded from the calibration set and saved for comparison with posterior
13 predictions (a “validation” set). In particular, those used for “validation” are one closed-chamber
14 experiment (Andersen et al., 1987), several data sets with only TCE blood data (D’Souza et al.,
15 1985; Jakobson et al., 1986; Lee et al., 1996, and selected time courses from Fisher et al. [1991]
16 and Lee et al. [2000a, b]), and one unpublished data set (Bruckner et al., unpublished). The
17 Andersen et al. (1987) data was selected randomly from the available closed chamber data, while
18 the other data sets were selected because they unpublished or because they more limited in scope
19 (e.g., TCE blood only) and so were not as efficient for use in the computationally-intensive
20 calibration stage. As with the mouse analyses, TCA and TCOH dosing data were incorporated to
21 better calibrate those pathways.

22 The human pharmacokinetic database of controlled exposure studies is extensive but also
23 more complicated. For the majority of the studies, only grouped or aggregated data were
24 available, and most of those data were saved for “validation” since there remained a large
25 number of studies for which individual data were available. However, some data that may be
26 uniquely informative are only available in grouped form, in particular DCVG blood
27 concentrations, NAcDCVC urinary excretion, and data from TCA and TCOH dosing. In
28 addition, several human data sets, while having individual data, involved sparse collection at
29 only one or a few time points per exposure (Bartonicek, 1962; Bloemen et al., 2001) and were
30 subsequently excluded to conserve computational resources. Lapare et al. (1995), which
31 involved multiple, complex exposure patterns over the course of a month and was missing the
32 individual urine data, was also excluded due to the relatively low amount of data given the large
33 computational effort required to simulate it. Several studies also investigated the effects of
34 exercise during exposure on human TCE toxicokinetics. The additional parameters in a model
35 including exercise would need to characterize the changes in cardiac output, alveolar ventilation,

This document is a draft for review purposes only and does not constitute Agency policy.

1 and regional blood flow as well as their inter-individual variability, and would have further
2 increased the computational burden. Therefore, it was decided that such data would be excluded
3 from this analysis. Even with these exclusions, data on a total of 42 individuals, some involving
4 multiple exposures, were included in the calibration.

6 **3.5.5.2. Updated Hierarchical Population Statistical Model**

7 Generally, only aggregated pharmacokinetic data (arithmetic mean and standard
8 deviation or standard error) are available from rodent studies. In the Hack et al. (2006) model,
9 each simulation was treated as a separate observational unit, so different dosing levels within the
10 same study were treated separately and assigned different PBPK model parameters. However,
11 the dose-response data are generally also only separated by sex and strain, and otherwise
12 aggregated, so the variability that is of interest is interstudy (e.g., lot-to-lot), interstrain, and
13 intersex variability, rather than interindividual variability. In addition, any particular lot of
14 animals within a study, which are generally inbred and kept under similarly controlled
15 conditions, are likely to be relatively homogeneous. Therefore, in the revised model, for rodents,
16 different animals of the same sex and strain in the same study (or series of studies conducted
17 simultaneously) were treated as identical, and grouped together. Thus, the predictions from the
18 population model in rodents simulate “average” pharmacokinetics for a particular “lot” of
19 rodents of a particular species, strain, and sex.

20 In humans, however, interindividual variability is of interest, and, furthermore,
21 substantial individual data are available in humans. However, in some studies, the same
22 individual was exposed more than once, and, so, those data should be grouped together (in the
23 Hack et al. [2006] model, they were treated as different “individuals”). Because the primary
24 interest here is chronic exposure, and because it would add substantially to the computational
25 burden, interoccasion variability—changes in pharmacokinetic parameters in a single individual
26 over time—is not addressed. Thus, the predictions from the population model in humans are the
27 “average” across different occasions for a particular individual (adult).

28 As discussed in Section 3.3.3.1, sex and (in rodents) strain differences in oxidative
29 metabolism were modest or minimal. While some sex-differences have been noted in GSH
30 metabolism (see Sections 3.3.3.2.7–3.3.3.2.8), almost all of the available *in vivo* data is in males,
31 making it more difficult to statistically characterize that difference with PBPK modeling.
32 Therefore, within a species, different sexes and (in rodents) strains were considered to be drawn
33 from a single, species-level population.

34 Figure A-1 in Appendix A illustrates the hierarchical structure. Informative prior
35 distributions reflecting the uncertainty in the population mean and variance, detailed in

This document is a draft for review purposes only and does not constitute Agency policy.

1 Appendix A, were updated from those used in Hack et al. (2006) based on an extensive analysis
2 of the available literature. Section 3.5.5.3, next, discusses specification of prior distributions in
3 the case where no data independent of the calibration data exist.

4 5 **3.5.5.3. Use of Interspecies Scaling to Update Prior Distributions in the Absence of Other** 6 **Data**

7 For many metabolic parameters, little or no *in vitro* or other prior information is available
8 to develop prior distributions. Initially, for such parameters, noninformative priors in the form of
9 log-uniform distributions with a range spanning at least 10^4 were specified. However, in the
10 time available for analysis (up to about 100,000 iterations), only for the mouse did all these
11 parameters achieve adequate convergence. This suggests that some of these parameters are
12 poorly identified for the rat and human. Additional preliminary runs indicated replacing the log-
13 uniform priors with lognormal priors and/or requiring more consistency between species could
14 improve identifiability sufficiently for adequate convergence. However, an objective method of
15 “centering” the lognormal distributions that did not rely on the *in vivo* data (e.g., via visual fitting
16 or limited optimization) being calibrated against was necessary in order to minimize potential
17 bias.

18 Therefore, the approach taken was to consider three species sequentially, from mouse to
19 rat to human, and to use interspecies scaling to update the prior distributions across species. This
20 sequence was chosen because the models are essentially “nested” in this order, the rat model
21 adds to the mouse model the “downstream” GSH conjugation pathways, and the human model
22 adds to the rat model the intermediary DCVG compartment. Therefore, for those parameters
23 with little or no independent data *only*, the mouse posteriors were used to update the rat priors,
24 and both the mouse and rat posteriors were used to update the human priors. Table 3-35 contains
25 a list of the parameters for which this scaling was used to update prior distributions. The scaling
26 relationship is defined by the “scaled parameters” listed in Appendix A (see Section A.4.1,
27 Table A-4), and generally follows standard practice. For instance, V_{MAX} and clearance rates
28 scale by body weight to the $3/4$ power, whereas K_M values are assumed to not scale, and rate
29 constants (inverse time units) scale by body weight to the $-1/4$ power.

Table 3-35. Parameters for which scaling from mouse to rat, or from mouse and rat to human, was used to update the prior distributions

Parameter with no or highly uncertain <i>a priori</i> data	Mouse → Rat	Rat → Human	Mouse+ Rat → Human	Comments
Respiratory lumen→tissue diffusion flow rate	√		√	No <i>a priori</i> information
TCOG body/blood partition coefficient	√		√	Prior centered on TCOH data, but highly uncertain
TCOG liver/body partition coefficient	√		√	Prior centered on TCOH data, but highly uncertain
Fraction of hepatic TCE oxidation not to TCA+TCOH	√		√	No <i>a priori</i> information
V _{MAX} for hepatic TCE GSH conjugation	√			Rat data on at 1 and 2 mM. Human data at more concentrations, so V _{MAX} and K _M can be estimated
K _M for hepatic TCE GSH conjugation	√			
V _{MAX} for renal TCE GSH conjugation	√			Rat data on at 1 and 2 mM. Human data at more concentrations, so V _{MAX} and K _M can be estimated
K _M for renal TCE GSH conjugation	√			
V _{MAX} for Tracheo-bronchial TCE oxidation	√		√	Prior based on activity at a single concentration
K _M for Tracheo-bronchial TCE oxidation	√		√	No <i>a priori</i> information
Fraction of respiratory oxidation entering systemic circulation	√		√	No <i>a priori</i> information
V _{MAX} for hepatic TCOH→TCA	√		√	No <i>a priori</i> information
K _M for hepatic TCOH→TCA	√		√	No <i>a priori</i> information
V _{MAX} for hepatic TCOH→TCOG	√		√	No <i>a priori</i> information
K _M for hepatic TCOH→TCOG	√		√	No <i>a priori</i> information
Rate constant for hepatic TCOH→other	√		√	No <i>a priori</i> information
Rate constant for TCA plasma→urine	√		√	Prior centered at GFR, but highly uncertain
Rate constant for hepatic TCA→other	√		√	No <i>a priori</i> information
Rate constant for TCOG liver→bile	√		√	No <i>a priori</i> information
Lumped rate constant for TCOG bile→TCOH liver	√		√	No <i>a priori</i> information
Rate constant for TCOG→urine	√		√	Prior centered at GFR, but highly uncertain
Lumped rate constant for DCVC→Urinary NAcDCVC		√		Not included in mouse model
Rate constant for DCVC bioactivation		√		Not included in mouse model

See Appendix A, Table A-4 for scaling relationships.

1 The scaling model is given explicitly as follows. If θ_i are the “scaled” parameters
2 (usually also natural-log-transformed) that are actually estimated, and A is the “universal”
3 (species-independent) parameter, then $\theta_i = A + \varepsilon_i$, where ε_i is the species-specific “departure”
4 from the scaling relationship, assumed to be normally distributed with variance σ_ε^2 . Therefore,
5 the mouse model gives an initial estimate of “A,” which is used to update the prior distribution
6 for $\theta_r = A + \varepsilon_r$ in the rat. The rat and mouse together then give a “better” estimate of A, which is
7 used to update the prior distribution for $\theta_h = A + \varepsilon_h$ in the human, with the assumed distribution
8 for ε_h . The mathematical details are given in Appendix A, but two key points in this model are
9 worth noting here:

- 11 • It is known that interspecies scaling is not an exact relationship, and that, therefore, in
12 any *particular* case it may either over- or underestimate. Therefore, the variance in the
13 new priors reflect a combination of (1) the uncertainty in the “previous” species’
14 posteriors as well as (2) a “prediction error” that is distributed lognormally with
15 geometric standard deviation (GSD) of 3.16-fold, so that the 95% confidence range about
16 the central estimate spans 100-fold. This choice was dictated partially by practicality, as
17 larger values of the GSD used in preliminary runs did not lead to adequate convergence
18 within the time available for analysis.
- 19 • The rat posterior is a product of its prior (which is based on the mouse posterior) and its
20 likelihood. Therefore, using the rat and mouse posteriors together to update the human
21 priors would use the mouse posterior “twice.” Therefore, the rat posterior is
22 disaggregated into its prior and its likelihood using a lognormal approximation (since the
23 prior is lognormal), and only the (approximate) likelihood is used along with the mouse
24 posterior to develop the human prior.

25
26 With this methodology for updating the prior distributions, adequate convergence was
27 achieved for the rat and human after 110,000~140,000 iterations (discussed further below).

28 29 **3.5.5.4. Implementation**

30 The PBPK model was coded in for use in the MCSim software (version 5.0.0), which was
31 developed particularly for implementing MCMC simulations. As a quality control (QC) check,
32 results were checked against the original Hack et al. (2006) model, with the original structures
33 restored and parameter values made equivalent, and the results were within the error tolerances
34 of the ordinary differential equation (ODE) solver after correcting an error in the Hack et al.
35 (2006) model for calculating the TCA liver plasma flow. In addition, the model was translated to
36 MatLab (version 7.2.0.232) with simulation results checked and found to be within the error
37 tolerances of the ODE solver (ode15s). Mass balances were also checked using the baseline

1 parameters, as well as parameters from preliminary MCMC simulations, and found to be within
2 the error tolerances of the ODE solver. Appendix A contains the MCSim model code.

4 **3.5.6. Evaluation of Updated Physiologically Based Pharmacokinetic (PBPK) Model**

5 **3.5.6.1. Convergence**

6 As in previous similar analyses (Gelman et al., 1996; Bois 2000a, b; Hack et al., 2006;
7 David et al., 2006), the potential scale reduction factor “ R ” is used to determine whether different
8 independent MCMC chains have converged to a common distribution. The R diagnostic is
9 calculated for each parameter in the model, and represents the factor by which the standard
10 deviation or other measure of scale of the posterior distribution (such as a confidence interval
11 [CI]) may potentially be reduced with additional samples (Gelman et al., 2004). This
12 convergence diagnostic declines to 1 as the number of simulation iterations approaches infinity,
13 so values close to 1 indicate approximate convergence, with values of 1.1 and below commonly
14 considered adequate (Gelman et al., 2004). However, as an additional diagnostic, the
15 convergence of model dose metric predictions was also assessed. Specifically, dose metrics for a
16 number of generic exposure scenarios similar to those used in long-term bioassays were
17 generated, and their natural log (due to their approximate lognormal posterior distributions) was
18 assessed for convergence using the potential scale reduction factor “ R .” This is akin to the idea
19 of utilizing sensitivity analysis so that effort is concentrated on calibrating the most sensitive
20 parameters for the purpose of interest. In addition, predictions of interest which do not
21 adequately converge can be flagged as such, so that the statistical uncertainty associated with the
22 limited sample size can be considered.

23 The mouse model had the most rapid reduction in potential scale reduction factors.
24 Initially, four chains of 42,500 iterations each were run, with the first 12,500 discarded as
25 “burn-in” iterations. The initial decision for determining “burn-in” was determined by visual
26 inspection. At this point, evaluating the 30,000 remaining iterations, all the population
27 parameters except for the V_{MAX} for DCVG formation had $R < 1.2$, with only the first-order
28 clearance rate for DCVG formation and the V_{MAX} and K_M for TCOH glucuronidation having
29 $R > 1.1$. For the samples used for inference, all of these initial iterations were treated as “burn-
30 in” iterations, and each chain was then restarted and run for an additional
31 68,700–71,400 iterations (chains were terminated at the same time, so the number of iterations
32 per chains was slightly different). For these iterations, all values of R were < 1.03 . Dose metric
33 predictions calculated for exposure scenarios 10–600 ppm either continuously or 7 hour/day,
34 5 day/week and 10–3,000 mg/kg/d either continuously or by gavage 5 day/week. These
35 predictions were all adequately converged, with all values of $R < 1.03$.

This document is a draft for review purposes only and does not constitute Agency policy.

1 As discussed above, for parameters with little or no *a priori* information, the posterior
2 distributions from the mouse model were used to update prior distributions for the rat model,
3 accounting for both the uncertainty reflected in the mouse posteriors as well as the uncertainty in
4 interspecies extrapolation. Four chains were run to 111,960–128,000 iterations each (chains
5 were terminated at the same time and run on computers with slightly different processing speeds,
6 so the number of iterations per chains was slightly different). As is standard, about the first
7 “half” of the chains—i.e., the first 64,000 iterations—were discarded as “burn-in” iterations, and
8 the remaining iterations were used for inferences. For these remaining iterations, the diagnostic
9 R was <1.1 for all population parameters except the fraction of oxidation not producing TCA or
10 TCOH ($R = 1.44$ for population mean, $R = 1.35$ for population variance), the K_M for TCOH \rightarrow
11 TCA ($R = 1.19$ for population mean), the V_{MAX} and K_m for TCOH glucuronidation ($R = 1.23$ and
12 1.12 , respectively for population mean, and $R = 1.13$ for both population variances), and the rate
13 of “other” metabolism of TCOH ($R = 1.29$ for population mean and $R = 1.18$ for population
14 variance). Due to resource constraints, chains needed to be stopped at this point. However,
15 these are similar to the degree of convergence reported in Hack et al. (2006). Dose metric
16 predictions calculated for two inhalation exposure scenarios (10–600 ppm continuously or
17 7 hours/day, 5 day/week) and two oral exposure scenarios (10–3,000 mg/kg/d continuously or by
18 gavage 5 day/week).

19 All dose metric predictions had $R < 1.04$, except for the amount of “other” oxidative
20 metabolism (i.e., not producing TCA or TCOH), which had $R = 1.12$ – 1.16 , depending on the
21 exposure scenario. The poorer convergence of this dose metric is expected given that a key
22 determining parameter, the fraction of oxidation not producing TCA or TCOH, had the poorest
23 convergence among the population parameters.

24 For the human model, a set of four chains was run for 74,160–84,690 iterations using
25 “preliminary” updated prior distributions based on the mouse posteriors and preliminary runs of
26 the rat model. Once the rat chains were completed, final updated prior distributions were
27 calculated and the last iteration of the preliminary runs were used as starting points for the final
28 runs. The center of the final updated priors shifted by less than 25% of the standard deviation of
29 either the preliminary or revised priors, so that the revised median was between the 40th
30 percentile and 60th percentile of the preliminary median, and vice versa. The standard deviations
31 changed by less than 5%. Therefore, the use of the preliminary chains as a starting point should
32 introduce no bias, as long as an appropriate burn-in period is used for the final runs.

33 The final chains were run for an additional 59,140–61,780 iterations, at which point, due
34 to resource constraints, chains needed to be stopped. After the first 20,000 iterations, visual
35 inspection revealed the chains were no longer dependent on the starting point. These iterations

1 were therefore discarded as “burn-in” iterations, and for the remaining ~40,000 iterations used
2 for inferences. All population mean parameters had $R < 1.1$ except for the respiratory tract
3 diffusion constant ($R = 1.20$), the liver:blood partition coefficient for TCOG ($R = 1.23$), the rate
4 of TCE clearance in the kidney producing DCVG ($R = 1.20$), and the rate of elimination of
5 TCOG in bile ($R = 1.46$). All population variances also had $R < 1.1$ except for the variance for
6 the fraction of oxidation not producing TCOH or TCA ($R = 1.10$). Dose metric predictions were
7 assessed for continuous exposure scenarios at 1–60 ppm in air or 1–300 mg/kg/d orally. These
8 predictions were all adequately converged with all values of $R < 1.02$.

10 **3.5.6.2. Evaluation of Posterior Parameter Distributions**

11 Posterior distributions of the population parameters need to be checked as to whether
12 they appear reasonable given the prior distributions. Inconsistency between the prior and
13 posterior distributions may indicate insufficiently broad (i.e., due to overconfidence) or
14 otherwise incorrectly specified priors, a misspecification of the model structure (e.g., leading to
15 pathological parameter estimates), or an error in the data. As was done with the evaluation of
16 Hack et al. (2006) in Appendix A, parameters were flagged if the interquartile regions of their
17 prior and posterior distributions did not overlap.

18 Appendix A contains detailed tables of the “sampled” parameters, and their prior and
19 posterior distributions. Because these parameters are generally scaled one or more times to
20 obtain a physically meaningful parameter, they are difficult to interpret. Therefore, in
21 Tables 3-36–3-40, the prior and posterior distributions for the PBPK model parameters obtained
22 *after* scaling are summarized. Note that because these model parameters are at the individual
23 (for humans) or sex/species/study unit (for rodents) level, they were generated using the
24 uncertainty distributions for the population mean and variance, and hence the distributions reflect
25 both uncertainty in the population characteristics as well as variability in the population.
26 Furthermore, they account for correlations among the population-level parameters.

27 The prior and posterior distributions for most physiological parameters were similar (see
28 Table 3-36). The posterior distribution was substantially narrower (i.e., less uncertainty) than the
29 prior distribution only in the case of the diffusion rate from the respiratory lumen to the
30 respiratory tissue, which also was to be expected given the very wide, noninformative prior for
31 that parameter.

Table 3-36. Physiological parameters: prior and posterior combined uncertainty and variability

Parameter description	PBPK parameter	Mouse		Rat		Human	
		Prior median (2.5%, 97.5%)	Posterior median (2.5%, 97.5%)	Prior median (2.5%, 97.5%)	Posterior median (2.5%, 97.5%)	Prior median (2.5%, 97.5%)	Posterior median (2.5%, 97.5%)
Cardiac output (L/h)	QC	0.84 (0.49, 1.4)	1 (0.46, 1.7)	5.4 (3.7, 7.9)	6.4 (3.5, 9.1)	390 (230, 670)	340 (190, 720)
Alveolar ventilation (L/h)	QP	2.1 (0.99, 4.4)	2.1 (0.84, 4.5)	10 (4.3, 25)	7.6 (3.4, 19)	370 (170, 780)	440 (170, 1,100)
Scaled fat blood flow	QFatC	0.07 (0.012, 0.13)	0.073 (0.015, 0.13)	0.07 (0.012, 0.13)	0.081 (0.023, 0.13)	0.05 (0.0082, 0.092)	0.044 (0.0076, 0.09)
Scaled gut blood flow	QGutC	0.14 (0.098, 0.18)	0.16 (0.11, 0.19)	0.15 (0.11, 0.2)	0.17 (0.12, 0.2)	0.19 (0.13, 0.25)	0.16 (0.12, 0.22)
Scaled liver blood flow	QLivC	0.02 (0.014, 0.026)	0.021 (0.014, 0.026)	0.021 (0.015, 0.027)	0.022 (0.015, 0.027)	0.064 (0.012, 0.12)	0.039 (0.0087, 0.091)
Scaled slowly perfused blood flow	QSlwC	0.22 (0.1, 0.33)	0.21 (0.1, 0.33)	0.34 (0.15, 0.52)	0.31 (0.15, 0.5)	0.22 (0.094, 0.35)	0.17 (0.085, 0.3)
Scaled rapidly perfused blood flow	QRapC	0.46 (0.31, 0.61)	0.44 (0.3, 0.59)	0.28 (0.073, 0.49)	0.28 (0.074, 0.45)	0.28 (0.11, 0.46)	0.39 (0.23, 0.51)
Scaled kidney blood flow	QKidC	0.091 (0.038, 0.14)	0.09 (0.038, 0.14)	0.14 (0.11, 0.17)	0.14 (0.11, 0.17)	0.19 (0.15, 0.23)	0.19 (0.15, 0.23)
Respiratory lumen:tissue diffusive clearance rate (L/h)	DResp	0.02 (0.000027, 16)	2.5 (0.8, 7.2)	10 (0.4, 100)	21 (6.6, 74)	570 (35, 3,900)	270 (63, 930)
Fat fractional compartment volume	VFatC	0.07 (0.014, 0.13)	0.089 (0.029, 0.13)	0.07 (0.013, 0.13)	0.068 (0.016, 0.12)	0.2 (0.038, 0.36)	0.16 (0.036, 0.31)
Gut fractional compartment volume	VGutC	0.049 (0.037, 0.06)	0.048 (0.037, 0.06)	0.032 (0.024, 0.04)	0.031 (0.025, 0.039)	0.02 (0.017, 0.023)	0.02 (0.017, 0.023)
Liver fractional compartment volume	VLivC	0.055 (0.031, 0.079)	0.046 (0.03, 0.073)	0.034 (0.023, 0.045)	0.033 (0.023, 0.044)	0.025 (0.015, 0.035)	0.026 (0.016, 0.035)
Rapidly perfused fractional compartment volume	VRapC	0.1 (0.082, 0.12)	0.1 (0.082, 0.12)	0.088 (0.069, 0.11)	0.088 (0.07, 0.11)	0.088 (0.075, 0.1)	0.088 (0.076, 0.099)

Table 3-36. Physiological parameters: prior and posterior combined uncertainty and variability (continued)

Parameter description	PBPK parameter	Mouse		Rat		Human	
		Prior median (2.5%, 97.5%)	Posterior median (2.5%, 97.5%)	Prior median (2.5%, 97.5%)	Posterior median (2.5%, 97.5%)	Prior median (2.5%, 97.5%)	Posterior median (2.5%, 97.5%)
Fractional volume of respiratory lumen	VRespLumC	0.0047 (0.0037, 0.0056)	0.0047 (0.0038, 0.0056)	0.0047 (0.0031, 0.0062)	0.0047 (0.0033, 0.0061)	0.0024 (0.0015, 0.0033)	0.0024 (0.0016, 0.0032)
Fractional volume of respiratory tissue	VRespEffC	0.0007 (0.00056, 0.00084)	0.0007 (0.00056, 0.00084)	0.0005 (0.00034, 0.00066)	0.0005 (0.00035, 0.00066)	0.00018 (0.00011, 0.00025)	0.00018 (0.00012, 0.00024)
Kidney fractional compartment volume	VKidC	0.017 (0.014, 0.02)	0.017 (0.014, 0.02)	0.007 (0.0051, 0.0089)	0.007 (0.0052, 0.0088)	0.0043 (0.003, 0.0056)	0.0043 (0.0031, 0.0055)
Blood fractional compartment volume	VBldC	0.049 (0.038, 0.06)	0.049 (0.039, 0.059)	0.074 (0.058, 0.09)	0.074 (0.059, 0.09)	0.077 (0.06, 0.094)	0.078 (0.062, 0.092)
Slowly perfused fractional compartment volume	VSlwC	0.55 (0.48, 0.62)	0.54 (0.48, 0.61)	0.59 (0.53, 0.66)	0.6 (0.54, 0.66)	0.44 (0.28, 0.61)	0.48 (0.32, 0.61)
Plasma fractional compartment volume	VPlasC	0.025 (0.012, 0.041)	0.022 (0.012, 0.036)	0.039 (0.019, 0.062)	0.04 (0.023, 0.059)	0.043 (0.033, 0.055)	0.044 (0.035, 0.054)
TCA body fractional compartment volume [not incl. blood+liver]	VBodC	0.79 (0.76, 0.81)	0.79 (0.77, 0.81)	0.79 (0.77, 0.81)	0.79 (0.77, 0.81)	0.75 (0.73, 0.77)	0.75 (0.74, 0.77)
TCOH/G body fractional compartment volume [not incl. liver]	VBodTCOHC	0.83 (0.81, 0.86)	0.84 (0.82, 0.86)	0.87 (0.85, 0.88)	0.87 (0.86, 0.88)	0.83 (0.82, 0.84)	0.83 (0.82, 0.84)

Table 3-37. Distribution parameters: prior and posterior combined uncertainty and variability

Parameter description	PBPK parameter	Mouse		Rat		Human	
		Prior median (2.5%, 97.5%)	Posterior median (2.5%, 97.5%)	Prior median (2.5%, 97.5%)	Posterior median (2.5%, 97.5%)	Prior median (2.5%, 97.5%)	Posterior median (2.5%, 97.5%)
TCE blood:air partition coefficient	PB	15 (8.2, 27)	14 (7.5, 29)	22 (12, 41)	19 (11, 34)	9.6 (5.9, 16)	9.3 (6.2, 14)
TCE fat:blood partition coefficient	PFat	36 (17, 74)	35 (18, 71)	27 (13, 56)	31 (17, 57)	67 (41, 110)	57 (41, 87)
TCE gut:blood partition coefficient	PGut	1.9 (0.72, 5.1)	1.5 (0.71, 3.8)	1.4 (0.53, 3.7)	1.2 (0.55, 2.7)	2.6 (0.99, 6.8)	2.8 (1.2, 6.1)
TCE liver:blood partition coefficient	PLiv	1.7 (0.65, 4.5)	2.2 (0.82, 4.7)	1.5 (1, 2.2)	1.5 (1.1, 2.1)	4.1 (1.5, 11)	4.1 (2, 8.3)
TCE rapidly perfused:blood partition coefficient	PRap	1.9 (0.72, 5)	1.8 (0.77, 4.5)	1.3 (0.5, 3.4)	1.3 (0.56, 3)	2.6 (0.99, 6.8)	2.4 (1, 6.2)
TCE respiratory tissue:air partition coefficient	PResp	2.6 (0.98, 6.8)	2.5 (1.1, 6.2)	1 (0.38, 2.6)	1 (0.45, 2.3)	1.3 (0.5, 3.5)	1.3 (0.64, 2.7)
TCE kidney:blood partition coefficient	PKid	2.1 (0.8, 5.6)	2.7 (0.9, 6.1)	1.3 (0.63, 2.7)	1.2 (0.66, 2.3)	1.6 (0.98, 2.6)	1.6 (1.1, 2.3)
TCE slowly perfused:blood partition coefficient	PSlw	2.4 (0.92, 6.4)	2.2 (0.96, 5.6)	0.58 (0.28, 1.2)	0.72 (0.37, 1.3)	2.1 (1, 4.4)	2.4 (0.96, 4.9)
TCA blood:plasma concentration ratio	TCAPlas	0.8 (0.35, 19)	1.1 (0.65, 2.6)	0.79 (0.53, 1.1)	0.78 (0.61, 0.97)	0.78 (0.53, 18)	0.64 (0.54, 2.7)
Free TCA body:blood plasma partition coefficient	PBodTCA	0.82 (0.21, 19)	0.89 (0.4, 2.5)	0.7 (0.12, 3.9)	0.77 (0.24, 2.7)	0.5 (0.15, 10)	0.43 (0.2, 1.7)
Free TCA liver:blood plasma partition coefficient	PLivTCA	1.1 (0.3, 25)	1.1 (0.48, 3.1)	0.92 (0.16, 5.1)	1.2 (0.31, 4)	0.63 (0.2, 13)	0.54 (0.26, 2.3)
Protein:TCA dissociation constant ($\mu\text{mole/L}$)	kDissoc	110 (5.8, 2,000)	130 (11, 1,600)	280 (62, 1,200)	270 (76, 860)	180 (160, 210)	180 (160, 200)
Maximum binding concentration ($\mu\text{mole/L}$)	B _{MAX}	95 (4.1, 2,200)	140 (9.3, 2,200)	330 (50, 2,100)	320 (68, 1,400)	840 (530, 1,300)	740 (520, 1,100)

Table 3-37. Distribution parameters: prior and posterior combined uncertainty and variability (continued)

Parameter description	PBPK parameter	Mouse		Rat		Human	
		Prior median (2.5%, 97.5%)	Posterior median (2.5%, 97.5%)	Prior median (2.5%, 97.5%)	Posterior median (2.5%, 97.5%)	Prior median (2.5%, 97.5%)	Posterior median (2.5%, 97.5%)
TCOH body:blood partition coefficient	PBodTCOH	1.1 (0.49, 2.5)	0.89 (0.48, 1.9)	1.1 (0.2, 5.9)	1 (0.26, 3.8)	0.9 (0.4, 2)	1.5 (0.76, 2.4)
TCOH liver:body partition coefficient	PLivTCOH	1.3 (0.58, 2.9)	1.9 (0.74, 3.4)	1.3 (0.24, 7.1)	1.2 (0.28, 5.6)	0.6 (0.26, 1.3)	0.64 (0.34, 1.1)
TCOG body:blood partition coefficient	PBodTCOG	1.1 (0.015, 84)	0.47 (0.13, 1.6)	0.47 (0.021, 15)	1.9 (0.09, 19)	0.75 (0.03, 18)	0.69 (0.014, 44)
TCOG liver:body partition coefficient	PLivTCOG	1.3 (0.017, 100)	1.3 (0.36, 4.6)	1.3 (0.052, 33)	9.7 (2.4, 47)	1.7 (0.092, 29)	3.1 (0.074, 43)
DCVG effective volume of distribution	VDCVG	—	—	—	—	64 (4.8, 37,000)	6.1 (4.8, 7.8)

PB = TCE blood-air partition coefficient.

Table 3-38. Absorption parameters: prior and posterior combined uncertainty and variability

Parameter description	PBPK parameter	Mouse		Rat		Human	
		Prior median (2.5%, 97.5%)	Posterior median (2.5%, 97.5%)	Prior median (2.5%, 97.5%)	Posterior median (2.5%, 97.5%)	Prior median (2.5%, 97.5%)	Posterior median (2.5%, 97.5%)
TCE stomach absorption coefficient (/h)	kAS	1.6 (0.0022, 890)	1.8 (0.052, 75)	1.3 (0.0022, 890)	2.4 (0.014, 310)	—	—
TCE stomach-duodenum transfer coefficient (/h)	kTSD	1.3 (0.019, 99)	5.2 (0.05, 98)	1.5 (0.019, 100)	3 (0.047, 94)	—	—
TCE duodenum absorption coefficient (/h)	kAD	0.78 (0.0012, 460)	0.26 (0.0078, 15)	0.71 (0.0011, 490)	0.19 (0.0057, 5.3)	—	—
TCA stomach absorption coefficient (/h)	kASTCA	0.7 (0.0011, 450)	3.9 (0.016, 300)	0.77 (0.0012, 470)	1.4 (0.032, 84)	0.69 (0.0012, 480)	4.4 (0.011, 490)
TCOH stomach absorption coefficient (/h)	kASTCOH	0.79 (0.0012, 490)	0.83 (0.0028, 160)	0.64 (0.0012, 470)	0.72 (0.0064, 110)	0.82 (0.0012, 490)	7.7 (0.022, 460)

Table 3-39. TCE metabolism parameters: prior and posterior combined uncertainty and variability

Parameter description	PBPK parameter	Mouse		Rat		Human	
		Prior median (2.5%, 97.5%)	Posterior median (2.5%, 97.5%)	Prior median (2.5%, 97.5%)	Posterior median (2.5%, 97.5%)	Prior median (2.5%, 97.5%)	Posterior median (2.5%, 97.5%)
V _{MAX} for hepatic TCE oxidation (mg/h)	V _{MAX}	4.3 (0.72, 27)	2.4 (0.7, 10)	6 (1, 36)	5.4 (1.8, 17)	430 (72, 2,500)	180 (59, 930)
K _M for hepatic TCE oxidation (mg/L)	K _M	35 (2.3, 520)	2.7 (0.69, 23)	21 (0.81, 610)	0.72 (0.35, 4)	3.8 (0.11, 140)	0.16 (0.017, 3.8)
Fraction of hepatic TCE oxidation not to TCA+TCOH	FracOther	0.47 (0.0015, 1)	0.023 (0.0025, 0.19)	0.026 (0.0014, 0.54)	0.28 (0.017, 0.87)	0.12 (0.0058, 0.77)	0.1 (0.0064, 0.67)
Fraction of hepatic TCE oxidation to TCA	FracTCA	0.07 (0.00021, 0.66)	0.13 (0.052, 0.31)	0.22 (0.024, 0.74)	0.047 (0.0072, 0.14)	0.18 (0.011, 0.78)	0.034 (0.0081, 0.21)
V _{MAX} for hepatic TCE GSH conjugation (mg/h)	V _{Max} DCVG	4.8 (0.0072, 3,300)	0.65 (0.0084, 640)	2.3 (0.012, 1,500)	6.5 (0.15, 330)	96 (0.0066, 1,200,000)	320 (8.5, 12,000)
K _M for hepatic TCE GSH conjugation (mg/L)	K _M DCVG	220 (0.0043, 8,200,000)	2,500 (0.11, 3,700,000)	1,700 (1, 4,000,000)	6,700 (87, 780,000)	2.9 (0.17, 50)	3.4 (0.16, 77)
V _{MAX} for renal TCE GSH conjugation (mg/h)	V _{Max} KidDCVG	0.3 (0.00046, 200)	0.029 (0.0011, 22)	0.038 (0.00024, 13)	0.0025 (0.00042, 0.02)	170 (0.018, 1,800,000)	2.1 (0.035, 120)
K _M for renal TCE GSH conjugation (mg/L)	K _M KidDCVG	180 (0.0043, 7,600,000)	220 (0.11, 430,000)	480 (0.34, 760,000)	0.27 (0.02, 3.6)	2.6 (0.15, 48)	0.78 (0.22, 7)
V _{MAX} for tracheo-bronchial TCE oxidation (mg/h)	V _{Max} Clara	0.3 (0.016, 6)	0.45 (0.012, 6.1)	0.19 (0.005, 4.1)	0.2 (0.0056, 2.3)	25 (0.84, 490)	17 (0.74, 160)
K _M for tracheo-bronchial TCE oxidation (mg/L)	K _M Clara	1.1 (0.0014, 670)	0.011 (0.0017, 0.18)	0.015 (0.0013, 0.67)	0.025 (0.0034, 0.84)	0.022 (0.0016, 0.6)	0.27 (0.0029, 65)
Fraction of respiratory metabolism to systemic circ.	FracLungSys	0.51 (0.0014, 1)	0.79 (0.15, 1)	0.81 (0.036, 1)	0.75 (0.049, 0.99)	0.75 (0.042, 0.99)	0.96 (0.81, 0.99)

Table 3-40. Metabolite metabolism parameters: prior and posterior combined uncertainty and variability

Parameter description	PBPK parameter	Mouse		Rat		Human	
		Prior median (2.5%, 97.5%)	Posterior median (2.5%, 97.5%)	Prior median (2.5%, 97.5%)	Posterior median (2.5%, 97.5%)	Prior median (2.5%, 97.5%)	Posterior median (2.5%, 97.5%)
V _{MAX} for hepatic TCOH→TCA (mg/h)	V _{Max} TCOH	0.066 (0.000012, 450)	0.12 (0.03, 0.52)	0.67 (0.023, 21)	0.71 (0.14, 3.8)	42 (0.61, 3,300)	9 (0.83, 110)
K _M for hepatic TCOH→TCA (mg/L)	K _M TCOH	0.85 (0.00017, 6,000)	0.92 (0.2, 4.1)	0.94 (0.029, 33)	19 (1.8, 130)	4.8 (0.23, 100)	2.2 (0.29, 21)
V _{MAX} for hepatic TCOH→TCOG (mg/h)	V _{Max} Gluc	0.085 (0.000012, 430)	4.8 (1.4, 25)	27 (0.8, 910)	11 (1.3, 120)	820 (11, 56,000)	890 (89, 5,800)
K _M for hepatic TCOH→TCOG (mg/L)	K _M Gluc	1.1 (0.0015, 670)	34 (2.7, 200)	28 (0.73, 580)	6.1 (0.25, 54)	11 (0.46, 250)	130 (20, 490)
Rate constant for hepatic TCOH→other (/h)	kMetTCOH	0.27 (0.000038, 1,500)	8.7 (1.3, 36)	4.5 (0.14, 160)	2.5 (0.25, 31)	0.79 (0.036, 18)	0.26 (0.0046, 6.9)
Rate constant for TCA plasma→urine (/h)	kUrnTCA	25 (0.3, 2,000)	3.1 (0.59, 15)	1.9 (0.16, 54)	0.98 (0.29, 3.5)	0.26 (0.031, 4.9)	0.12 (0.032, 0.45)
Rate constant for hepatic TCA→other (/h)	kMetTCA	0.26 (0.00036, 160)	1.5 (0.45, 5)	0.82 (0.026, 24)	0.47 (0.11, 1.7)	0.16 (0.0079, 3.2)	0.1 (0.011, 0.67)
Rate constant for TCOG liver→bile (/h)	kBile	0.25 (0.00035, 160)	2.4 (0.5, 13)	1.3 (0.04, 44)	12 (1.7, 64)	1.1 (0.053, 20)	2.6 (0.55, 11)
Lumped rate constant for TCOG bile→TCOH liver (/h)	kEHR	0.23 (0.00034, 160)	0.036 (0.0024, 0.16)	0.016 (0.00045, 0.69)	1.8 (0.12, 11)	0.076 (0.0031, 1.8)	0.054 (0.016, 0.19)
Rate constant for TCOG→urine (/h)	kUrnTCOG	0.67 (0.000089, 4,800)	12 (0.62, 420)	10 (0.078, 1,200)	9.1 (0.27, 540)	2.6 (0.027, 230)	2.2 (0.0067, 640)
Rate constant for hepatic DCVG→DCVC (/h)	kDCVG	–	–	–	–	0.034 (0.000053, 22)	2.5 (1.1, 5.9)
Lumped rate constant for DCVC→urinary NAcDCVC (/h)	kNAT	–	–	0.13 (0.00021, 92)	0.003 (0.00048, 0.022)	0.00085 (0.00005, 0.034)	0.00011 (0.000038, 0.00099)
Rate constant for DCVC bioactivation (/h)	kKidBioact	–	–	0.14 (0.00021, 90)	0.0087 (0.00091, 0.057)	0.0021 (0.000072, 0.09)	0.023 (0.0036, 0.095)

1 For distribution parameters (see Table 3-37), there were only relatively minor changes
2 between prior and posterior distributions for TCE and TCOH partition coefficients. The
3 posterior distributions for several TCA partition coefficients and plasma binding parameters
4 were substantially narrower than their corresponding priors, but the central estimates were
5 similar, meaning that values at the high and low extremes were not likely. For TCOG as well,
6 partition coefficient posterior distributions were substantially narrower, which was expected
7 given the greater uncertainty in the prior distributions (TCOH partition coefficients were used as
8 a proxy). Again, posterior distributions indicated that the high and low extremes were not likely.
9 Finally, posterior distribution for the distribution volume for DCVG was substantially narrower
10 than the prior distribution, which only provided a lower bound given by the blood volume. In
11 this case, the upper bounds were substantially lower in the posterior.

12 Posterior distributions for oral absorption parameters (see Table 3-38) in mice and rats
13 (there were no oral studies in humans) were also informed by the data, as reflected in their being
14 substantially more narrow than the corresponding priors. Finally, with a few exceptions, TCE
15 and metabolite kinetic parameters (see Tables 3-39–3-40) showed substantially narrower
16 posterior distributions than prior distributions, indicating that they were fairly well specified by
17 the *in vivo* data. The exceptions were the V_{MAX} for hepatic oxidation in humans (for which there
18 was substantial *in vitro* data) and the V_{MAX} for respiratory metabolism in mice and rats (although
19 the posterior distribution for the K_M for this pathway was substantially narrower than the
20 corresponding prior).

21 In terms of general consistency between prior and posterior distributions, in only a few
22 cases did the interquartile regions of the prior and posterior distributions not overlap. In most of
23 these cases, including the diffusion rate from respiratory lumen to tissue, the K_{MS} for renal TCE
24 GSH conjugation and respiratory TCE oxidation, and several metabolite kinetic parameters, the
25 prior distributions themselves were noninformative. For a noninformative prior, the lack of
26 overlap would only be an issue if the posterior distributions were affected by the truncation limit,
27 which was not the case here. The only other parameter for which there was a lack of
28 interquartile overlap between the prior and posterior distribution was the K_M for hepatic TCE
29 oxidation in mice and in rats, though the prior and posterior 95% confidence intervals did
30 overlap within each species. As discussed Section 3.3, there is some uncertainty in the
31 extrapolation of *in vitro* K_M values to *in vivo* values (within the same species). In addition, in
32 mice, it has been known for some time that K_M values appear to be discordant among different
33 studies (Abbas and Fisher, 1997; Greenberg et al., 1999; Fisher et al., 1991).

34 In sum, the Bayesian analysis of the updated PBPK model and data exhibited no major
35 inconsistencies in prior and posterior parameter distributions. The most significant issue was the
36 K_M for hepatic oxidative metabolism, for which the posterior estimates were low compared to,

This document is a draft for review purposes only and does not constitute Agency policy.

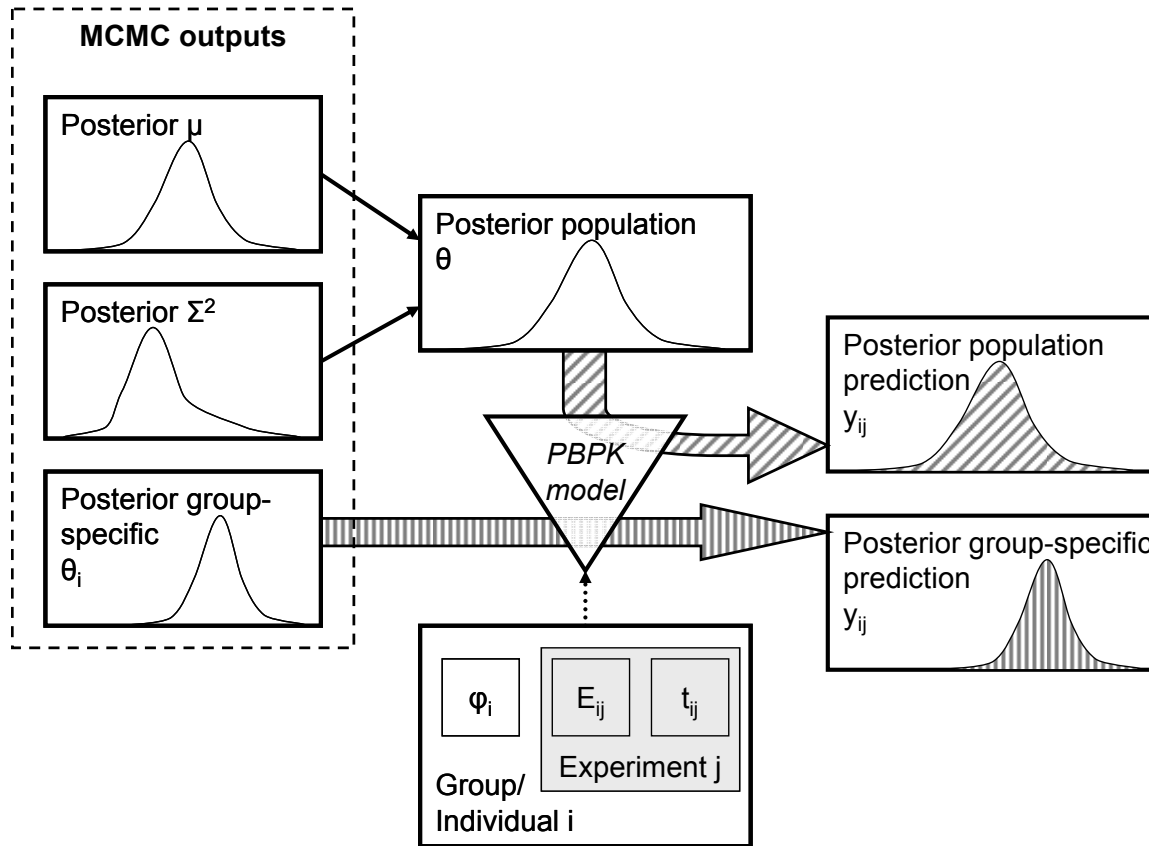
1 albeit somewhat uncertain, *in vitro* estimates, and it could be argued that a wider prior
2 distribution would have been better. However, the central estimates were not at or near the
3 truncation boundary, so it is unlikely that wider priors would change the results substantially.
4 Therefore, there were no indications based on this evaluation of prior and posterior distributions
5 either that prior distributions were overly restrictive or that model specification errors led to
6 pathological parameter estimates.

8 **3.5.6.3. Comparison of Model Predictions With Data**

9 As with the Hack et al. (2006) model, initially the sampled group- or individual-specific
10 parameters were used to generate predictions for comparison to the calibration data (see
11 Figure 3-8). Thus, the predictions for a particular data set are conditioned on the posterior
12 parameter distributions for same data set. Because these parameters were “optimized” for each
13 experiment, these group- or individual-specific predictions should be accurate by design—and,
14 on the whole, were so. In addition, the “residual error” estimate for each measurement (see
15 Table 3-41) provides some quantitative measure of the degree to which there were deviations due
16 to intrastudy variability and model misspecification, including any difficulties fitting multiple
17 dose levels in the same study using the same model parameters.

18 Next, only samples of the population parameters (means and variances) were used, and
19 “new” groups or individuals were sampled from appropriate distribution using these population
20 means and variances (see Figure 3-8). That is, the predictions were only conditioned on the
21 population-level parameters distributions, representing an “average” over all the data sets, and
22 not on the specific predictions for that data set. These “new” groups or individuals then
23 represent the predicted population distribution, incorporating variability in the population as well
24 as uncertainty in the population means and variances. Because of the limited amount of mouse
25 data, all available data for that species was utilized for calibration, and there was no data
26 available for “out-of-sample” evaluation (often referred to as “validation data,” but this term is
27 not used here due to ambiguities as to its definition). In rats, several studies that contained
28 primarily blood TCE data, which were abundant, were used for out-of-sample evaluation. In
29 humans, there were substantial individual and aggregated (group mean) data that was available
30 for out-of-sample evaluation, as computational intensity limited the number of individuals that
31 could be used in the MCMC-based calibration.

1



2

3

4

5

6

7

Figure 3-8. Schematic of how posterior predictions were generated for comparison with experimental data. Two sets of posterior predictions were generated: population predictions (diagonal hashing) and group-specific predictions (vertical hashing). (Same as Figure A-2 in Appendix A)

1
2

Table 3-41. Estimates of the residual error

Measurement abbreviation	Measurement description	GSD for "residual" error (median estimate)		
		Mouse	Rat	Human
RetDose	Retained TCE dose (mg)	-	-	1.13
CAIvPPM	TCE concentration in alveolar air (ppm)	-	-	1.44~1.83
CIvhPPM	TCE concentration in closed chamber (ppm)	1.18	1.11~1.12	-
CMixExh	TCE concentration in mixed exhaled air (mg/L)	-	1.5	-
CArt	TCE concentration in arterial blood (mg/L)	-	1.17~1.52	-
CVen	TCE concentration in venous blood (mg/L)	2.68	1.22~ 4.46	1.62~ 2.95
CBldMix	TCE concentration in mixed arterial and venous blood (mg/L)	1.61	1.5	-
CFat	TCE concentration in fat (mg/L)	2.49	1.85~ 2.66	-
CGut	TCE concentration in gut (mg/L)	-	1.86	-
CKid	TCE concentration in kidney (mg/L)	2.23	1.47	-
CLiv	TCE concentration in liver (mg/L)	1.71	1.67~1.78	-
CMus	TCE concentration in muscle (mg/L)	-	1.65	-
AExhpost	Amount of TCE exhaled postexposure (mg)	1.23	1.12~1.17	-
CTCOH	Free TCOH concentration in blood (mg/L)	1.54	1.14~1.64	1.14~ 2.1
CLivTCOH	Free TCOH concentration in liver (mg/L)	1.59	-	-
CPlasTCA	TCA concentration in plasma (mg/L)	1.40	1.13~1.21	1.12~1.17
CBldTCA	TCA concentration in blood (mg/L)	1.49	1.13~1.59	1.12~1.49
CLivTCA	TCA concentration in liver (mg/L)	1.34	1.67	-
AUrnTCA	Cumulative amount of TCA excreted in urine (mg)	1.34	1.18~1.95	1.11~1.54
AUrnTCA_collect	Cumulative amount of TCA collected in urine (noncontinuous sampling) (mg)	-	-	2~2.79
ABileTCOG	Cumulative amount of bound TCOH excreted in bile (mg)	-	2.13	-
CTCOG	Bound TCOH concentration in blood	-	2.76	-
CTCOGTCOH	Bound TCOH concentration in blood in free TCOH equivalents	1.49	-	-
CLivTCOGTCOH	Bound TCOH concentration in liver in free TCOH equivalents (mg/L)	1.63	-	-
AUrnTCOGTCOH	Cumulative amount of total TCOH excreted in urine (mg)	1.26	1.12~ 2.27	1.11~1.13
AUrnTCOGTCOH_collect	Cumulative amount of total TCOH collected in urine (noncontinuous sampling) (mg)	-	-	1.3~1.63
CDCVGmol	DCVG concentration in blood (mmol/L)	-	-	1.53
AUrnNDCVC	Cumulative amount of NAcDCVC excreted in urine (mg)	-	1.17	1.17
AUrnTCTotMole	Cumulative amount of TCA+total TCOH excreted in urine (mmol)	-	1.12~1.54	-
TotCTCOH	Total TCOH concentration in blood (mg/L)	1.85	1.49	1.2~1.69

3
4

Values higher than 2-fold are in bold.

This document is a draft for review purposes only and does not constitute Agency policy.

1 **3.5.6.3.1. Mouse model and data.** Table 3-42 provides an evaluation of the predictions of the
2 mouse model for each data set, with figures showing data and predictions in Appendix A. With
3 exception of the remaining over-prediction of TCE in blood following inhalation exposure, the
4 parent PBPK model (for TCE) appears to now be robust in mice. Most of the problems
5 previously encountered with the Abbas and Fisher (1997) gavage data were solved by allowing
6 absorption from both of the stomach and duodenal compartments. Notably, the addition of
7 possible wash-in/wash-out, respiratory metabolism, and extrahepatic metabolism (i.e., kidney
8 GSH conjugation) was insufficient to remove the long-standing discrepancy of PBPK models
9 over-predicting TCE blood levels, suggesting another source of model or experimental error is
10 the cause. However, the availability of tissue concentration levels of TCE somewhat ameliorates
11 this limitation.

12 In terms of TCA and TCOH, the overall mass balance and metabolic disposition to these
13 metabolites also appeared to be robust, as urinary excretion following dosing with TCE, TCOH,
14 as well as TCA could be modeled accurately. This improvement over the Hack et al. (2006)
15 model was likely due in part to the addition of nonurinary clearance (“untracked” metabolism) of
16 TCA and TCOH. Also, the addition of a liver compartment for TCOH and TCOG, so that first-
17 pass metabolism could be properly accounted for, was essential for accurate simulation of the
18 metabolite pharmacokinetics both from i.v. dosing of TCOH and from exposure to TCE.

19 These conclusions are corroborated by the estimated “residual” errors, which include
20 intrastudy variability, interindividual variability, and measurement and model errors. The
21 implied GSD for this error in each *in vivo* measurement is presented in Table 3-41. As expected,
22 the venous blood TCE concentration had the largest residual error, with a GSD of 2.7, reflecting
23 largely the difficulty in fitting TCE blood levels following inhalation exposure. In addition, the
24 fat and kidney TCE concentrations also are somewhat uncertain, with a GSD for the residual
25 error of 2.5 and 2.2, respectively, while other residual errors had GSD of less than 2-fold. These
26 tissues were only measured in two studies, Abbas and Fisher (1997) and Greenberg et al. (1999),
27 and the residual error reflects the difficulties in simultaneously fitting the model to the different
28 dose levels with the same parameters.

1
2
3

Table 3-42. Summary comparison of updated PBPK model predictions and *in vivo* data in mice

Study	Exposure(s)	Discussion
Abbas and Fisher, 1997	TCE gavage (corn oil)	<p>Generally, model predictions were quite good, especially with respect to tissue concentrations of TCE, TCA, and TCOH. There were some discrepancies in TCA and TCOG urinary excretion and TCA and TCOG concentrations in blood due to the requirement (unlike in Hack et al. [2006]) that all experiments in the same study utilize the same parameters. Thus, for instance, TCOG urinary excretion was accurately predicted at 300 mg/kg, underpredicted at 600 mg/kg, over-predicted at 1,200 mg/kg, and underpredicted again at 2,000 mg/kg, suggesting significant intraexperimental variability (not addressed in the model).</p> <p>Population predictions were quite good, with the almost all of the data within the 95% CI of the predictions, and most within the interquartile region.</p>
Abbas et al., 1997	TCOH, TCA i.v.	<p>Both group-specific and population predictions were quite good. Urinary excretion, which was over-predicted by the Hack et al. (2006) model, was accurately predicted due to the allowance of additional “untracked” clearance. In the case of population predictions, almost all of the data were within the 95% CI of the predictions, and most within the interquartile region.</p>
Fisher and Allen, 1993	TCE gavage (corn oil)	<p>Both group-specific and population predictions were quite good. Some discrepancies in the time-course of TCE blood concentrations were evidence across doses in the group-specific predictions, but not in the population predictions, suggesting significant intragroup variability (not addressed in the model).</p>
Fisher et al., 1991	TCE inhalation	<p>Blood TCE levels during and following inhalation exposures were still over-predicted at the higher doses. However, there was the stringent requirement (absent in Hack et al. [2006]) that the model utilize the same parameters for all doses and in both the closed and open chamber experiments. Moreover, the Hack et al. (2006) model required significant differences in the parameters for the different closed chamber experiments, while predictions here were accurate utilizing the same parameters across different initial concentrations. These conclusions were the same for group-specific and population predictions (e.g., TCE blood levels remained over-predicted in the later case).</p>
Green and Prout, 1985	TCE gavage (corn oil)	<p>Both group-specific and population predictions were adequate, though the data collection was sparse. In the case of population predictions, almost all of the data were within the 95% CI of the predictions, and about half within the interquartile region.</p>
Greenberg et al., 1999	TCE inhalation	<p>Model predictions were quite good across a wide variety of measures that included tissue concentrations of TCE, TCA, and TCOH. However, as with the Hack et al. (2006) predictions, TCE blood levels were over-predicted by up to 2-fold. Population predictions were quite good, with the exception of TCE blood levels. Almost all of the other data was within the 95% CI of the predictions, and most within the interquartile region.</p>

This document is a draft for review purposes only and does not constitute Agency policy.

Table 3-42. Summary comparison of updated PBPK model predictions and *in vivo* data in mice (continued)

Study	Exposure(s)	Discussion
Larson and Bull, 1992a	TCE gavage (aqueous)	Both group-specific and population predictions were quite good, though the data collection was somewhat sparse. In the case of population predictions, all of the data were within the 95% CI of the predictions,
Larson and Bull, 1992b	TCA gavage (aqueous)	Both group-specific and population predictions were quite good. In the case of population predictions, most of the data were within the interquartile region.
Merdink et al., 1998	TCE i.v.	Both group-specific and population predictions were quite good, though the data collection was somewhat sparse. In the case of population predictions, all of the data were within the 95% CI of the predictions,
Prout et al., 1985	TCE gavage (corn oil)	Both group-specific and population predictions were adequate, though there was substantial scatter in the data due to the use of single animals at each data point.
Templin et al., 1993	TCE gavage (aqueous)	Both group-specific and population predictions were quite good. With respect to population predictions, almost all of the other data was within the 95% CI of the predictions, and most within the interquartile region.

2

3

4

5

6

7

8

9

10

11

12

13

14

15

16

17

18

19

20

21

In terms of total metabolism, closed-chamber data were fit accurately with the updated model. While the previous analyses of Hack et al. (2006) allowed for each chamber experiment to be fit with different parameters, the current analysis made the more restrictive assumption that all experiments in a single study utilize the same parameters. Furthermore, the accuracy of closed chamber predictions did not require the very high values for cardiac output that were used by Fisher et al. (1991), confirming the suggestion (discussed in Appendix A) that additional respiratory metabolism would resolve this discrepancy. The accurate model means that uncertainty with respect to possible wash-in/wash-out, respiratory metabolism, and extrahepatic metabolism could be well characterized. For instance, the absence of *in vivo* data on GSH metabolism in mice means that this pathway remains relatively uncertain; however, the current model should be reliable for estimating lower and upper bounds on the GSH pathway flux.

3.5.6.3.2. Rat model and data. A summary evaluation of the predictions of the rat model as compared to the data are provided in Tables 3-43 and 3-44, with figures showing data and predictions in Appendix A. Similar to previous analyses (Hack et al., 2006), the TCE submodel for the rat appears to be robust, with blood and tissue concentrations accurately predicted. Unlike in the mouse, some data consisting of TCE blood and tissue concentrations were used for “out-of-sample evaluation” (sometimes loosely termed “validation”). These data were generally

This document is a draft for review purposes only and does not constitute Agency policy.

1 well simulated; most of the data within the 95% confidence interval of posterior predictions.
2 This provides additional confidence in the predictions for the parent compound.

3 In terms of TCA and TCOH, as with the mouse, the overall mass balance and metabolic
4 disposition to these metabolites also appeared to be robust: urinary excretion following dosing
5 with TCE, TCOH, as well as TCA, could be modeled accurately, and, secondly, the residual
6 errors did not indicate substantial mis-fit ($GSD \leq 1.25$). This improvement over the Hack et al.
7 (2006) model was likely due in part to the addition of nonurinary clearance (“untracked”
8 metabolism) of TCA and TCOH. In addition, the addition of a liver compartment for TCOH and
9 TCOG, so that first-pass metabolism could be properly accounted for, was essential for accurate
10 simulation of the metabolite pharmacokinetics both from i.v. dosing of TCOH and from TCE
11 exposure. Blood and plasma concentrations of TCA and TCOH were fairly well simulated, with
12 GSD for the residual error of 1.2–1.3, but a bit more discrepancy was evident with TCA liver
13 concentrations. However, TCA liver concentrations were only available in one study (Yu et al.,
14 2000), and the data show a change in the ratio of liver to blood concentrations at the last time
15 point, which may be the source of the added residual error.

16 In terms of total metabolism, as with the mouse, closed-chamber data were fit accurately
17 with the updated model (residual error GSD of about 1.11). In addition, the data on NAcDCVC
18 urinary excretion was well predicted (residual error GSD of 1.18), in particular the fact that
19 excretion was still ongoing at the end of the experiment (see Figure 3-9, panels A and B). Thus,
20 there is greater confidence in the estimate of the flux through the GSH pathway than there was
21 from the Hack et al. (2006) model. However, the overall flux is still estimated indirectly, and
22 there remains some ambiguity as to the relative contributions respiratory wash-in/wash-out,
23 respiratory metabolism, extrahepatic metabolism, DCVC bioactivation versus *N*-acetylation, and
24 oxidation in the liver producing something other than TCOH or TCA. Therefore, there remain a
25 large range of possible values for the flux through the GSH conjugation and other indirectly
26 estimated pathways that are nonetheless consistent with all the available *in vivo* data. The use of
27 noninformative priors for the metabolism parameters for which there were no *in vitro* data means
28 that a fuller characterization of the uncertainty in these various metabolic pathways could be
29 achieved. Thus, the model should be reliable for estimating lower and upper bounds on several
30 of these pathways.

1
2
3

Table 3-43. Summary comparison of updated PBPK model predictions and *in vivo* data used for “calibration” in rats

Study	Exposure(s)	Discussion
Bernauer et al., 1996	TCE inhalation	<p>Posterior fits to these data were adequate, especially with the requirement that all predictions for dose levels utilize the same PBPK model parameters. Predictions of TCOG and TCA urinary excretion was relatively accurate, though the time-course of TCA excretion seemed to proceed more slowly with increasing dose, an aspect not captured in by model. Importantly, unlike the Hack et al. (2006) results, the time-course of NAcDCVC excretion was quite well simulated, with the excretion rate remaining non-negligible at the last time point (48 h). It is likely that the addition of the DCVG submodel between TCE and DCVC, along with prior distributions that accurately reflected the lack of reliable independent (e.g., <i>in vitro</i>) data on bioactivation, allowed for the better fit.</p>
Dallas et al., 1991	TCE inhalation	<p>These data, consisting of arterial blood and exhaled breath concentrations of TCE, were accurately predicted by the model using both group-specific and population sampled parameters. In the case of population predictions, most of the data were within the 95% CI of the predictions.</p>
Fisher et al., 1989	TCE inhalation	<p>These data, consisting of closed chamber TCE concentrations, were accurately simulated by the model using both group-specific and population sampled parameters. In the case of population predictions, most of the data were within the 95% CI of the predictions.</p>
Fisher et al., 1991	TCE inhalation	<p>These data, consisting of TCE blood, and TCA blood and urine time-courses, were accurately simulated by the model using both group-specific and population sampled parameters. In the case of population predictions, most of the data were within the 95% CI of the predictions.</p>
Green and Prout, 1985	TCE gavage (corn oil) TCA i.v. TCA gavage (aqueous)	<p>For TCE treatment, these data, consisting of one time point each in urine for TCA, TCA +TCOG, and TCOG, were accurately simulated by both group-specific and population predictions.</p> <p>For TCA i.v. treatment, the single datum of urinary TCA+TCOG at 24 h was at the lower 95% CI in the group-specific simulations, but accurately predicted with the population sampled parameters, suggesting intrastudy variability is adequately accounted for by population variability.</p> <p>For TCA gavage treatment, the single datum of urinary TCA+TCOG at 24 h was accurately simulated by both group-specific and population predictions.</p>
Hissink et al., 2002	TCE gavage (corn oil) TCE i.v.	<p>These data, consisting of TCE blood, and TCA+TCOG urinary excretion time-courses, were accurately simulated by the model using group-specific parameters. In the case of population predictions, TCA+TCOH urinary excretion appeared to be somewhat under-predicted.</p>
Kaneko et al., 1994	TCE inhalation	<p>These data, consisting of TCE blood and TCA and TCOG urinary excretion time-courses, were accurately predicted by the model using both group-specific and population sampled parameters. In the case of population predictions, TCA+TCOH urinary excretion appeared to be somewhat underpredicted, However, all of the data were within the 95% CI of the predictions.</p>

This document is a draft for review purposes only and does not constitute Agency policy.

Table 3-43. Summary comparison of updated PBPK model predictions and *in vivo* data used for “calibration” in rats (continued)

Study	Exposure(s)	Discussion
Keys et al., 2003	TCE inhalation, gavage (aqueous), i.a.	These data, consisting of TCE blood, gut, kidney, liver, muscle and fat concentration time-courses, were accurately predicted by the model using both group-specific and population sampled parameters. In the case of population predictions, most of the data were within the 95% CI of the predictions.
Kimmerle and Eben, 1973a	TCE inhalation	Some inaccuracies were noted in group-specific predictions, particularly with TCA and TCOG urinary excretion, TCE exhalation postexposure, and TCE venous blood concentrations. In the case of TCA excretion, the rate was underpredicted at the lowest dose (49 mg/kg) and over-predicted at 330 ppm. In terms of TCOG urinary excretion, the rate was over-predicted at 175 ppm and underpredicted at 330 ppm. Similarly for TCE exhaled postexposure, there was some over-prediction at 175 ppm and some underprediction at 300 ppm. Finally, venous blood concentrations were over-predicted at 3,000 ppm. However, for population predictions, most of the data were within with 95% confidence region.
Larson and Bull, 1992a	TCA gavage (aqueous)	These data, consisting of TCA plasma time-courses, were accurately predicted by the model using both group-specific and population sampled parameters. In the case of population predictions, all of the data were within the 95% CI of the predictions.
Larson and Bull, 1992b	TCE gavage (aqueous)	These data, consisting of TCE, TCA, and TCOH in blood, were accurately predicted by the model using both group-specific and population sampled parameters. In the case of population predictions, all of the data were within the 95% CI of the predictions.
Lee et al., 2000a	TCE i.v., p.v.	These data, consisting of TCE concentration time course in mixed arterial and venous blood and liver, were predicted using both the group specific and population predictions. In both cases, most of the data were within the 95% CI of the predictions.
Merdink et al., 1999	TCOH i.v.	TCOH blood concentrations were accurately predicted using group-specific parameters. However, population-based parameters seemed to lead to some under-prediction, though most of the data were within the 95% CI of the predictions.
Prout et al., 1985	TCE gavage (corn oil)	Most of these data were accurately predicted using both group-specific and population-sampled parameters. However, at the highest two doses (1,000 and 2,000 mg/kg), there were some discrepancies in the (very sparsely collected) urinary excretion measurements. In particular, using group-specific parameters, TCA+TCOH urinary excretion was under-predicted at 1,000 mg/kg and over-predicted at 2,000 mg/kg. Using population-sampled parameters, this excretion was underpredicted in both cases, though not entirely outside of the 95% CI.
Simmons et al., 2002	TCE inhalation	Most of these data were accurately predicted using both group-specific and population-sampled parameters. In the open chamber experiments, there was some scatter in the data that did not seem to be accounted for in the model. The closed chamber data were accurately fit.

This document is a draft for review purposes only and does not constitute Agency policy.

Table 3-43. Summary comparison of updated PBPK model predictions and *in vivo* data used for “calibration” in rats (continued)

Study	Exposure(s)	Discussion
Stenner et al., 1997	TCE intraduodenal TCOH i.v. TCOH i.v., bile-cannulated	These data, consisting of TCA and TCOH in blood and TCA and TCOG in urine, were generally accurately predicted by the model using both group-specific and population sampled parameters. However, using group-specific parameters, the amount of TCOG in urine was over-predicted for 100 TCOH mg/kg i.v. dosing, though total TCOH in blood was accurately simulated. In addition, in bile-cannulated rats, the TCOG excretions at 5 and 20 mg/kg i.v. were underpredicted, while the amount at 100 mg/kg was accurately predicted. On the other hand, in the case of population predictions, all of the data were within the 95% CI of the predictions, and mostly within the interquartile region, even for TCOG urinary excretion. This suggests that intrastudy variability may be a source of the poor fit in using the group-specific parameters.
Templin et al., 1995	TCE oral (aqueous)	These data, consisting of TCE, TCA, and TCOH in blood, were accurately predicted by the model using both group-specific and population sampled parameters. In the case of population predictions, all of the data were within the 95% CI of the predictions.
Yu et al., 2000	TCA i.v.	These data, consisting of TCA in blood, liver, plasma, and urine, were generally accurately predicted by the model using both group-specific and population sampled parameters. The only notable discrepancy was at the highest dose of 50 mg/kg, in which the rate of urinary excretion from 0–6 h appeared to more rapid than the model predicted. However, all of the data were within the 95% CI of the predictions based on population-sampled parameters.

1
2 i.a. = intra-arterial, i.v. = intravenous, p.v. = intraperivenous.

1
2
3

Table 3-44. Summary comparison of updated PBPK model predictions and *in vivo* data used for “out-of-sample” evaluation in rats

Study	Exposure(s)	Discussion
Andersen et al., 1987	TCE inhalation	These closed chamber data were well within the 95% CI of the predictions based on population-sampled parameters.
Bruckner et al., unpublished	TCE inhalation	These data on TCE in blood, liver, kidney, fat, muscle, gut, and venous blood, were generally accurately predicted based on population-sampled parameters. The only notable exception was TCE in the kidney during the exposure period at the 500 ppm level, which were somewhat under-predicted (though levels postexposure were accurately predicted).
Fisher et al., 1991	TCE inhalation	These data on TCE in blood were well within the 95% CI of the predictions based on population-sampled parameters.
Jakobson et al., 1986	TCE inhalation	These data on TCE in arterial blood were well within the 95% CI of the predictions based on population-sampled parameters.
Lee et al., 1996	TCE i.a., i.v., p.v., gavage	Except at some very early time-points (<0.5 h), these data on TCE in blood were well within the 95% CI of the predictions based on population-sampled parameters.
Lee et al., 2000a, b	TCE gavage	These data on TCE in blood were well within the 95% CI of the predictions based on population-sampled parameters.

4
5

i.a. = intra-arterial, i.v. = intravenous, p.v. = intraperivenous.

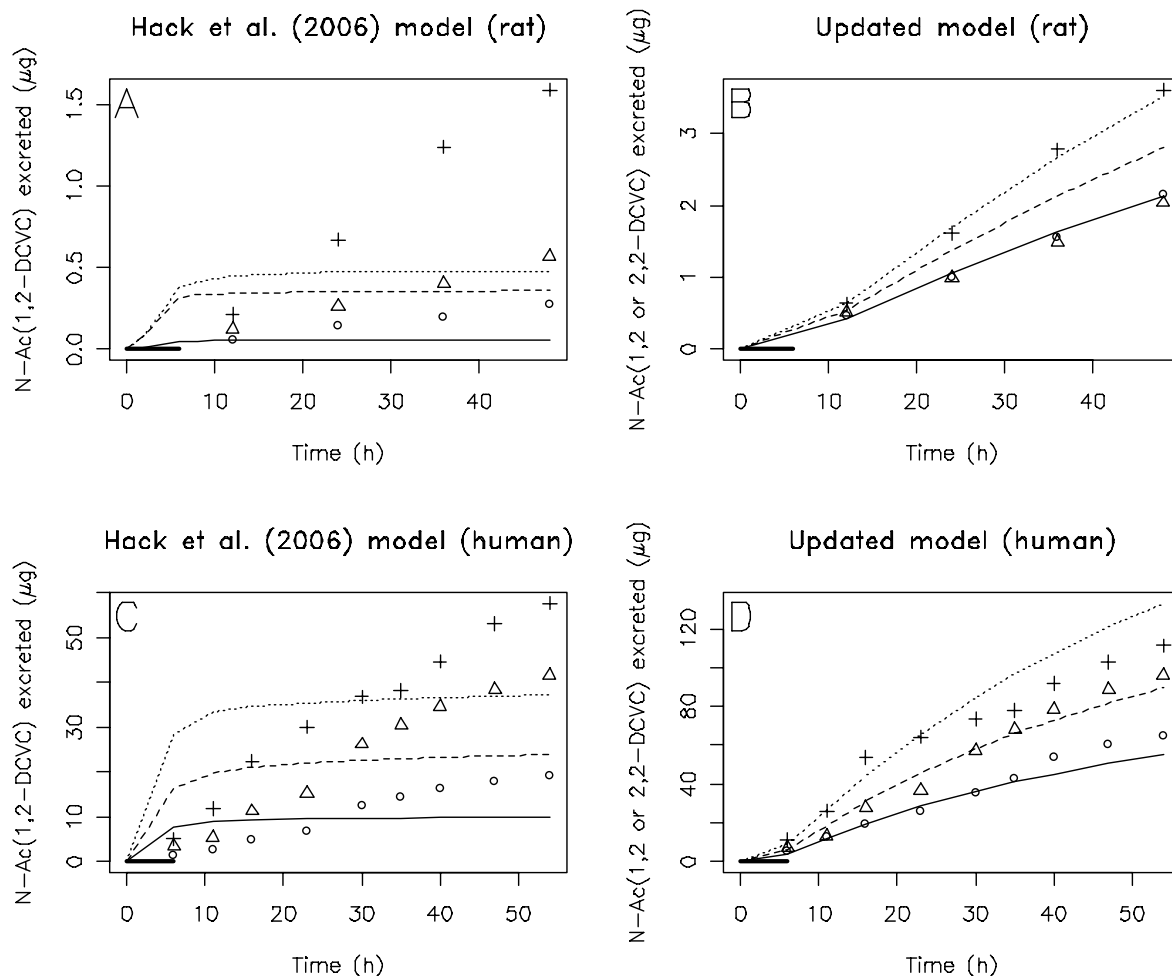


Figure 3-9. Comparison of urinary excretion data for NAcDCVC and predictions from the Hack et al. (2006) and the updated PBPK models. Data are from Bernauer et al. (1996) for (A and B) rats or (C and D) humans exposed for 6 h to 40 (○), 80 (△), or 160 (+) ppm in air (thick horizontal line denotes the exposure period). Predictions from Hack et al. (2006) and the corresponding data (A and C) are only for the 1,2 isomer, whereas those from the updated model (B and D) are for both isomers combined. Parameter values used for each prediction are a random sample from the group- or individual-specific parameters from the rat and human MCMC chains (the last iteration of the first chain was used in each case). Note that in the Hack et al. (2006) model, each dose group had different model parameters, whereas in the updated model, all dose groups are required to have the same model parameters. See files linked to Appendix A for comparisons with the full distribution of predictions.

1 **3.5.6.3.3. Human model.** Table 3-45–3-46 provide a summary evaluation of the predictions of
2 the model as compared to the human data, with figures showing data and predictions in
3 Appendix A. With respect to the TCE submodel, blood and exhaled air measurements appeared
4 more robust than previously found from the Hack et al. (2006) model. TCE blood concentrations
5 from most studies were well predicted. However, those from Chiu et al. (2007) were
6 consistently over-predicted, and a few of those from Fisher et al. (1998) were consistently
7 underpredicted. Alveolar or mixed exhaled breath concentrations of TCE from all studies except
8 Fisher et al. (1998) were well predicted, though the discrepancy appeared smaller than that
9 originally reported by Fisher et al. (1998) for their PBPK model. In addition, the majority of the
10 “out-of-sample” evaluation data consisted of TCE in blood or breath, and were generally well
11 predicted, lending confidence to the model predictions for the parent compound.

12 In terms of TCA and TCOH, as with the mouse and rat, the overall mass balance and
13 metabolic disposition to these metabolites also appeared to be robust, as urinary excretion
14 following TCE exposure could be modeled accurately. However, data from Chiu et al. (2007)
15 indicated substantial interoccasion variability, as the same individual exposed to the same
16 concentration on different occasions sometimes had substantial differences in urinary excretion.
17 Since Chiu et al. (2007) was the only calibration study for which this urine collection was
18 intermittent, this interoccasion variability was also reflected in the larger residual error (GSD of
19 1.55 and 1.59 for TCA and TCOH, respectively—Table 3-41) for intermittent urine collection as
20 compared to cumulative collection (respective residual error GSD of 1.36 and 1.11). Blood and
21 plasma concentrations of TCA and free TCOH were fairly well simulated, with GSD for the
22 residual error of 1.1–1.4, though total TCOH in blood had greater residual error with GSD of
23 about 1.6. This partially reflects the “sharper” peak concentrations of total TCOH in the Chiu et
24 al. (2007) data relative to the model predictions. In addition, TCA and TCOH blood and urine
25 data were available from several studies for “out-of-sample” evaluation and were generally well
26 predicted by the model, lending further confidence to the model predictions for these
27 metabolites.

1
2
3

Table 3-45. Summary comparison of updated PBPK model predictions and *in vivo* data used for “calibration” in humans

Reference	Exposure(s)	Discussion
Bernauer et al., 1996	TCE inhalation	<p>These data, consisting of TCA, TCOG and NAcDCVC excreted in urine, were accurately predicted by the model using both individual-specific and population sampled parameters. The posterior NAcDCVC predictions were an important improvement over the predictions of Hack et al. (2006), which predicted much more rapid excretion than observed. The fit improvement is probably a result of the addition of the DCVG submodel between TCE and DCVC, along with the broader priors on DCVC excretion and bioactivation. Interestingly, in terms of population predictions, the NAcDCVC excretion data from this study were on the low end, though still within the 95% CI.</p>
Chiu et al., 2007	TCE inhalation	<p>Overall, posterior predictions were quite accurate across most of the individuals and exposure occasions. TCE alveolar breath concentrations were well simulated for both individual-specific and population-generated simulations, though there was substantial scatter (intraoccasion variability). However, TCE blood concentrations were consistently over-predicted in most of the experiments, both using individual-specific and population-generated parameters. This was not unexpected, as Chiu et al. (2007) noted the TCE blood measurements to be lower by about 2-fold relative to previously published studies. As discussed in Chiu et al. (2007), wash-in/wash-out and extrahepatic (including respiratory) metabolism were not expected to be able to account for the difference, and indeed all these processes were added to the current model without substantially improving the discrepancy.</p> <p>With respect to metabolite data, TCA and total TCOH in blood were relatively accurately predicted. There was individual experimental variability observed for both TCA and TCOH in blood at six hours (end of exposure). The population-generated simulations over-predicted TCA in blood, while they were accurate in predicting blood TCOH. Predictions of free TCOH in blood also showed over-prediction for individual experiments, with variability at the end of exposure timepoint. However, TCOH fits were improved for the population-generated simulations. TCA and TCOG urinary excretion was generally well simulated, with simulations slightly under- or over-predicting the individual experimental data in some cases.</p>
Fisher et al., 1998	TCE inhalation	<p>The majority of the predictions for these data were quite accurate. Interestingly, in contrast to the predictions for Chiu et al. (2007), TCE blood levels were somewhat underpredicted in a few cases, both from using individual-specific and population-generated predictions. These two results together suggest some unaccounted-for study-to-study variance, though interindividual variability cannot be discounted as the data from Chiu et al. (2007) were from individuals in the Netherlands and that from Fisher et al. (1998) were from individuals in the United States. As reported by Fisher et al. (1998), TCE in alveolar air was somewhat over-predicted in several cases, however, the discrepancies seemed smaller than originally reported for the Fisher et al. (1998) model.</p>

This document is a draft for review purposes only and does not constitute Agency policy.

Table 3-45. Summary comparison of updated PBPK model predictions and *in vivo* data used for “calibration” in humans (continued)

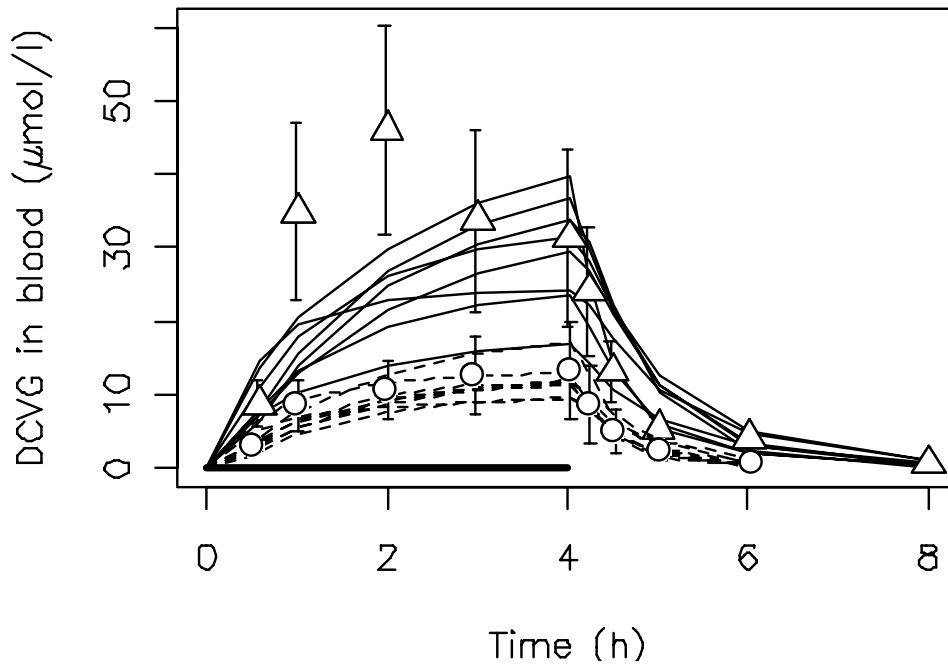
Reference	Exposure(s)	Discussion
Fisher et al., 1998 (continued)	TCE inhalation (continued)	<p>With respect to metabolite data, TCOH and TCA in blood and TCOG and TCA in urine were generally well predicted, though data for some individuals appeared to exhibit inter- and/or intraoccasion variability. For example, in one case in which the same individual (female) was exposed to both 50 and 100 ppm, the TCOH blood data was over-predicted at the higher one exposure. In addition, in one individual, initial individual-specific simulations for TCA in urine were underpredicted but shifted to over-predictions towards the end of the simulations. The population-generated results over-predicted TCA in urine for the same individual. Given the results from Chiu et al. (2007), interoccasion variability is likely to be the cause, though some dose-related effect cannot be ruled out.</p> <p>Finally, DCVG data was well predicted in light of the high variability in the data and availability of only grouped data or data from multiple individual who cannot be matched to the appropriate TCE and oxidative metabolite data set. In all cases, the basic shape (plateau and then sharp decline) and order of magnitude of the time-course were well predicted. Furthermore, the range of the data was well-captured by the 95% CI of the population-generated predictions.</p>
Kimmerle and Eben, 1973b	TCE inhalation	These data were well fit by the model, using either individual-specific or population-generated parameters.
Monster et al., 1976	TCE inhalation	The data simulated in this case were exhaled alveolar TCE, TCE in venous blood, TCA in blood, TCA in urine, and TCOG in urine. Both using individual-specific and population-generated simulations, all fits are within the 95% CI. The one exception was the retained dose for a male exposed to 65 ppm, which was outside the 95% CI for the population-generated results.
Muller et al., 1974	TCA, TCOH oral	<p>The data measured after oral TCA was timecourse TCA measured in plasma and urine. Individual-specific predictions were accurate, but both data sets were over-predicted in the population-generated simulations.</p> <p>The data measured after oral TCOH was timecourse TCOH in blood, TCOG in urine, TCA in plasma, and TCA in urine. Individual-specific predictions were accurate, but the population-generated simulations over-predicted TCOH in blood and TCOG in urine. The population-based TCA predictions were accurate.</p> <p>These results indicate that “unusual” parameter values were necessary in the individual-specific simulations to give accurate predictions.</p>
Paykoc et al., 1945	TCA i.v.	These data were well fit by the model, using either individual-specific or population-generated parameters.

1 **Table 3-46. Summary comparison of updated PBPK model predictions and**
 2 ***in vivo* data used for “out-of-sample” evaluation in humans**
 3

Reference	Exposure(s)	Discussion
Bartonicek, 1962	TCE inhalation	While these data were mostly within the 95% CI of the predictions, they tended to be at the high end for all the individuals in the study.
Bloemen et al., 2001	TCE inhalation	These data were all well within the 95% CI of the predictions.
Fernandez et al., 1977	TCE inhalation	These data were all well within the 95% CI of the predictions.
Lapare et al., 1995	TCE inhalation	These data were all well within the 95% CI of the predictions.
Monster et al., 1979	TCE inhalation	These data were all well within the 95% CI of the predictions.
Muller et al., 1974, 1975	TCE inhalation	Except for TCE in alveolar air, which was over-predicted during exposure, these data were all well within the 95% CI of the predictions.
Sato et al., 1977	TCE inhalation	These data were all well within the 95% CI of the predictions.
Stewart et al., 1970	TCE inhalation	These data were all well within the 95% CI of the predictions.
Treibig et al., 1976	TCE inhalation	Except for TCE in alveolar air, these data were all well within the 95% CI of the predictions.

4
 5
 6 In terms of total metabolism, no closed-chamber data exist in humans, but alveolar breath
 7 concentrations were generally well simulated, suggesting that total metabolism may be fairly
 8 robust. In addition, as with the rat, the data on NAcDCVC urinary excretion was well predicted
 9 (residual error GSD of 1.12), in particular the fact that excretion was still ongoing at the end of
 10 the experiment (48 hrs after the end of exposure). Thus, there is greater confidence in the
 11 estimate of the flux through the GSH pathway than there was from the Hack et al. (2006) model,
 12 in which excretion was completed within the first few hours after exposure (see Figure 3-9,
 13 panels C and D). If only urinary data were available, as is the case for the rat, the overall flux
 14 would still estimated indirectly, and there would remain some ambiguity as to the relative
 15 contributions respiratory wash-in/wash-out, respiratory metabolism, extrahepatic metabolism,
 16 DCVC bioactivation versus *N*-acetylation, and oxidation in the liver producing something other
 17 than TCOH or TCA. However, unlike in the rat, the blood DCVG data, while highly variable,
 18 nonetheless provide substantial constraints (at least a strong lower bound) on the flux of GSH
 19 conjugation, and is well fit by the model (see Figure 3-10). Importantly, the high residual error
 20 GSD for blood DCVG reflects the fact that only grouped or unmatched individual data were
 21 available, so in this case, the residual error includes interindividual variability, which is not
 22 included in the other residual error estimates. For the other indirectly estimated pathways, there
 23 remain a large range of possible values that are nonetheless consistent with all the available *in*
 24 *vivo* data. The use of noninformative priors for the metabolism parameters for which there were
 25 no *in vitro* data means that a fuller characterization of the uncertainty in these various metabolic

1 pathways could be achieved. Thus, as with the rat, the model should be reliable for estimating
2 lower and upper bounds on several of these pathways.



3
4 **Figure 3-10. Comparison of DCVG concentrations in human blood and**
5 **predictions from the updated model.** Data are mean concentrations for males
6 (Δ) and females (\circ) reported in Lash et al. (1999b) for humans exposed for
7 4 hours to 100 ppm TCE in air (thick horizontal line denotes the exposure period).
8 Data for oxidative metabolites from the same individuals were reported in Fisher
9 et al. (1998) but could not be matched with the individual DCVG data (Lash
10 2007, personal communication). The vertical error bars are standard errors of the
11 mean as reported in Lash et al. (1999b) ($n = 8$, so standard deviation is 80.5-fold
12 larger). Lines are PBPK model predictions for individual male (solid) and female
13 (dashed) subjects. Parameter values used for each prediction are a random sample
14 from the individual-specific parameters from the human MCMC chains (the last
15 iteration of the 1st chain was used). See files linked to Appendix A for
16 comparisons with the full distribution of predictions.

17
18
19 **3.5.6.4. Summary Evaluation of Updated Physiologically Based Pharmacokinetic (PBPK)**
20 **Model**

21 Overall, the updated PBPK model, utilizing parameters consistent with the available
22 physiological and *in vitro* data from published literature, provides reasonable fits to an extremely
23 large database of *in vivo* pharmacokinetic data in mice, rats, and humans. Posterior parameter
24 distributions were obtained by MCMC sampling using a hierarchical Bayesian population
25 statistical model and a large fraction of this *in vivo* database. Convergence of the MCMC

This document is a draft for review purposes only and does not constitute Agency policy.

1 samples for model parameters was good for mice, and adequate for rats and humans. In addition,
2 in rats and humans, the model produced predications that are consistent with *in vivo* data from
3 many studies not used for calibration (insufficient studies were available in mice for such “out of
4 sample” evaluation).

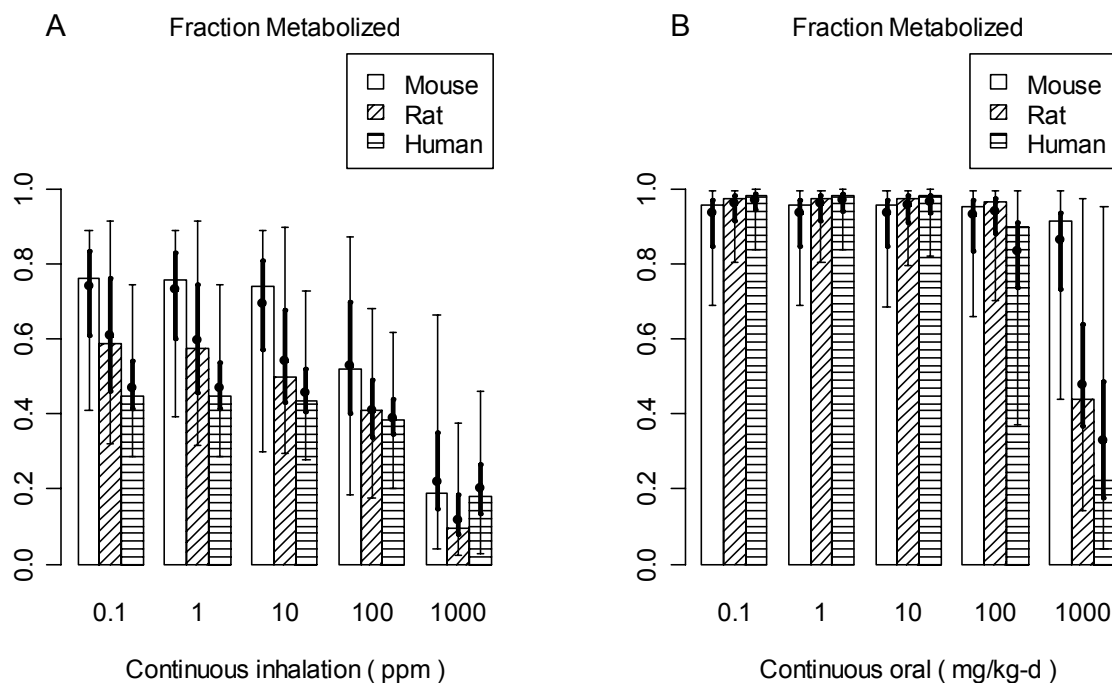
6 **3.5.7. Physiologically Based Pharmacokinetic (PBPK) Model Dose Metric Predictions**

7 **3.5.7.1. Characterization of Uncertainty and Variability**

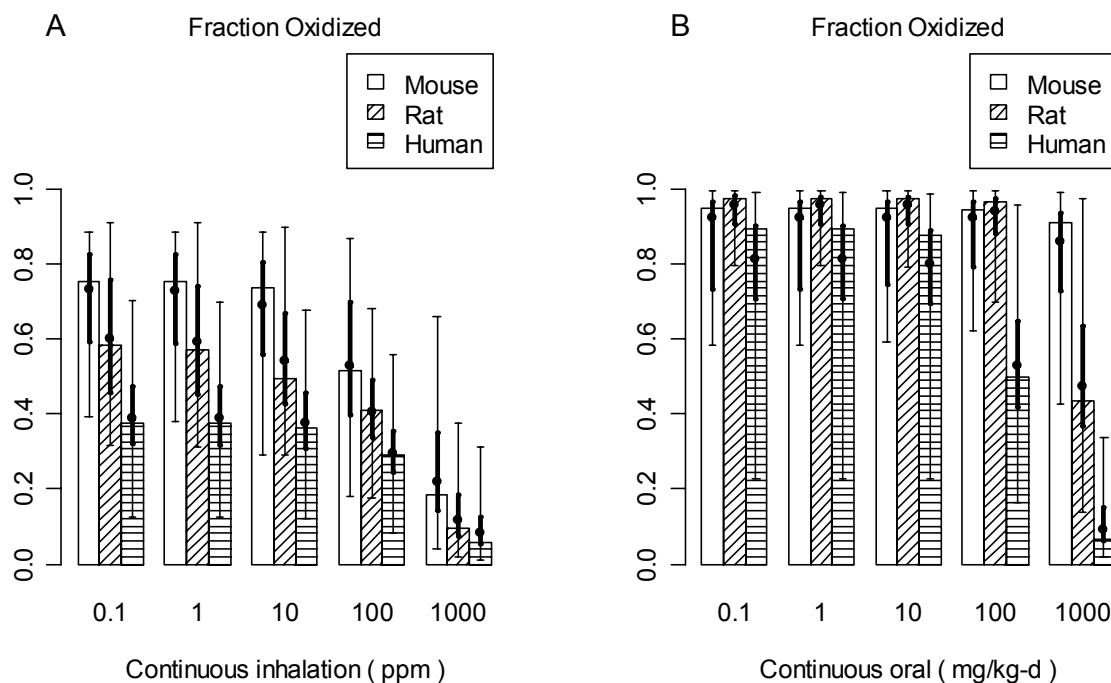
8 Since it is desirable to characterize the contributions from both uncertainty in population
9 parameters and variability within the population, so the following procedure is adopted. First,
10 500 sets of population parameters (i.e., population mean and variance for each parameter) are
11 extracted from the posterior MCMC samples—these represent the uncertainty in the population
12 parameters. To minimize autocorrelation, they were obtained by “thinning” the chains to the
13 appropriate degree. From each of these sets of population parameters, 100 sets of “individual,”
14 or “study group” in the case of rodents, parameters were generated by Monte Carlo—each of
15 these represents the population variability, given a *particular* set of population parameters. Thus
16 a total of 50,000 individuals (or study groups, for rodents), representing 100 (variability) each for
17 500 different populations (uncertainty), were generated.

18 Each set was run for a variety of generic exposure scenarios. The combined distribution
19 of all 50,000 individuals reflects both uncertainty and variability—i.e., the case in which one is
20 trying to predict the dosimetry for a single random study (for rodents) or individual (for humans).
21 In addition, for each dose metric, the mean predicted internal dose was calculated from set of the
22 500 sets of 100 individuals, resulting in a distribution for the uncertainty in the population mean.
23 Comparing the combined uncertainty and variability distribution with the uncertainty distribution
24 in the population mean gives a sense of how much of the overall variation is due to uncertainty
25 versus variability.

26 Figures 3-11–3-19 show the results of these simulations for a number of representative
27 dose metrics across species continuously exposed via inhalation or orally. For display purposes,
28 dose metrics have been scaled by total intake (resulting in a predicted “fraction” metabolized) or
29 exposure level (resulting in an internal dose per ppm for inhalation or per mg/kg/d for oral
30 exposures). In these figures, the thin error bars representing the 95% confidence interval for
31 overall uncertainty and variability, and the thick error bars representing the 95% confidence
32 interval for the uncertainty in the population mean. The interpretation of these figures is that if
33 the thick error bars are much smaller (or greater) than the think error bars, then variability (or
34 uncertainty) contributes the most to overall uncertainty and variability.

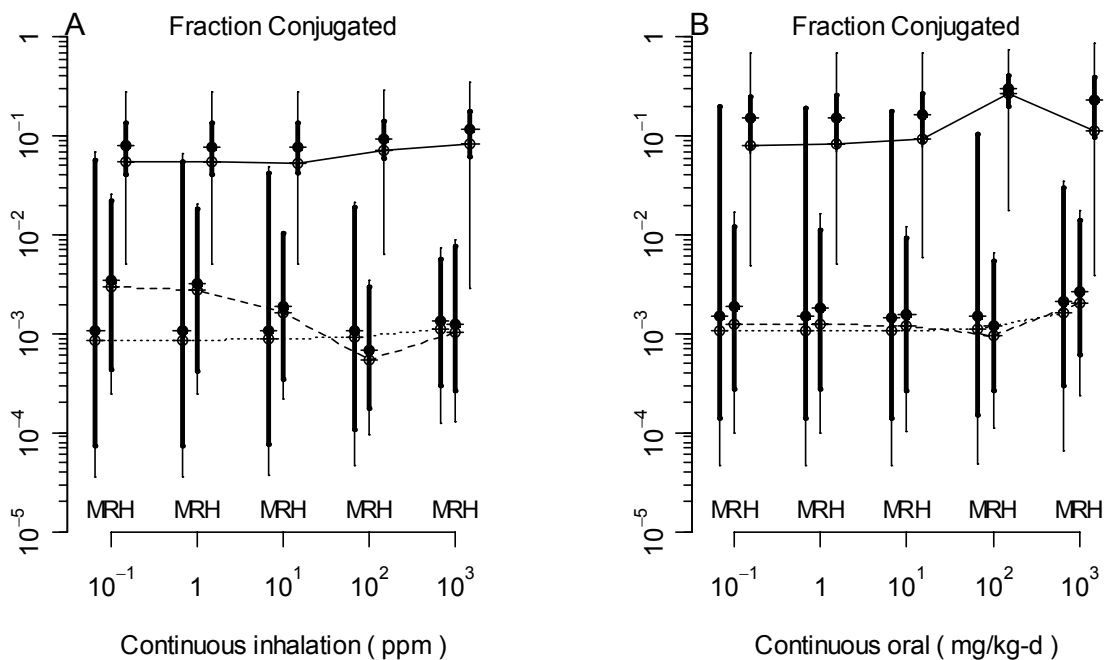


1
2
3 **Figure 3-11. PBPK model predictions for the fraction of intake that is**
4 **metabolized under continuous inhalation (A) and oral (B) exposure**
5 **conditions in mice (white), rats (diagonal hashing), and humans (horizontal**
6 **hashing).** Bars and thin error bars represent the median estimate and 95%
7 confidence interval for a random rodent group or human individual, and reflect
8 combined uncertainty and variability. Circles and thick error bars represent the
9 median estimate and 95% confidence interval for the population mean, and reflect
10 uncertainty only.

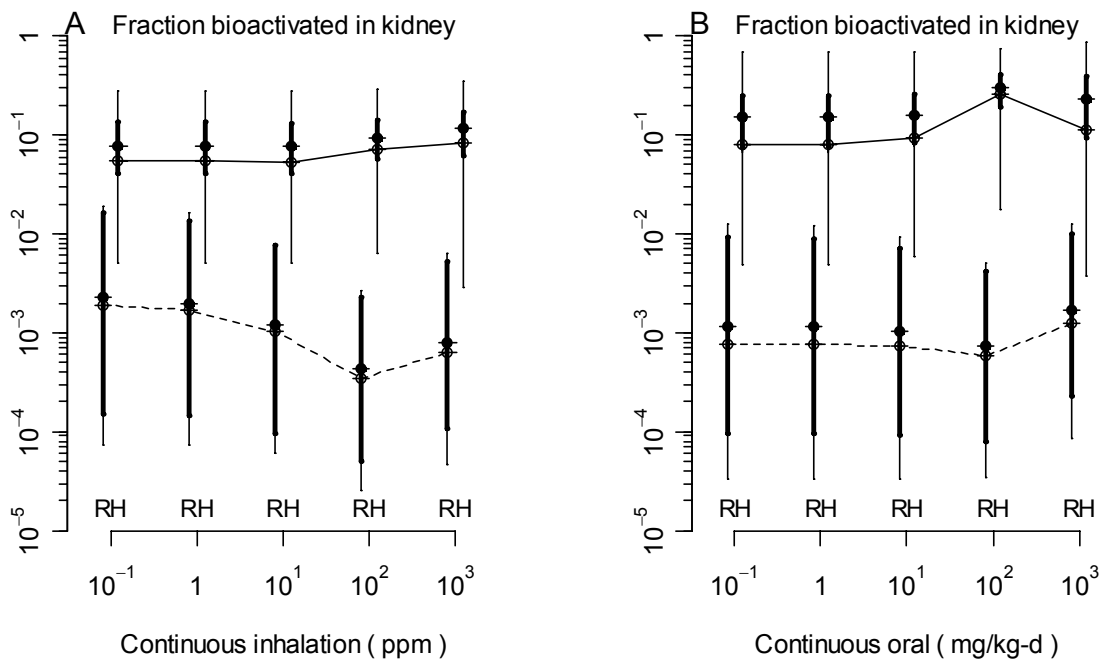


1
2
3
4
5
6
7
8
9
10

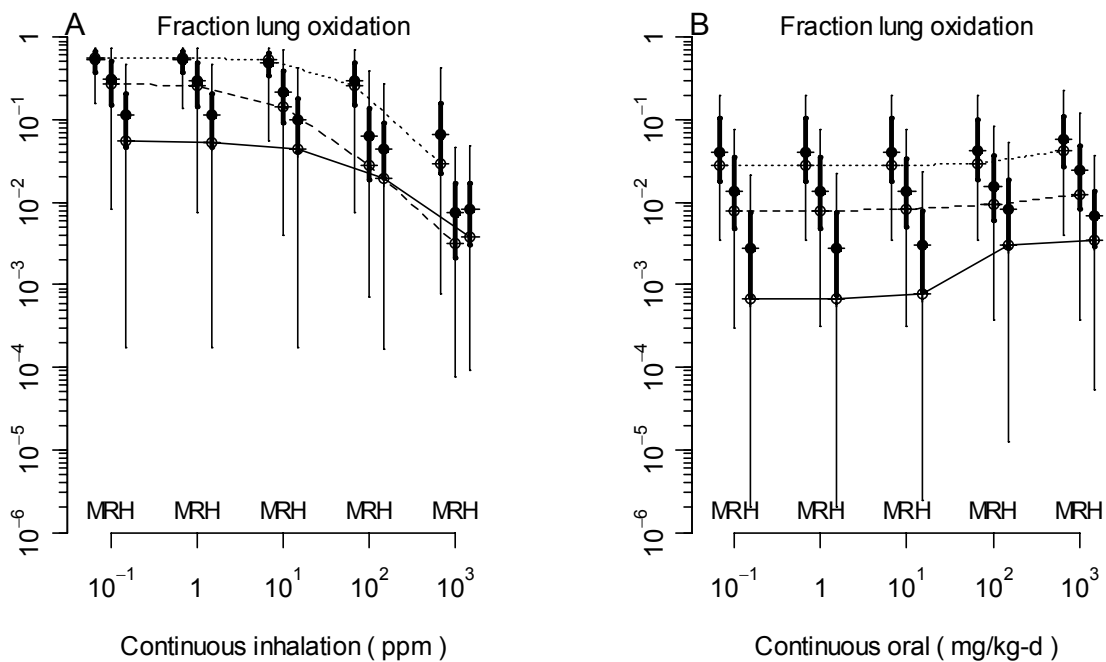
Figure 3-12. PBPK model predictions for the fraction of intake that is metabolized by oxidation (in the liver and lung) under continuous inhalation (A) and oral (B) exposure conditions in mice (white), rats (diagonal hashing), and humans (horizontal hashing). Bars and thin error bars represent the median estimate and 95% confidence interval for a random rodent group or human individual, and reflect combined uncertainty and variability. Circles and thick error bars represent the median estimate and 95% confidence interval for the population mean, and reflect uncertainty only.



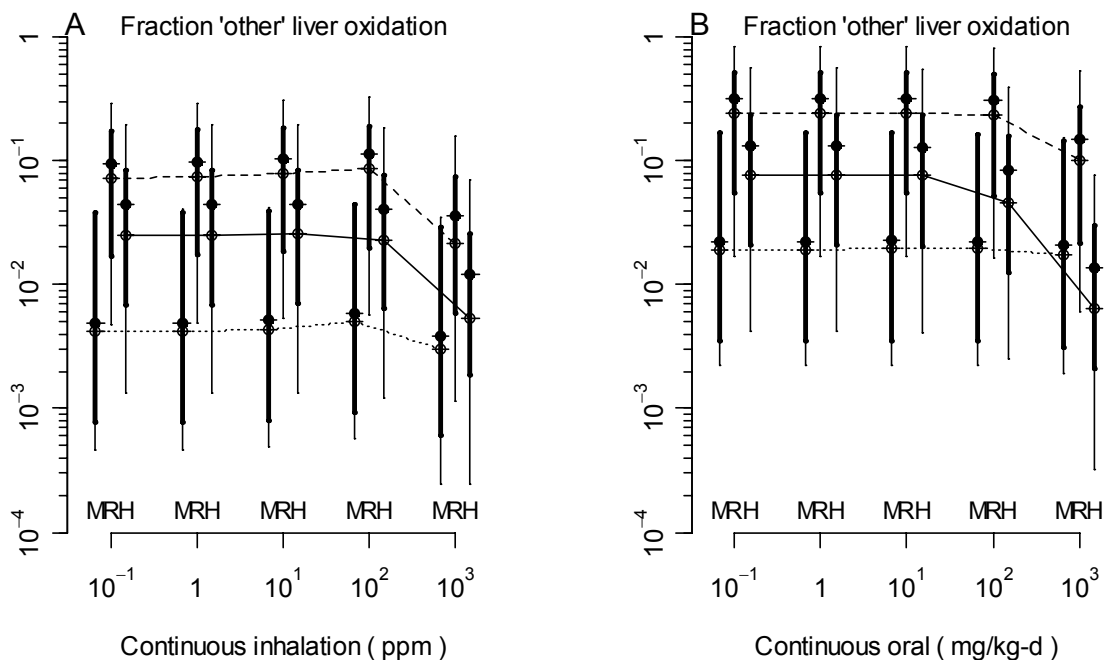
1
 2 **Figure 3-13. PBPK model predictions for the fraction of intake that is**
 3 **metabolized by GSH conjugation (in the liver and kidney) under continuous**
 4 **inhalation (A) and oral (B) exposure conditions in mice (dotted line), rats**
 5 **(dashed line), and humans (solid line). X-values are slightly offset for clarity.**
 6 Open circles (connected by lines) and thin error bars represent the median
 7 estimate and 95% confidence interval for a random rodent group or human
 8 individual, and reflect combined uncertainty and variability. Filled circles and
 9 thick error bars represent the median estimate and 95% confidence interval for the
 10 population mean, and reflect uncertainty only.



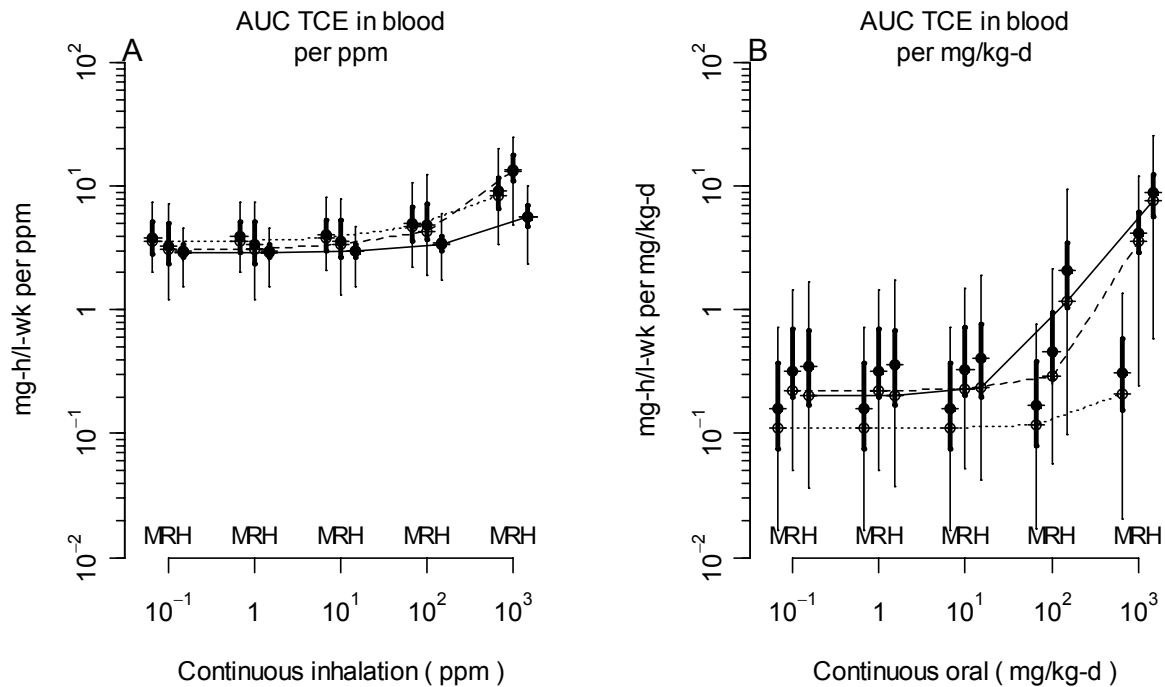
1
 2 **Figure 3-14. PBPK model predictions for the fraction of intake that is**
 3 **bioactivated DCVC in the kidney under continuous inhalation (A) and oral**
 4 **(B) exposure conditions in rats (dashed line) and humans (solid line).**
 5 *X*-values are slightly offset for clarity. Open circles (connected by lines) and thin
 6 error bars represent the median estimate and 95% confidence interval for a
 7 random rodent group or human individual, and reflect combined uncertainty and
 8 variability. Filled circles and thick error bars represent the median estimate and
 9 95% confidence interval for the population mean, and reflect uncertainty only.



1
 2 **Figure 3-15. PBPK model predictions for fraction of intake that is oxidized**
 3 **in the respiratory tract under continuous inhalation (A) and oral (B)**
 4 **exposure conditions in mice (dotted line), rats (dashed line), and humans**
 5 **(solid line).** X-values are slightly offset for clarity. Open circles (connected by
 6 lines) and thin error bars represent the median estimate and 95% confidence
 7 interval for a random rodent group or human individual, and reflect combined
 8 uncertainty and variability. Filled circles and thick error bars represent the
 9 median estimate and 95% confidence interval for the population mean, and reflect
 10 uncertainty only.



1
 2 **Figure 3-16. PBPK model predictions for the fraction of intake that is**
 3 **“untracked” oxidation of TCE in the liver under continuous inhalation (A)**
 4 **and oral (B) exposure conditions in mice (dotted line), rats (dashed line), and**
 5 **humans (solid line)** *X*-values are slightly offset for clarity. Open circles
 6 (connected by lines) and thin error bars represent the median estimate and 95%
 7 confidence interval for a random rodent group or human individual, and reflect
 8 combined uncertainty and variability. Filled circles and thick error bars represent
 9 the median estimate and 95% confidence interval for the population mean, and
 10 reflect uncertainty only.



2

3

4 **Figure 3-17. PBPK model predictions for the weekly AUC of TCE in venous**
 5 **blood (mg-hour/L-week) per unit exposure (ppm or mg/kg/d) under**
 6 **continuous inhalation (A) and oral (B) exposure conditions in mice (dotted**

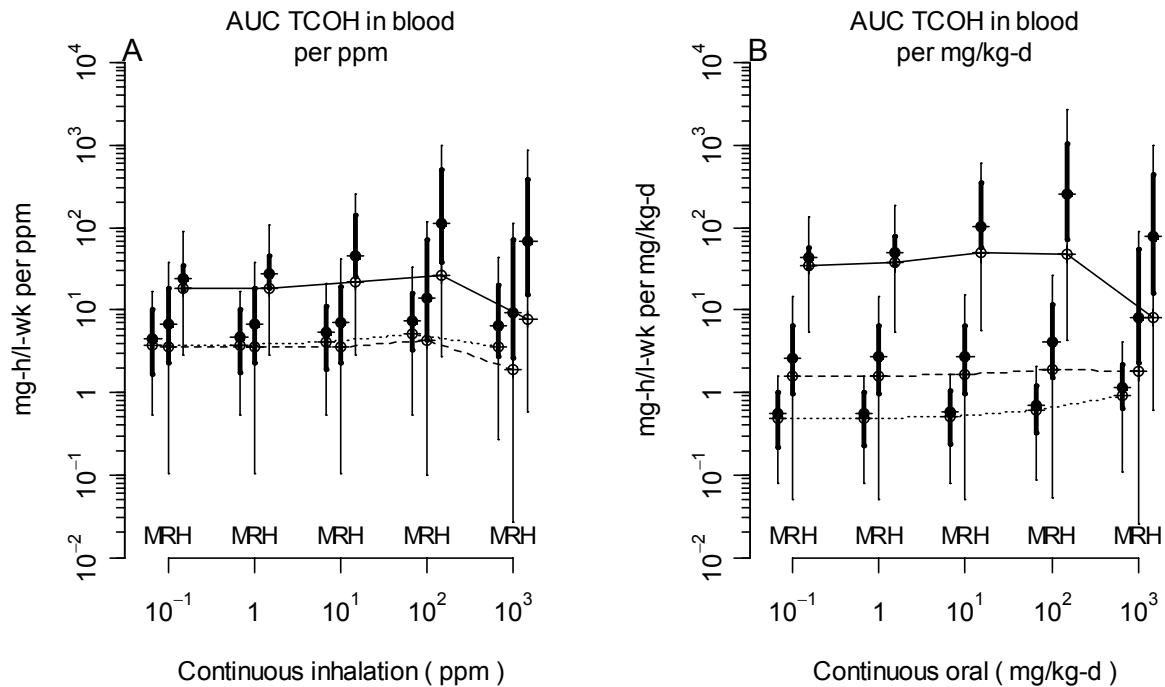
7 **line), rats (dashed line), and humans (solid line). X-values are slightly offset**
 8 for clarity. Open circles (connected by lines) and thin error bars represent the

9 median estimate and 95% confidence interval for a random rodent group or

10 human individual, and reflect combined uncertainty and variability. Filled circles

11 and thick error bars represent the median estimate and 95% confidence interval

12 for the population mean, and reflect uncertainty only.



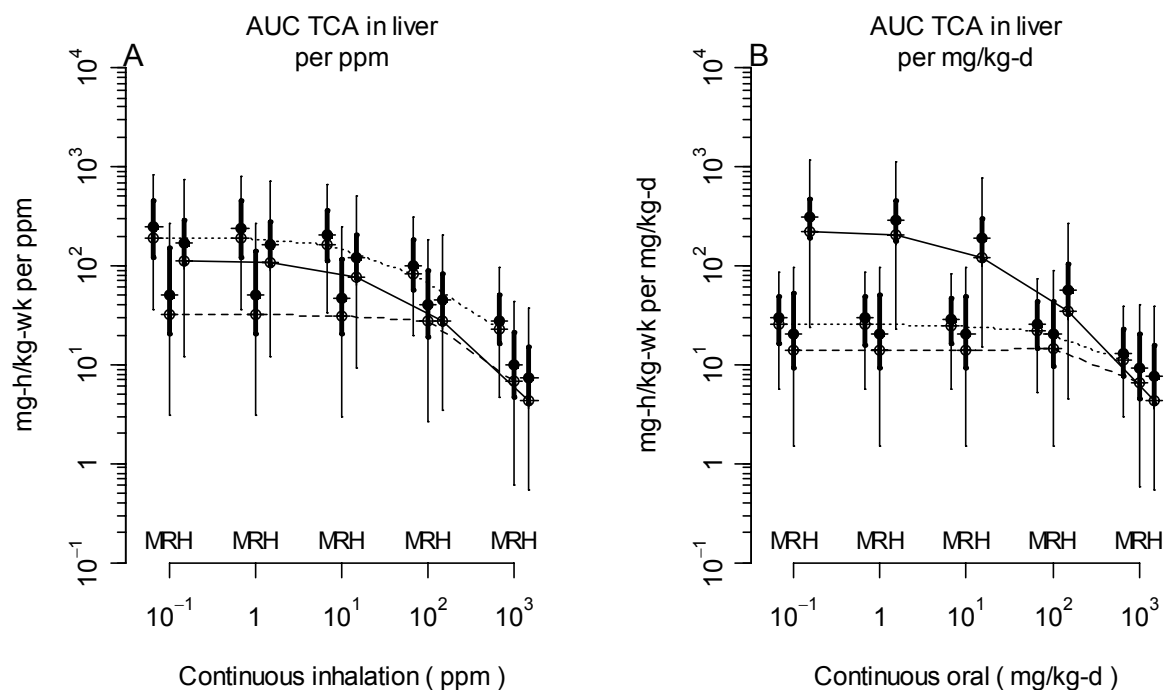
2

3

4 **Figure 3-18. PBPK model predictions for the weekly AUC of TCOH in blood**
 5 **(mg-hour/L-week) per unit exposure (ppm or mg/kg/d) under continuous**
 6 **inhalation (A) and oral (B) exposure conditions in mice (dotted line), rats**
 7 **(dashed line), and humans (solid line).** *X*-values are slightly offset for clarity.

8 Open circles (connected by lines) and thin error bars represent the median
 9 estimate and 95% confidence interval for a random rodent group or human

10 individual, and reflect combined uncertainty and variability. Filled circles
 11 and thick error bars represent the median estimate and 95% confidence interval for the
 12 population mean, and reflect uncertainty only.



1
2
3 **Figure 3-19. PBPK model predictions for the weekly AUC of TCA in the**
4 **liver (mg-hour/L-week) per unit exposure (ppm or mg/kg/d) under**
5 **continuous inhalation (A) and oral (B) exposure conditions in mice (dotted**
6 **line), rats (dashed line), and humans (solid line). X-values are slightly offset**
7 **for clarity. Open circles (connected by lines) and thin error bars represent the**
8 **median estimate and 95% confidence interval for a random rodent group or**
9 **human individual, and reflect combined uncertainty and variability. Filled circles**
10 **and thick error bars represent the median estimate and 95% confidence interval**
11 **for the population mean, and reflect uncertainty only.**
12
13

14 For application to human health risk assessment, the uncertainty in and variability among
15 rodent internal dose estimates *both* contribute to *uncertainty* in human risk estimates. Therefore,
16 it is appropriate to combine uncertainty and variability when applying rodent dose metric
17 predictions to quantitative risk assessment. The median and 95% confidence interval for each
18 dose metric at some representative exposures in rodents are given in Tables 3-47–3-48, and the
19 confidence interval in these tables includes both uncertainty in the population mean and variance
20 as well as variability in the population. On the other hand, for use in predicting human risk, it is
21 often necessary to separate, to the extent possible, interindividual variability from uncertainty,
22 and this disaggregation is summarized in Table 3-49.

This document is a draft for review purposes only and does not constitute Agency policy.

10/20/09

This document is a draft for review purposes only and does not constitute Agency policy.

3-123

DRAFT—DO NOT CITE OR QUOTE

Table 3-47. Posterior predictions for representative internal doses: mouse

Dose metric	Posterior predictions for mouse dose metrics: median (2.5%, 97.5%)				Units
	100 ppm, 7 h/d, 5 d/wk	600 ppm, 7 h/d, 5 d/wk	300 mg/kg/d, 5 d/wk	1,000 mg/kg/d, 5 d/wk	
ABioactDCVCBW34	0.304 (0.000534, 12.4)	2.35 (0.00603, 37)	0.676 (0.00193, 18.4)	2.81 (0.0086, 42.4)	mg/wk-kg ^{3/4}
ABioactDCVCKid	43.7 (0.0774, 1780)	336 (0.801, 5,240)	96.8 (0.281, 2,550)	393 (1.23, 6,170)	mg/wk-kg tissue
AMetGSHBW34	0.684 (0.0307, 17.6)	5.15 (0.285, 44.9)	1.66 (0.0718, 24.5)	6.37 (0.567, 49.4)	mg/wk-kg ^{3/4}
AMetLiv1BW34	170 (61.2, 403)	878 (342, 2,030)	400 (125, 610)	874 (233, 1,960)	mg/wk-kg ^{3/4}
AMetLivOtherBW34	3.81 (0.372, 38.4)	20 (1.86, 192)	8.38 (0.773, 80.1)	20 (1.55, 202)	mg/wk-kg ^{3/4}
AMetLivOtherLiv	196 (19, 2,070)	1,030 (96.5, 10,100)	437 (39.5, 4,180)	1,020 (82.1, 10,400)	mg/wk-kg tissue
AMetLngBW34	187 (7.75, 692)	263 (10.9, 2,240)	38.5 (3.49, 147)	127 (8.59, 484)	mg/wk-kg ^{3/4}
AMetLngResp	638,000 (26,500, 2,510,000)	918,000 (36,800, 7,980,000)	134,000 (12,500, 514,000)	433,000 (30,200, 1,690,000)	mg/wk-kg tissue
AUCCBid	96.9 (45, 211)	822 (356, 2,040)	110 (6.95, 411)	592 (56, 1,910)	mg-h/L-wk
AUCCTOH	87.9 (9.9, 590)	480 (42.1, 4,140)	132 (14.4, 670)	389 (34, 2,600)	mg-h/L-wk
AUCLivTCA	1,880 (444, 7,190)	5,070 (1,310, 18,600)	2,260 (520, 8,750)	4,660 (939, 18,900)	mg-h/L-wk
TotMetabBW34	377 (140, 917)	1,260 (475, 3,480)	472 (165, 617)	1,110 (303, 2,010)	mg/wk-kg ^{3/4}
TotOxMetabBW34	375 (139, 916)	1,250 (451, 3,450)	465 (161, 616)	1,100 (294, 2,010)	mg/wk-kg ^{3/4}
TotTCAInBW	272 (88.9, 734)	729 (267, 1,950)	334 (106, 875)	694 (185, 1,910)	mg/wk-kg

Note: Mouse body weight is assumed to be 0.03 kg. Predictions are weekly averages over 10 weeks of the specified exposure protocol. Confidence interval reflects both uncertainties in population parameters (mean, variance) as well as population variability.

Table 3-48. Posterior predictions for representative internal doses: rat

Dose metric	Posterior predictions for rat dose metrics: median (2.5%,97.5%)				Units
	100 ppm, 7 h/d, 5 d/wk	600 ppm, 7 h/d, 5 d/wk	300 mg/kg/d, 5 d/wk	1,000 mg/kg/d, 5 d/wk	
ABioactDCVCBW34	0.341 (0.0306, 2.71)	2.3 (0.175, 22.6)	2.15 (0.17, 20.2)	8.89 (0.711, 84.1)	mg/wk-kg ^{3/4}
ABioactDCVCKid	67.8 (6.03, 513)	450 (35.4, 4,350)	420 (31.6, 3,890)	1,720 (134, 15,800)	mg/wk-kg tissue
AMetGSHBW34	0.331 (0.0626, 2.16)	2.27 (0.315, 19.3)	2.13 (0.293, 16)	8.84 (1.35, 69.3)	mg/wk-kg ^{3/4}
AMetLiv1BW34	176 (81.1, 344)	623 (271, 1,270)	539 (176, 1,060)	951 (273, 2,780)	mg/wk-kg ^{3/4}
AMetLivOtherBW34	45.5 (2.52, 203)	160 (7.84, 749)	134 (6.83, 659)	238 (11.3, 1390)	mg/wk-kg ^{3/4}
AMetLivOtherLiv	1,870 (92.1, 8,670)	6,660 (313, 31,200)	5,490 (280, 27,400)	9,900 (492, 59,600)	mg/wk-kg tissue
AMetLngBW34	15 (0.529, 173)	24.5 (0.819, 227)	15.1 (0.527, 115)	32.1 (1.01, 311)	mg/wk-kg ^{3/4}
AMetLngResp	41,900 (1,460, 496,000)	67,900 (2,350, 677,000)	40,800 (1,500, 325,000)	85,700 (2,660, 877,000)	mg/wk-kg tissue
AUCCBld	86.7 (39.2, 242)	1,160 (349, 2,450)	670 (47.8, 1,850)	3,340 (828, 8,430)	mg-h/L-wk
AUCCTCOH	83.6 (1.94, 1,560)	446 (6, 10,900)	304 (4.71, 7,590)	685 (8.14, 32,500)	mg-h/L-wk
AUCLivTCA	587 (53.7, 4,740)	2,030 (186, 13,400)	1,730 (124, 11,800)	3,130 (200, 21,000)	mg-h/L-wk
TotMetabBW34	206 (103, 414)	682 (288, 1,430)	572 (199, 1,080)	1,030 (302, 2,920)	mg/wk-kg ^{3/4}
TotOxMetabBW34	206 (103, 414)	677 (285, 1,430)	568 (191, 1,080)	1,010 (286, 2,910)	mg/wk-kg ^{3/4}
TotTCAInBW	31.7 (3.92, 174)	110 (13.8, 490)	90.1 (10.4, 417)	164 (17.3, 800)	mg/wk-kg

Note: Rat body weight is assumed to be 0.3 kg. Predictions are weekly averages over 10 weeks of the specified exposure protocol. Confidence interval reflects both uncertainties in population parameters (mean, variance) as well as population variability.

Table 3-49. Posterior predictions for representative internal doses: human

Dose metric	Posterior predictions for human dose metrics: 2.5% population: median (2.5%, 97.5%) 50% population: median (2.5%, 97.5%) 97.5% population: median (2.5%, 97.5%)			
	Female 0.001 ppm continuous	Male 0.001 ppm continuous	Female 0.001 mg/kg/d continuous	Male 0.001 mg/kg/d continuous
ABioactDCVCBW 34	0.000256 (6.97e-5, 0.000872) 0.00203 (0.00087, 0.00408) 0.0119 (0.00713, 0.0177)	0.000254 (6.94e-5, 0.000879) 0.00202 (0.000859, 0.00413) 0.012 (0.00699, 0.0182)	0.000197 (6.13e-5, 0.000502) 0.00262 (0.0012, 0.00539) 0.021 (0.0118, 0.0266)	0.0002 (6.24e-5, 0.000505) 0.00271 (0.00125, 0.00559) 0.022 (0.0124, 0.0277)
ABioactDCVCKid	0.02 (0.00549, 0.0709) 0.16 (0.0671, 0.324) 0.95 (0.56, 1.45)	0.0207 (0.00558, 0.0743) 0.163 (0.0679, 0.342) 0.979 (0.563, 1.51)	0.0152 (0.0048, 0.0384) 0.207 (0.0957, 0.43) 1.68 (0.956, 2.26)	0.016 (0.00493, 0.0407) 0.22 (0.102, 0.459) 1.81 (1.03, 2.43)
AMetGSHBW34	0.000159 (4.38e-05, 0.000539) 0.00126 (0.000536, 0.00253) 0.00736 (0.00442, 0.011)	0.000157 (4.37e-05, 0.00054) 0.00125 (0.000528, 0.00254) 0.00736 (0.00434, 0.0112)	0.000121 (3.82e-05, 0.000316) 0.00161 (0.000748, 0.00331) 0.013 (0.00725, 0.0164)	0.000123 (3.82e-05, 0.000323) 0.00167 (0.000777, 0.00343) 0.0136 (0.00759, 0.0171)
AMetLiv1BW34	0.00161 (0.000619, 0.00303) 0.00637 (0.00501, 0.00799) 0.0157 (0.0118, 0.0206)	0.00157 (0.000608, 0.00292) 0.00619 (0.00484, 0.00779) 0.0152 (0.0115, 0.02)	0.00465 (0.00169, 0.0107) 0.0172 (0.0153, 0.0183) 0.0192 (0.019, 0.0193)	0.00498 (0.00184, 0.0112) 0.018 (0.0161, 0.0191) 0.02 (0.0198, 0.0201)
AMetLivOtherBW 34	4.98e-5 (8.59e-6, 0.000222) 0.000671 (0.000134, 0.00159) 0.00507 (0.00055, 0.00905)	4.87e-5 (8.33e-6, 0.000214) 0.000652 (0.000129, 0.00153) 0.00491 (0.000531, 0.00885)	0.000143 (2.35e-5, 0.000681) 0.00166 (0.00035, 0.00365) 0.00993 (0.00109, 0.0153)	0.00015 (2.49e-5, 0.000713) 0.00173 (0.000365, 0.00382) 0.0103 (0.00113, 0.0159)
AMetLivOtherLiv	0.000748 (0.000138, 0.00335) 0.0104 (0.00225, 0.0237) 0.0805 (0.00871, 0.147)	0.00065 (0.000119, 0.00288) 0.00898 (0.00193, 0.0203) 0.0691 (0.00751, 0.127)	0.00214 (0.000354, 0.00979) 0.0253 (0.00564, 0.0543) 0.157 (0.0188, 0.251)	0.00197 (0.00033, 0.00907) 0.0234 (0.00526, 0.0503) 0.146 (0.0173, 0.232)
AMetLngBW34	6.9e-6 (6.13e-7, 7.99e-5) 0.00122 (0.000309, 0.0032) 0.0123 (0.00563, 0.0197)	7.25e-6 (6.44e-7, 8.39e-5) 0.00127 (0.000325, 0.00329) 0.0124 (0.00582, 0.0199)	7.54e-8 (6.59e-9, 7.85e-7) 1.51e-5 (3.44e-6, 4.6e-5) 0.000396 (0.000104, 0.00097)	7.05e-8 (6.1e-9, 7.25e-7) 1.39e-5 (3.21e-6, 4.24e-5) 0.000366 (9.54e-5, 0.000906)

Table 3-49. Posterior predictions for representative internal doses: human (continued)

Dose metric	Posterior predictions for human dose metrics: 2.5% population: median (2.5%, 97.5%) 50% population: median (2.5%, 97.5%) 97.5% population: median (2.5%, 97.5%)			
	Female 0.001 ppm continuous	Male 0.001 ppm continuous	Female 0.001 mg/kg/d continuous	Male 0.001 mg/kg/d continuous
AMetLngResp	0.0144 (0.00116, 0.155) 2.44 (0.613, 6.71) 25.8 (12.4, 42.3)	0.0146 (0.00118, 0.157) 2.44 (0.621, 6.65) 25.3 (12.2, 41.2)	0.00015 (1.27e-05, 0.00153) 0.0313 (0.00725, 0.0963) 0.813 (0.216, 2.13)	0.000134 (1.15e-05, 0.00137) 0.0279 (0.00644, 0.086) 0.716 (0.189, 1.9)
AUCCBld	0.00151 (0.00122, 0.00186) 0.00285 (0.00252, 0.00315) 0.00444 (0.00404, 0.00496)	0.00158 (0.00127, 0.00191) 0.00295 (0.00262, 0.00326) 0.00456 (0.00416, 0.00507)	4.33e-05 (3.3e-05, 6.23e-05) 0.000229 (0.000122, 0.000436) 0.00167 (0.000766, 0.00324)	3.84e-05 (2.89e-05, 5.61e-05) 0.000204 (0.000109, 0.000391) 0.00153 (0.000693, 0.00303)
AUCCTCOH	0.00313 (0.00135, 0.00547) 0.0181 (0.0135, 0.0241) 0.082 (0.0586, 0.118)	0.00305 (0.00134, 0.00532) 0.0179 (0.0133, 0.0238) 0.0812 (0.0585, 0.117)	0.00584 (0.00205, 0.0122) 0.0333 (0.025, 0.0423) 0.115 (0.0872, 0.163)	0.00615 (0.00213, 0.0127) 0.035 (0.0264, 0.0445) 0.122 (0.0919, 0.172)
AUCLivTCA	0.0152 (0.00668, 0.0284) 0.126 (0.0784, 0.194) 0.754 (0.441, 1.38)	0.0137 (0.00598, 0.0258) 0.114 (0.0704, 0.177) 0.699 (0.408, 1.3)	0.029 (0.0116, 0.0524) 0.227 (0.138, 0.343) 1.11 (0.661, 1.87)	0.0279 (0.0114, 0.0501) 0.219 (0.133, 0.33) 1.09 (0.64, 1.88)
TotMetabBW34	0.0049 (0.00383, 0.00595) 0.0107 (0.00893, 0.0129) 0.0246 (0.0185, 0.0326)	0.00482 (0.0038, 0.00585) 0.0105 (0.00877, 0.0127) 0.0244 (0.0183, 0.0324)	0.0163 (0.0136, 0.0181) 0.0191 (0.0188, 0.0193) 0.0194 (0.0194, 0.0194)	0.0173 (0.0147, 0.019) 0.0199 (0.0196, 0.0201) 0.0202 (0.0202, 0.0202)
TotOxMetabBW34	0.00273 (0.00143, 0.00422) 0.00871 (0.0069, 0.0111) 0.0224 (0.0158, 0.0309)	0.00269 (0.00143, 0.00415) 0.00857 (0.00675, 0.011) 0.0222 (0.0155, 0.0308)	0.0049 (0.00183, 0.0108) 0.0173 (0.0154, 0.0183) 0.0192 (0.019, 0.0193)	0.00516 (0.00194, 0.0114) 0.018 (0.0161, 0.0191) 0.02 (0.0198, 0.0201)

Table 3-49. Posterior predictions for representative internal doses: human (continued)

Dose metric	Posterior predictions for human dose metrics: 2.5% population: median (2.5%, 97.5%) 50% population: median (2.5%, 97.5%) 97.5% population: median (2.5%, 97.5%)			
	Female 0.001 ppm continuous	Male 0.001 ppm continuous	Female 0.001 mg/kg/d continuous	Male 0.001 mg/kg/d continuous
TotTCAInBW	0.000259 (0.000121, 0.000422) 0.00154 (0.00114, 0.00202) 0.00525 (0.00399, 0.00745)	0.000246 (0.000114, 0.000397) 0.00146 (0.00109, 0.00193) 0.00499 (0.0038, 0.0071)	0.000501 (0.000189, 0.000882) 0.00286 (0.00222, 0.00357) 0.00659 (0.00579, 0.00724)	0.000506 (0.000192, 0.00089) 0.00289 (0.00222, 0.0036) 0.00662 (0.00581, 0.00726)

Note: Human body weight is assumed to be 70 kg for males, 60 kg for females. Predictions are weekly averages over 100 weeks of continuous exposure (dose metric units same as previous tables). Each row represents a different population percentile (2.5, 50, and 97.5%), and the confidence interval in each entry reflects uncertainty in population parameters (mean, variance).

1 **3.5.7.2. Implications for the Population Pharmacokinetics of Trichloroethylene (TCE)**

2 **3.5.7.2.1. Results.** The overall uncertainty and variability in key toxicokinetic predictions, as a
3 function of dose and species, is shown in Figures 3-11–3-19. As expected, TCE that is inhaled
4 or ingested is substantially metabolized in all species, predominantly by oxidation
5 (Figures 3-11–3-12). At higher exposures, metabolism becomes saturated and the fraction
6 metabolized declines. Mice on average have a greater capacity to oxidized TCE than rats or
7 humans, and this is reflected in the predictions at the two highest levels for each route. The
8 uncertainty in the predictions for the population means for total and oxidative metabolism is
9 relatively modest, therefore, the wide confidence interval for combined uncertainty and
10 variability largely reflects intergroup (for rodents) or interindividual (for humans) variability. Of
11 particular note is the high variability in oxidative metabolism at low doses in humans, with the
12 95% confidence interval spanning from 0.1–0.7 for inhalation and 0.2–1.0 for ingestion.

13 Predictions of GSH conjugation and renal bioactivation of DCVC are highly uncertain in
14 rodents, spanning more than 1,000-fold in mice and 100-fold in rats (Figures 3-13–3-14). In
15 both mice and rats, the uncertainty in the population mean virtually overlaps with the combined
16 uncertainty and variability, reflecting the lack of GSH-conjugate specific data in mice (the
17 bounds are based on mass balance) and the availability of only urinary NAcDCVC excretion in
18 one study in rats. In humans, however, the blood concentrations of DCVG from Lash et al.
19 (1999b) combined with the urinary NAcDCVC data from Bernauer et al. (1996) were able to
20 better constrain GSH conjugation and bioactivation of DCVC, with 95% confidence intervals on
21 the population mean spanning only 3-fold or so. However, substantial variability is predicted
22 (reflecting variability in the measurements of Lash et al., 1999b), for the error bars for the
23 population mean are substantially smaller than that for overall uncertainty and variability. Of
24 particular note is the prediction of one or two orders of magnitude more GSH conjugation and
25 DCVC bioactivation, on average, in humans than in rats, although importantly, the 95%
26 confidence intervals for the predicted population means do overlap.

27 Predictions for respiratory tract oxidative metabolism were, as expected, greatest in mice,
28 followed by rats and then humans (see Figure 3-15). In addition, due to the “presystemic” nature
29 of the respiratory tract metabolism model as well as the hepatic first-pass effect, substantially
30 more metabolism was predicted from inhalation exposures as compared to oral exposures.
31 Interestingly, the population means appeared to be fairly well constrained despite the lack of
32 direct data, suggesting that overall mass balance is an important constraint for the presystemic
33 respiratory tract metabolism modeled here.

34 Some constraints were also placed on “other” hepatic oxidation—i.e., through a pathway
35 that does not result in chloral formation and subsequent formation of TCA and TCOH

This document is a draft for review purposes only and does not constitute Agency policy.

1 (Figure 3-16). The 95% confidence interval for overall uncertainty and variability spanned about
2 100-fold, a large fraction of that due to uncertainty in the population mean. Interestingly, a
3 higher rate per kg tissue was predicted for rats than for mice or humans, although importantly,
4 the 95% confidence intervals for the population means overlap among all three species.

5 The AUC of TCE in blood (see Figure 3-17) showed the expected nonlinear behavior
6 with increasing dose, with the nonlinearity more pronounced with oral exposure, as would be
7 expected by hepatic first-pass. Notably, the predicted AUC of TCE in blood from inhalation
8 exposures corresponds closely with cross-species ppm-equivalence, as is often assumed. For low
9 oral exposures (≤ 1 mg/kg-d), cross-species mg/kg-d equivalence appears to be fairly accurate
10 (within 2-fold), implying the usual assumption of $\text{mg/kg}^{3/4}$ -d equivalence would be somewhat less
11 accurate, at least for humans. Interestingly, the AUC of TCOH in blood (see Figure 3-18) was
12 relatively constant with dose, reflecting the parallel saturation of both TCE oxidation and TCOH
13 glucuronidation. In fact, in humans, the mean AUC for TCOH in blood increases up to 100 ppm
14 or 100 mg/kg/d, due to saturation of TCOH glucuronidation, before decreasing at 1,000 ppm or
15 1,000 mg/kg-d, due to saturation of TCE oxidation.

16 The predictions for the AUC for TCA in the liver showed some interesting features (see
17 Figure 3-19). The predictions for all three species with within an order of magnitude of each
18 other, with a relatively modest uncertainty in the population mean (reflecting the substantial
19 amount of data on TCA). The shape of the curves, however, differs substantially, with humans
20 showing saturation at much lower doses than rodents, especially for oral exposures. In fact, the
21 ratio between the liver TCA AUC and the rate of TCA production, although differing between
22 species, is relatively constant as a function of dose within species (not shown). Therefore, the
23 shape of the curves largely reflect saturation in the production of TCA from TCOH, *not* in the
24 oxidation of TCE itself, for which saturation is predicted at higher doses, particularly via the oral
25 route (see Figure 3-12). In addition, while for the same exposure (ppm or mg/kg/d TCE) more
26 TCA (on a mg/kg/d basis) is produced in mice relative to rats and humans, humans and rats have
27 longer TCA half-lives even though plasma protein binding of TCA is on average greater.

28
29 **3.5.7.2.2. Discussion.** This analysis substantially informs four of the major areas of
30 pharmacokinetic uncertainty previously identified in numerous reports (reviewed in Chiu et al.,
31 2006): GSH conjugation pathway, respiratory tract metabolism, alternative pathways of TCE
32 oxidation including DCA formation, and the impact of plasma binding on TCA kinetics
33 particularly in the liver. In addition, the analysis helps identify data that have the potential to
34 further reduce the uncertainties in TCE toxicokinetics and risk assessment.

1 With respect to the first, previous estimates of the degree of TCE GSH conjugation and
2 subsequent bioactivation of DCVC in humans were based on urinary excretion data alone
3 (Bernauer et al., 1996; Birner et al., 1993). For instance, Bloemen et al. (2001) concluded that
4 due to the low yield of identified urinary metabolites through this pathway (<0.05% as compared
5 to 20–30% in urinary metabolites of TCE oxidation), GSH conjugation of TCE is likely of minor
6 importance. However, as noted by Lash et al. (2000a, b), urinary excretion is a poor quantitative
7 marker of flux through the GSH pathway because it only accounts for the portion detoxified, and
8 not the portion bioactivated (a limitation acknowledged by Bloemen et al., 2001). A
9 re-examination of the available *in vitro* data on GSH conjugation by Chiu et al. (2006) suggested
10 that the difference in flux between TCE oxidation and GSH conjugation may not be as large as
11 suggested by urinary excretion data. For example, the formation rate of DCVG from TCE in
12 freshly isolated hepatocytes was similar in order of magnitude to the rate measured for oxidative
13 metabolites (Lipscomb et al., 1998; Lash et al., 1999a). A closer examination of the only other
14 available human *in vivo* data on GSH conjugation, the DCVG blood levels reported in Lash et al.
15 (1999b) also suggests a substantially greater flux through this pathway than inferred from urinary
16 data. In particular, the peak DCVG blood levels reported in this study were comparable on a
17 molar basis to peak blood levels of TCOH, the major oxidative metabolite, in the same subjects,
18 as previously reported by Fisher et al. (1998). A lower bound estimate of the GSH conjugation
19 flux can be derived as follows. The reported mean peak blood DCVG concentrations of 46 μM
20 in males exposed to 100 ppm TCE for 4 hrs (Lash et al., 1999b), multiplied by a typical blood
21 volume of 5 l (ICRP, 2002), yields a peak amount of DCVG in blood of 0.23 mmoles. In
22 comparison, the retained dose from 100 ppm exposure for 4 hours is 4.4 mmol, assuming
23 retention of about 50% (Monster et al., 1976) and minute-volume of 9 L/minute (ICRP, 2002).
24 Thus, in these subjects, about 5% of the retained dose is present in blood as DCVG at the time of
25 peak blood concentration. This is a strong lower bound on the total fraction of retained TCE
26 undergoing GSH conjugation because DCVG clearance is ongoing at the time of peak
27 concentration, and DCVG may be distributed to tissues other than blood. It should be reiterated
28 that only grouped DCVG blood data were available for PBPK model-based analysis; however,
29 this should only result in an underestimation of the degree of *variation* in GSH conjugation.
30 Finally, this hypothesis of a significant flux through the human GSH conjugation pathway is
31 consistent with the limited available total recovery data in humans in which only 60–70% of the
32 TCE dose is recovered as TCE in breath and excreted urinary metabolites (reviewed in Chiu et
33 al., 2007).

34 Thus, there is already substantial qualitative and semi-quantitative evidence to suggest a
35 substantially greater flux through the GSH conjugation pathway than previously estimated based

This document is a draft for review purposes only and does not constitute Agency policy.

1 on urinary excretion data alone. The scientific utility of applying a combination of PBPK
2 modeling and Bayesian statistical methods to this question comes from being able to
3 systematically integrate these different types of data—*in vitro* and *in vivo*, direct (blood DCVG)
4 and indirect (total recovery, urinary excretion)—and quantitatively assess their consistency and
5 implications. For example, the *in vitro* data discussed above on GSH conjugation were used for
6 developing prior distributions for GSH conjugation rates, and were not used in previous PBPK
7 models for TCE. Then, both the direct and indirect *in vivo* data were used to the extent possible
8 either in the Bayesian calibration or model evaluation steps.

9 Several other aspects of the predictions related to GSH conjugation of TCE are worthy of
10 note. Predictions for rats and mice remain more uncertain due to their having less direct
11 toxicokinetic data, but are better constrained by total recovery studies. For instance, the total
12 recovery of 60-70% of dose in exhaled breath and oxidative metabolites in human studies is
13 substantially less than the >90% reported in rodent studies (also noted by Goepfert et al., 1995).
14 In addition, it has been suggested that “saturation” of the oxidative pathway for volatiles in
15 general, and TCE in particular, may lead to marked increases in flux through the GSH
16 conjugation pathway (Slikker et al., 2004a, b; Goepfert et al., 1995), but the PBPK model predicts
17 only a modest, at most ~2-fold, change in flux. This is because there is evidence that both
18 pathways are saturable in the liver for this substrate at similar exposures and because GSH
19 conjugation also occurs in the kidney. Therefore, the available data are not consistent with
20 toxicokinetics alone causing substantially nonlinearities in TCE kidney toxicity or cancer, or in
21 any other effects associated with GSH conjugation of TCE.

22 Finally, the present analysis suggests a number of areas where additional data can further
23 reduce uncertainty in and better characterize the TCE GSH conjugation pathway. The Bayesian
24 analysis predicts a relatively low distribution volume for DCVG in humans, a hypothesis that
25 could be tested experimentally. In addition, corroboration of the DCVG blood levels reported in
26 Lash et al. (1999b) in future studies would further increase confidence in the predictions.
27 Moreover, it would be useful in such studies to be able to match individuals with respect to
28 toxicokinetic data on oxidative and GSH conjugation metabolites so as to better characterize
29 variability. A consistent picture as to which GST isozymes are involved in TCE GSH
30 conjugation, along with data on variability in isozyme polymorphisms and activity levels, can
31 further inform the extent of human variability. In rodents, more direct data on GSH metabolites,
32 such as reliably-determined DCVG blood concentrations, preferably coupled with simultaneous
33 data on oxidative metabolites, would greatly enhance the assessment of GSH conjugation flux in
34 laboratory animals. Given the large apparent variability in humans, data on inter-strain
35 variability in rodents may also be useful.

This document is a draft for review purposes only and does not constitute Agency policy.

1 With respect to oxidative metabolism, as expected, the liver is the major site of oxidative
2 metabolism in all three species, especially after oral exposure, where >85% of total metabolism
3 is oxidation in the liver in all three species. However, after inhalation exposure, the model
4 predicts a greater proportion of metabolism via the respiratory tract than previous models for
5 TCE. This is primarily because previous models for TCE respiratory tract metabolism (Clewell
6 et al., 2000; Hack et al., 2006) were essentially flow-limited—i.e., the amount of respiratory tract
7 metabolism (particularly in mice) was determined primarily by the (relatively small) blood flow
8 to the tracheobronchial region. However, the respiratory tract structure used in the present model
9 is more biologically plausible, is more consistent with that of other volatile organics metabolized
10 in the respiratory tract (e.g., styrene), and leads to a substantially better fit to closed chamber data
11 in mice.

12 Consistent with the qualitative suggestions from *in vitro* data, the analysis here predicts
13 that mice have a greater rate of respiratory tract oxidative metabolism as compared to rats and
14 humans. However, the predicted difference of 50-fold or so on average between mice and
15 humans is not as great as the 600-fold suggested by previous reports (Green et al., 1997; Green,
16 2000; NRC, 2006). The suggested factor of 600-fold was based on multiplying the Green et al.
17 (1997) data on TCE oxidation in lung microsomes from rats versus mice (23-fold lower) by a
18 factor for the total CYP content of human lung compared to rat lung (27-fold lower) (Wheeler et
19 al. [1990], incorrectly cited as being from Raunio et al. [1998]). However, because of the
20 isozyme-specificity of TCE oxidation, and the differing proportions of different isozymes across
21 species, total CYP content may not be the best measure of inter-species differences in TCE
22 respiratory tract oxidative metabolism. Wheeler et al. (1992) reported that CYP2E1 content of
23 human lung microsomes is about 10-fold lower than that of human liver microsomes. Given that
24 Green et al. (1997) report that TCE oxidation by human liver microsomes is about 3-fold lower
25 than that in mouse lung microsomes, this suggests that the mouse-to-human comparison TCE
26 oxidation in lung microsomes would be about 30-fold. Moreover, the predicted amount of
27 metabolism corresponds to about the detection limit reported by Green et al. (1997) in their
28 experiments with human lung microsomes, suggesting overall consistency in the various results.
29 Therefore, the 50-fold factor predicted by our analysis is biologically plausible given the
30 available *in vitro* data. More direct *in vivo* measures of respiratory tract metabolism would be
31 especially beneficial to reduce its uncertainty as well as better characterize its human variability.

32 TCA dosimetry is another uncertainty that was addressed in this analysis. In particular,
33 the predicted inter-species differences in liver TCA AUC are modest, with a range of 10-fold or
34 so across species, due to the combined effects of inter-species differences in the yield of TCA
35 from TCE, plasma protein binding, and elimination half-life. This result is in contrast to

1 previous analyses which did not include TCA protein binding (Clewell et al., 2000; Fisher,
2 2000), which predicted significantly more than an order of magnitude difference in TCA AUC
3 across species. In addition, in order to be consistent with available data, the model requires some
4 metabolism or other clearance of TCA in addition to urinary excretion. That urinary excretion
5 does not represent 100% of TCA clearance is evident empirically, as urinary recovery after TCA
6 dosing is not complete even in rodents (Abbas et al., 1997; Yu et al., 2000). Additional
7 investigation into possible mechanisms, including metabolism to DCA or enterohepatic
8 recirculation with fecal excretion, would be beneficial to provide a stronger biological basis for
9 this empirical finding.

10 With respect to “untracked” oxidative metabolism, this pathway appears to be a relatively
11 small contribution to total oxidative metabolism. While it is tempting to use this pathway as a
12 surrogate for DCA production through from the TCE epoxide (Cai and Guengerich, 1999), one
13 should be reminded that DCA may be formed through multiple pathways (see Section 3.3).
14 Therefore, this pathway at best represents a lower bound on DCA production. In addition, better
15 quantitative markers of oxidative metabolism through the TCE epoxide pathway (e.g.,
16 dichloroacetyl lysine protein adducts, as reported in Forkert et al., 2006) are needed in order to
17 more confidently characterize its flux.

18 In a situation such as TCE in which there is large database of studies coupled with
19 complex toxicokinetics, the Bayesian approach provides a systematic method of simultaneously
20 estimating model parameters and characterizing their uncertainty and variability. While such an
21 approach is not necessarily needed for all applications, such as route-to-route extrapolation (Chiu
22 and White, 2006), as discussed in Barton et al. (2007), characterization of uncertainty and
23 variability is increasingly recognized as important for risk assessment while representing a
24 continuing challenge for both PBPK modelers and users. If there is sufficient reason to
25 characterize uncertainty and variability in a highly transparent and objective manner, there is no
26 reason why our approach could not be applied to other chemicals. However, such an endeavor is
27 clearly not trivial, though the high level of effort for TCE is partially due to the complexity of its
28 metabolism and the extent of its toxicokinetic database.

29 It is notable that, with experience, the methodology for the Bayesian approach to PBPK
30 modeling of TCE has evolved significantly from that of Bois (2000a, 2000b), to Hack et al.
31 (2006), to the present analysis. Part of this evolution has been a more refined specification of the
32 problem being addressed, showing the importance of “problem formulation” in risk assessment
33 applications of PBPK modeling. The particular hierarchical population model for each species
34 was specified based on the intended use of the model predictions, so that relevant data can be
35 selected for analysis (e.g., excluding most grouped human data in favor of individual human

This document is a draft for review purposes only and does not constitute Agency policy.

1 data) and data can be appropriately grouped (e.g., in rodent data, grouping by sex and strain
2 within a particular study). Thus, the predictions from the population model in rodents are the
3 “average” for a particular “lot” of rodents of a particular species, strain, and sex. This is in
4 contrast to the Hack et al. (2006) model, in which each dose group was treated as a separate
5 “individual.” As discussed above, this previous population model structure led to the unlikely
6 result that different dose groups within a closed chamber study had significantly different V_{MAX}
7 values. In humans, however, interindividual variability is of interest, and furthermore,
8 substantial individual data are available in humans. Hack et al. (2006) mixed individual- and
9 group-level data, depending on the availability from the published study, but this approach likely
10 underestimates population variability due to group means being treated as individuals. In
11 addition, in some studies, the same individual was exposed more than once, and in Hack et al.
12 (2006), these were treated as different “individuals.” In this case, actual interindividual
13 variability may be either over- or underestimated, depending on the degree of interoccasion
14 variability. While it is technically feasible to include interoccasion variability, it would have
15 added substantially to the computational burden and reduced parameter identifiability. In
16 addition, a primary interest for this risk assessment is chronic exposure, so the predictions from
17 the population model in humans are the “average” across different occasions for a particular
18 individual (adult).

19 The second aspect of this evolution is the drive towards increased objectivity and
20 transparency. For instance, available information, or the lack thereof, is formally codified and
21 explicit either in prior distributions or in the data used to generate posterior distributions, and not
22 both. Methods at minimizing subjectivity (and hence improving reproducibility) in parameter
23 estimation include: (1) clear separation between the *in vitro* or physiologic data used to develop
24 prior distributions and the *in vivo* data used to generate posterior distributions; (2) use of
25 noninformative distributions, first updated using a probabilistic model of interspecies-scaling
26 that allows for prediction error, for parameters lacking in prior information; and (3) use of a
27 more comprehensive database of physiologic data, *in vitro* measurements, and *in vivo* data for
28 parameter calibration or for out-of-sample evaluation (“validation”). These measures increase
29 the confidence that the approach employed also provides adequate characterization of the
30 uncertainty in metabolic pathways for which available data was sparse or relatively indirect, such
31 as GSH conjugation in rodents and respiratory tract metabolism. Moreover, this approach yields
32 more confident insights into what additional data can reduce these uncertainties than approaches
33 that rely on more subjective methods.

34 Like all analyses, this one has a number of limitations and opportunities for refinement,
35 both biological and statistical. One would be the inclusion of a CH submodel, so that

This document is a draft for review purposes only and does not constitute Agency policy.

1 pharmacokinetic data, such as that recently published by Merdink et al. (2008), could be
2 incorporated. In addition, our probabilistic analysis is still dependent on a model structure
3 substantially informed by deterministic analyses that test alternative model structures (Evans et
4 al., submitted), as probabilistic methods for discrimination or selection among complex,
5 nonlinear models such as that for TCE toxicokinetics have not yet been widely accepted.
6 Therefore, additional refinement of the respiratory tract model may be possible, though more
7 direct *in vivo* data would likely be necessary to strongly discriminating among models.
8 Furthermore, additional model changes that may be of utility to risk assessment, such as
9 development of models for different lifestages (including childhood and pregnancy), would
10 likely require additional *in vivo* or *in vitro* data, particularly as to metabolism, to ensure model
11 identifiability. Finally, improvements are possible in the statistical and population models and
12 analyses, such as incorporation of interoccasion variability (Bernillon and Bois, 2000),
13 application of more sophisticated “validation” methods (such as cross-validation), and more
14 rigorous treatment of grouped data (Chiu and Bois, 2007).

15

16 **3.5.7.3. Overall Evaluation of Physiologically Based Pharmacokinetic (PBPK) Model-Based** 17 **Internal Dose Predictions**

18 The utility of the PBPK model developed here for making predictions of internal dose
19 can be evaluated based on four different components: (1) the degree to which the simulations
20 have converged to the true posterior distribution; (2) the degree of overall uncertainty and
21 variability; (3) for humans, the degree of uncertainty in the population; and (4) the degree to
22 which the model predictions are consistent with *in vivo* data that are informative to a particular
23 dose metric. Table 3-50 summarizes these considerations for each dose metric prediction. Note
24 that this evaluation does not consider in any way the extent to which a dose metric may be the
25 appropriate choice for a particular toxic endpoint.

26 Overall, the least uncertain dose metrics are the fluxes of total metabolism
27 (TotMetabBW34), total oxidative metabolism (TotOxMetabBW34), and hepatic oxidation
28 (AMetLiv1BW34). These all have excellent posterior convergence (R diagnostic ≤ 1.01),
29 relatively low uncertainty and variability (GSD < 2), and relatively low uncertainty in human
30 population variability (GSD for population percentiles < 2). In addition, the PBPK model
31 predictions compare well with the available *in vivo* pharmacokinetic data.

32

Table 3-50. Degree of variance in dose metric predictions due to incomplete convergence (columns 2–4), combined uncertainty and population variability (columns 5–7), uncertainty in particular human population percentiles (columns 8–10), model fits to *in vivo* data (column 11). The GSD is the geometric standard deviation, which is a “fold-change” from the central tendency.

Dose metric abbreviation	Convergence: <i>R</i> for generic scenarios			GSD for combined uncertainty and variability			GSD for uncertainty in human population percentiles			Comments regarding model fits to <i>in vivo</i> data
	Mouse	Rat	Human	Mouse	Rat	Human	1~5%	25~75%	95~99%	
ABioactDCVCBW34, ABioactDCVCKid	–	≤1.016	≤1.015	–	≤3.92	≤3.77	≤2.08	≤1.64	≤1.30	Good fits to urinary NAcDCVC, and blood DCVG.
AMetGSHBW34	≤1.011	≤1.024	≤1.015	≤9.09	≤3.28	≤3.73	≤2.08	≤1.64	≤1.29	Good fits to urinary NAcDCVC, and blood DCVG.
AMetLiv1BW34	≤1.000	≤1.003	≤1.004	≤2.02	≤1.84	≤1.97	≤1.82	≤1.16	≤1.16	Good fits to oxidative metabolites.
AMetLivOtherBW34, AMetLivOtherLiv	≤1.004	≤1.151	≤1.012	≤3.65	≤3.36	≤3.97	≤2.63	≤1.92	≤2.05	No direct <i>in vivo</i> data.
AMetLngBW34, AMetLngResp	≤1.001	≤1.003	≤1.002	≤4.65	≤4.91	≤10.4	≤4.02	≤2.34	≤1.83	No direct <i>in vivo</i> data, but good fits to closed chamber.
AUCCBld	≤1.001	≤1.004	≤1.005	≤3.04	≤3.16	≤3.32	≤1.20	≤1.43	≤1.49	Generally good fits, but poor fit to a few mouse and human studies
AUCCTCOH	≤1.001	≤1.029	≤1.002	≤3.35	≤8.78	≤5.84	≤1.73	≤1.20	≤1.23	Good fits across all three species.
AUCLivTCA	≤1.000	≤1.005	≤1.002	≤2.29	≤3.18	≤2.90	≤1.65	≤1.30	≤1.40	Good fits to rodent data.
TotMetabBW34	≤1.001	≤1.004	≤1.004	≤1.92	≤1.82	≤1.81	≤1.13	≤1.12	≤1.18	Good fits to closed chamber.
TotOxMetabBW34	≤1.001	≤1.003	≤1.004	≤1.94	≤1.85	≤1.96	≤1.77	≤1.15	≤1.20	Good fits to closed chamber and oxidative metabolites.
TotTCAInBW	≤1.002	≤1.002	≤1.001	≤1.96	≤2.69	≤2.30	≤1.68	≤1.19	≤1.19	Good fits to TCA data.

1 Predictions for TCE in blood (AUCCBld) are somewhat more uncertain. Although
2 convergence was excellent across species ($R \leq 1.01$), overall uncertainty and variability was
3 about 3-fold. In humans, the uncertainty in human population variability was relatively low
4 (GSD for population percentiles <1.5). TCE blood level predictions were somewhat high in
5 comparison to the Chiu et al. (2006) study at 1 ppm, though the predictions were better for most
6 of the other studies at higher exposure levels. In mice, TCE blood levels were somewhat over-
7 predicted in open-chamber inhalation studies. In both mice and rats, there were some cases in
8 which fits were inconsistent across dose groups if the same parameters were used across dose
9 groups, indicating unaccounted-for dose-related effects or intrastudy variability. However, in
10 both rats and humans, TCE blood (humans and rats) and tissue (rats only) concentrations from
11 studies not used for calibration (i.e., saved for “out-of-sample” evaluation/“validation”) were
12 well simulated, adding confidence to the parent compound dose metric predictions.

13 For the TCA dose metric predictions (TotTCAInBW, AUCLivTCA) convergence in all
14 three species was excellent ($R \leq 1.01$). Overall uncertainty and variability was intermediate
15 between dose metrics for metabolism and that for TCE in blood, with GSD of about 2 to 3-fold.
16 Uncertainty in human population percentiles was relatively low (GSD of 1.2 to 1.7). While liver
17 TCA levels were generally well fit, the data was relatively sparse. Plasma and blood TCA levels
18 were generally well fit, though in mice, there were again some cases in which fits were
19 inconsistent across dose groups if the same parameters were used across dose groups, indicating
20 unaccounted-for dose-related effects or intrastudy variability. In humans, the accurate
21 predictions for TCA blood and urine concentrations from studies used for “out of sample”
22 evaluation lends further confidence to dose metrics involving TCA.

23 The evaluation of TCOH in blood followed a similar pattern. Convergence in all three
24 species was good, though the rat model had slightly worse convergence ($R \sim 1.03$) than the
25 mouse and humans ($R \leq 1.01$). In mice, overall uncertainty and variability was slightly more
26 than for TCE in blood. There much higher overall uncertainty and variability in the rat
27 predictions (GSD of almost 9) that likely reflects true interstudy variability. The
28 population-generated predictions for TCOH and TCOG in blood and urine were quite wide, with
29 some *in vivo* data both at the upper and lower ends of the range of predictions. In humans, the
30 overall uncertainty and variability was intermediate between mice and rats (GSD = 5.8). As with
31 the rats, this likely reflects true population heterogeneity, as the uncertainty in human population
32 percentiles was relatively low (GSD of around 1.2~1.7-fold). For all three species, fits to *in vivo*
33 data are generally good. In mice, however, there were again some cases in which fits were
34 inconsistent across dose groups if the same parameters were used across dose groups, indicating
35 unaccounted-for dose-related effects or intrastudy variability. In humans, the accurate

1 predictions for TCOH blood and urine concentrations from studies used for “out of sample”
2 evaluation lends further confidence to those dose metrics involving TCOH.

3 GSH metabolism dose metrics (ABioactDCVCBW34, ABioactDCVCKid,
4 AMetGSHBW34) had the greatest overall uncertainty in mice but was fairly well characterized
5 in rats and humans. In mice, there was no *in vivo* data informing this pathway except for the
6 indirect constraint of overall mass balance. So although convergence was adequate ($R < 1.02$),
7 the uncertainty/variability was very large, with a GSD of 9-fold for the overall flux (the amount
8 of bioactivation was not characterized because there are no data constraining downstream GSH
9 pathways). For rats, there were additional constraints from (well-fit) urinary NAcDCVC data,
10 which reduced the overall uncertainty and variability substantially (GSD < 4 -fold). In humans,
11 in addition to urinary NAcDCVC data, DCVG blood concentration data was available, though
12 only at the group level. However, these data, both of which were well fit, in addition to the
13 greater amount of *in vitro* metabolism data, allowed for the flux through the GSH pathway and
14 the rate of DCVC bioactivation to be fairly well constrained, with overall uncertainty and
15 variability having GSD < 4 -fold, and uncertainty in population percentiles no more than about
16 2-fold.

17 The final two dose metrics, respiratory metabolism (AMetLngBW34, AMetLngResp)
18 and “other” oxidative metabolism (AMetLivOtherBW34, AMetLivOtherLiv), also lacked direct
19 *in vivo* data and were predicted largely on the basis of mass balance and physiological
20 constraints. Respiratory metabolism had good convergence ($R < 1.01$), helped by the availability
21 of closed chamber data in rodents. In rats and mice, overall uncertainty and variability was
22 rather uncertain (GSD of 4~5-fold), but the overall uncertainty and variability was much greater
23 in humans, with a GSD of about 10-fold. This largely reflects the significant variability across
24 individuals as well as substantial uncertainty in the low population percentiles (GSD of 4-fold).
25 However, the middle (i.e., “typical” individuals) and upper percentiles (i.e., the individuals at
26 highest risk) are fairly well constrained with a GSD of around 2-fold. For the “other” oxidative
27 metabolism dose metric, convergence was good in mice and humans ($R < 1.02$), but less than
28 ideal in rats ($R \sim 1.15$). In rodents, the overall uncertainty and variability were moderate, with a
29 GSD around 3.5-fold, slightly higher than that for TCE in blood. The overall uncertainty and
30 variability in this metric in humans had a GSD of about 4-fold, slightly higher than for GSH
31 conjugation metrics. However, uncertainty in the middle and upper population percentiles had
32 GSDs of only about 2-fold, similar to that for respiratory metabolism.

33 Overall, as shown in Table 3-50, the updated PBPK model appears to be most reliable for
34 the fluxes of total, oxidative, and hepatic oxidative metabolism. In addition, dose metrics related
35 to blood levels of TCE and oxidative metabolites TCOH and TCA had only modest uncertainty.

This document is a draft for review purposes only and does not constitute Agency policy.

1 In the case of TCE in blood, for some data sets, model predictions over-predicted the *in vivo*
2 data, and, in the case of TCOH in rats, substantial interstudy variability was evident. For GSH
3 metabolism, dose-metric predictions for rats and humans had only slightly greater uncertainty
4 than the TCE and metabolism metrics. Predictions for mice were much more uncertain,
5 reflecting the lack of GSD-specific *in vivo* data. Finally, for “other” oxidative metabolism and
6 respiratory oxidative metabolism, predictions also had somewhat more uncertainty than the TCE
7 and metabolism metrics, though uncertainty in middle and upper human population percentiles
8 was modest.

This document is a draft for review purposes only and does not constitute Agency policy.